HAL
open science

Wireless sensor networks for indoor mapping and accurate localization for low speed navigation in smart cities

Dinh-Van Nguyen

To cite this version:

Dinh-Van Nguyen. Wireless sensor networks for indoor mapping and accurate localization for low speed navigation in smart cities. Robotics [cs.RO]. Université Paris sciences et lettres, 2018. English. NNT : 2018PSLEM029 . tel-02274361

HAL Id: tel-02274361

https://pastel.hal.science/tel-02274361v1

Submitted on 29 Aug 2019

HAL is a multi-disciplinary open access archive for the deposit and dissemination of scientific research documents, whether they are published or not. The documents may come from teaching and research institutions in France or abroad, or from public or private research centers.

L'archive ouverte pluridisciplinaire **HAL**, est destinée au dépôt et à la diffusion de documents scientifiques de niveau recherche, publiés ou non, émanant des établissements d'enseignement et de recherche français ou étrangers, des laboratoires publics ou privés.

PSL UNIVERSITÉ PARIS

THÈSE DE DOCTORAT
DE L'UNIVERSITÉ PSL

Préparée à MINES ParisTech

Wireless Sensors Networks for Indoor Mapping and Accurate Localization for Low Speed Navigation in Smart Cities

Réseaux de capteurs sans-fil pour la cartographie à l'intérieur et la localisation précise servant la navigation à basse vitesse dans les villes intelligentes

Soutenue par

Dinh-Van NGUYEN

Le 05 Dec 2018

Ecole doctorale n° 432

Sciences des Métiers de l'Ingénieur

Spécialité

Informatique temps réel, robotique et automatique

Composition du jury :

Paul, MUHLETHALER *Directeur de recherche, INRIA*	*Président*
Vincent, FREMONT *Professeur, Ecole Central Nantes*	*Rapporteur*
Samia, AINOUZ *Maître de conférences, INSA de Rouen*	*Rapporteur*
Trung-kien, DAO *Lecturer-Researcher, MICA Institute*	*Co-Directeur de these*
Eric, CASTELLI *Chargé de recherche, CNRS*	*Co-Directeur de thèse*
Fawzi, NASHASHIBI *Directeur de recherche, INRIA*	*Directeur de thèse*

MINES ParisTech | PSL

ABSTRACT

With the increasing demand for urban space, more and more multistory carparks are needed. Although these carparks help to utilize urban space more efficient, they also introduce a new problem. Reports suggest approximately 70 million hours of parking slot searching each year, equivalently 700 million euros loss for France alone. In addition, carparks uses are exceeding their original purposes. Demanding features such as electric charger, online booking of parking spaces, dynamic guidance or mobile payment etc. turn a carpark into a competitive smart environment. One solution to this problem is to develop an autonomous navigation system for intelligent vehicles in the carpark situation. The thesis will identify one of these sub-tasks namely localization in GPS-denied environments. This thesis will present a novel method to solve the indicated problem while keeping the system follows four criteria: availability, scalability, universality and accuracy. There are two main steps: (1) a solution to replicate the GPS behaviour for the GPS-denied environment, and (2) a framework that allows the fusion of GPS-like systems with other localization methods to achieve a high localization accuracy. First, a Wi-Fi Fingerprinting localization system is employed. An approach using an ensemble neural network on a hybrid Wi-Fi fingerprinting database is proposed in this thesis. Experiments in a year-long duration show that this system is capable of localizing vehicles with 2.25m of mean error in the global coordinate frame (WGS84). Second, a complete localization solution must be a fusion of multiple techniques. This allows global as well as local levels of localization to function together. At the same time, having redundancy in the system boosts accuracy and reliability. In this thesis, a flexible fusion framework for multiple localization sensors is proposed. This fusion framework will not only deal with the GPS-denied environment but could be potentially used in the GPS-aided environment and provide a smooth transition between the two areas. To accomplish this demanding task, a Gaussian Mixture Model Particle Filter is developed. While the motion model of this particle filter incorporates data from the IMU (Inertial Measurement Unit) or laser-SLAM, the correction model is a Gaussian mixture model of multiple observations obtained from the Wi-Fi fingerprinting localization system. With two intelligent vehicles (a Cybercar and a Citroen C1 car), 64 experiments were carried out to validate the framework. A mean localization error of 0.5m is achieved in a global coordinate frame. Compare to other solutions with 0.2m of mean localization error in local coordinate frames; this proposed solution has advantages in terms of scalability, availability and universality as well.

MINES ParisTech

Unité Mathématiques et Systèmes

ACKNOWLEDGEMENTS

I would like to thank my family, my wife Linh, my parents, my sister and our little cat for all the support. No word can describe how much they mean to me.

To my supervisors, thank you! You all have been so patient and thoughtful with me. You gave me this extraordinary opportunity at the beginning and accomplishing this thesis would not be possible without your advices.

To my colleagues, Raoul, Anne, Jean-Marc, and the PhD gang, thank you! You all have been fantastic. I could not ask for a better team.

And finally, to my future baby boy, this is for you!

MINES ParisTech

Unité Mathématiques et Systèmes

CONTENTS

1. INTRODUCTION 1

1.1 CONTEXT 2

1.2 SCOPE 4

1.3 MAIN CONTRIBUTIONS 6

1.4 THESIS OVERVIEW 7

2. INTELLIGENT VEHICLES LOCALIZATION 10

2.1 OVERVIEW OF INTELLIGENT VEHICLES LOCALIZATION 14

2.2 GPS-BASED LOCALIZATION 15

2.3 LASER-BASED LOCALIZATION 20

2.3.1 Filter-based Laser SLAM 21

2.3.2 Optimization-based Laser SLAM 23

2.4 VISION-BASED LOCALIZATION 24

2.5 DEAD-RECKONING 25

2.6 INTELLIGENT VEHICLES LOCALIZATION IN GPS-DENIED ENVIRONMENTS 27

2.6.1 Absolute Localization 27

2.6.2 Relative Localization 31

2.7 DISCUSSION 32

3. WIRELESS SENSOR NETWORKS LOCALIZATION 36

3.1 INTRODUCTION 37

3.2 LOCALIZATION STRATEGIES OVERVIEW 38

3.3 RANGE-BASED APPROACH 38

3.3.1 Time of Arrival 38

3.3.2 Angle of Arrival 40

3.3.3 Received Signal Strength Indicator 42

3.4 RANGE-FREE APPROACH 43

3.4.1 Distance Vector Hop 43

3.4.2 Approximate Point-in-Triangulation Test 45

3.4.3 Fingerprinting Localization 45

3.4.4 Centroid Localization 47

3.5 DISCUSSION 47

4. WI-FI FINGERPRINTING LOCALIZATION 50

4.1 INTRODUCTION 52

4.2 RELATED WORKS 56
4.3 ENSEMBLE APPROACH FOR WI-FI FINGERPRINTING LOCALIZATION OF INTELLIGENT VEHICLES 61
4.3.1 Hybrid Database Offline Phase 62
4.3.2 Wi-Fi Ensemble Neural Network 65
4.4 EXPERIMENTS AND RESULTS 70
4.4.1 Survey of the Wi-Fi Characteristics in the Experiment Area 72
4.4.2 Wi-Fi localization Experiments 75
4.5 DISCUSSION 78
5. FUSION STRATEGY FOR LOCALIZATION ENHANCEMENT 81
5.1 INTRODUCTION 83
5.2 THE PARTICLE FILTER 86
5.2.1 Initialization Step 87
5.2.2 Prediction Step 87
5.2.3 Correction Step 88
5.2.4 Selection & Resampling Step 89
5.3 GAUSSIAN MIXTURE MODEL PARTICLE FILTER 90
5.3.1 Initialization Step 91
5.3.2 Correction Step 92
5.4 FUSION OF WI-FI FINGERPRINTING AND IMU 95
5.4.1 Inputs Synchronization 96
5.4.2 Particles Propagation 97
5.4.3 Motion model 97
5.4.4 Selection & Resampling 98
5.5 FUSION OF WI-FI FINGERPRINTING, IMU AND LASER-SLAM 99
5.5.1 Evidential SLAM 100
5.5.2 PML-SLAM 102
5.5.3 SLAM in Global Coordinate Frame 104
5.5.4 SLAM as Odometry Measurements 106
5.6 EXPERIMENTS AND RESULTS 108
5.6.1 Wi-Fi Fingerprinting Localization and IMU Fusion 108
5.6.2 Wi-Fi Fingerprinting Localization, IMU and Laser-SLAM fusion 118
5.7 DISCUSSION 122

6. CONCLUSION 126
6.1 THESIS MOTIVATION 127
6.2 THESIS CONTRIBUTIONS 128
6.3 FUTURE WORK 130
6.4 CONCLUSION 131
7. REFERENCES 133
8. APPENDIX 1: RÉSUMÉ 149
9. APPENDIX 2: ABSTRACT 162

LIST OF TABLES

Table 1 Service performance standard for SPS (Department Of Defense 2008; "GPS Performances - Navipedia" 2018) 16

Table 2 Service performance standard for PPS ("GPS Performances - Navipedia" 2018; GPS Directorate 2007) 16

Table 3 Comparison between global positioning systems (Hofmann-Wellenhof, Lichtenegger, and Wasle 2018) 20

Table 4 Comparison of different WSNs localization techniques 54

Table 5 Positioning Error using BLE and Wi-Fi fingerprinting (Wilfinger and Thesis 2015) 58

Table 6 Wi-Fi fingerprinting localization using 13 fingerprints 73

Table 7 Correlation between the average Wi-Fi signal strength and the localization error 74

Table 8 Top 3 highest confidence fingerprints as the classification result 77

Table 9 Wi-Fi ensemble fingerprinting localization error 77

Table 10 Comparison of Algorithms for Nonlinear Filtering (Daum 2005) 85

Table 11 Particles count and the localization error statistic 114

LIST OF FIGURES

Figure 1.1 Parkmatic – Automated Parking System ("Parkmatic - Multi Parking" 2018) 3

Figure 1.2 OneSITU – Parking Management System ("Parking Solutions - Solutions - OneSITU" 2018) 4

Figure 1.3 World Geodetic Coordinate System WGS84 (Malys et al. 2015) 5

Figure 2.1 Fusion of localization systems 15

Figure 2.2 GPS principle 16

Figure 2.3 The Galileo satellites navigation system commercial service architecture (Fernández-Hernández et al. 2018) 18

Figure 2.4 The kinematic high precision positioning results of Galileo (Ignacio, Irma, and Guillermo 2015) 19

Figure 2.5 The GLONASS accuracy evolution ("GLONASS Performances - Navipedia" 2018) 19

Figure 2.6 Graphical representation of (a) Full SLAM problem; (b) Online SLAM problem (Bresson et al. 2017) 20

Figure 2.7 Particle Filter based Evidential SLAM (Trehard et al. 2014) 22

Figure 2.8 GraphSLAM visualization of large scale forest mapping (Pierzchała, Giguère, and Astrup 2018) 23

Figure 2.9 GPS-aided SLAM for large scale uban mapping (Carlson, Thorpe, and Browning 2010) 24

Figure 2.10 Edge-filtered map of the environment (Borges et al. 2010) 25

Figure 2.11 Camera image to edge image transformation (Borges et al. 2010) 25

Figure 2.12 Dead-reckoning and static map (Fouque et al. 2008) 27

Figure 2.13 Graphical representation of SLAM with a static map (Wahl et al. 2015) 28

Figure 2.14 2D map and LiDAR reading of the obstacle-free environment (Ibisch et al. 2013) 29

Figure 2.15 Sensor setup for camera-based carpark localization (Schwesinger et al. 2016) ... 30

Figure 2.16 Flow chart of 3D map-matching based on particle filter (Bojja et al. 2013) 31

Figure 2.17 Fisheye-based parking lot searching (Houben et al. 2013) 32

Figure 2.18 Two levels of localization system 33

Figure 3.1 Two-way scheme of TOA 39

Figure 3.2 Angle of Arrival (AOA) localization method (Yin et al. 2016) 41

Figure 3.3 Angel of Arrival confidence zone 41

Figure 3.4 Array Track localization error 42

Figure 3.5 Signal propagation through obstacles (Dao et al. 2014) 43

Figure 3.6 DV-Hop distance 44

Figure 3.7 Approximate point-in-triangulation test (F. Liu and Tan 2012) 45

Figure 3.8 Fingerprinting localization concept 46

Figure 3.9 Centroid algorithm concept (Hongyang Chen et al. 2008) 47

Figure 4.1 Fingerprints illustration 54

Figure 4.2 iParking system architecture (J. Liu et al. 2012) 56

Figure 4.3 Thondorf carpark (Wilfinger and Thesis 2015) 57

Figure 4.4 Time series for a test run (Wilfinger and Thesis 2015) 57

Figure 4.5 Sensors setup and testing environment (Gikas et al. 2016) 59

Figure 4.6 The Universidad Carlos II de Madrid campus (Hernandez et al. 2017) 59

Figure 4.7 General architecture of the system (Hernandez et al. 2017) 60

Figure 4.8 Cumulative Distribution of Error (Hernandez et al. 2017) 60

Figure 4.9 Wi-Fi localization in urban area (Ang 2018) 61

Figure 4.10 Cumulative distribution of error in urban area (Ang 2018) 61

Figure 4.11 Online scan range for different speeds 62

Figure 4.12 Distance between two adjacent fingerprints 64

Figure 4.13 Ensemble of estimators motivation (Dietterich 2000) 67

Figure 4.14 Fully connected neural network with 1 hidden layer 68

Figure 4.15 Boostrap hybrid database 69

Figure 4.16 Testing area in INRIA Rocquencourt campus 71

Figure 4.17 Blue Cybercar and Red Citroen C1 71

Figure 4.18 The Wi-Fi heat map of the testing area 72

Figure 4.19 13 Reference points in the environment 73

Figure 4.20Number of detected access points for each reference point 73

Figure 4.21 Distribution of localization error for each fingerprint 74

Figure 4.22 Cumulative distribution of the localization error for fingerprints 1-9 75

Figure 4.23 The experiment area with 25 fingerprints 75

Figure 4.24 Localization result for 1 run 77

Figure 5.1 Particle Filter Flowchart 88

Figure 5.2 Particle filter and Wi-Fi fingerprinting flowchart 91

Figure 5.3 Gaussian Mixture Model Estimation 93

Figure 5.4 Single Gaussian Model Estimation 93

Figure 5.5 Gaussian Mixture Model in Practice 1 94

Figure 5.6 Gaussian Mixture Model in Practice 2 95

Figure 5.7 Gaussian Mixture Model Particle Filter with IMU and Wi-Fi fingerprinting 96

Figure 5.8 Input Synchronization Timestamp 96

Figure 5.9 General architecture for Evidential SLAM (Trehard et al. 2014) 101

Figure 5.10 Evidential SLAM test drive in KITTI database (Trehard et al. 2014) 102

Figure 5.11 General flowchart of the PML-SLAM algorithm (Alsayed et al. 2015) 103

Figure 5.12 Test drive on KITTI database with PML-SLAM (Alsayed et al. 2015) 103

Figure 5.13 Deviation of distance and heading for PML SLAM (Alsayed et al. 2015) 104

Figure 5.14 Fusion of laser-SLAM, Wi-Fi fingerprinting and IMU 106

Figure 5.15 Laser-SLAM and IMU particles clouds 107

Figure 5.16 True position during the initialization step: within fingerprint area (red) and outside fingerprint area (blue) 109
Figure 5.17 Initial position within the defined fingerprint area case 111
Figure 5.18 Experiment test run 111
Figure 5.19 Localization error with corresponding ground truth quality 112
Figure 5.20 Travel path with RTK GPS quality 112
Figure 5.21 Initial position outside the defined fingerprint area case 113
Figure 5.22 Experiment test run 114
Figure 5.23 Initial position within a fingerprint area 115
Figure 5.24 Initial position outside a fingerprint area 115
Figure 5.25 Localization error histogram of all experiments 116
Figure 5.26 Cumulative sum of errors for all experiments 116
Figure 5.27 Localization error histogram (good initial position) 117
Figure 5.28 Cumulative sum of localization error (good initial position) 117
Figure 5.29 laser-SLAM in Global Coordinate 118
Figure 5.30 Fusion System (Wi-Fi and laser-SLAM) in the Global Coordinate Frame 119
Figure 5.31 Localization error of fusion solution 120
Figure 5.32 Experiment test run 120
Figure 5.33 PML-SLAM online map 121
Figure 5.34 Evidential SLAM online map 122

LIST OF ABBREVIATIONS AND ACRONYMS

Abbreviation	*Full Name*
AOA	Angle of Arrival
APIT	Approximate Point In Triangulation Test
CV	Coefficient of Variation
DGPS	Differential Global Positioning System
DV-hop	Distance Vector Hop
EKF	Extended Kalman Filter
EPS	Effective Particle Size
FP	Fingerprint
GMM	Gaussian Mixture Model
GNSS	Global Navigation Satellite System
GPS	Global Positioning Systems
ICP	Iterative Closest Points
IMU	Inertial Measurement Unit
IoT	Internet of Things
ITS	Intelligent Transportation Systems
KNN	K-Nearest Neighbours
OOI	Object of Interest
PML	Probabilistic Maximum Likelihood
PPS	Precise Positioning Service
RIOs	Road Infrastructure Objects
RMSE	Root Mean Square Error
RSSI	Received Signal Strength Indicator

RTK	Real-time Kinematic
SLAM	Simultaneous Localization and Mapping
SPS	Standard Positioning Service
SVM	Support Vector Machine
TDOA	Time Difference of Arrival
TOA	Time of Arrival
V2I	Vehicle to Infrastructure
WEFLS	Wi-Fi Ensemble Fingerprinting Localization System
WLAN	Wireless Local Area Network
WSNs	Wireless Sensors Networks

1. INTRODUCTION

Résumé

Le chapitre présente la motivation, la portée et le but de la thèse. Cette thèse débute avec la collaboration de deux unités de recherche, l'équipe RITS, l'INRIA France et l'institut MICA, et est financée par le programme de bourses d'études 911 du gouvernement vietnamien. comme autoroute, rues urbaines, etc. L'environnement sans GPS, qui est également un scénario important pour les applications de véhicules intelligents, n'a pas encore été totalement traité. Un environnement notable pour un tel scénario est un parking couvert. Cette thèse a pour objectif de trouver une nouvelle solution au problème de localisation dans un environnement sans GPS. Les solutions existantes pour ce scénario sont coûteuses à déployer ou ne permettent pas de résoudre complètement le problème. Par conséquent, la solution doit être une méthode de localisation globale qui permette une transition transparente entre la localisation d'environnement assistée par GPS et celle qui est refusée par le GPS et satisfasse à quatre critères: disponibilité, évolutivité, universalité et précision. Deux contributions principales sont proposées: un système de localisation d'empreintes digitales d'ensemble Wi-Fi capable de reproduire le comportement du GPS pour l'environnement sans GPS et un cadre de fusion de filtres à particules mélangées gaussien permettant la fusion de techniques de localisation multiples.

1.1 Context

The thesis is conducted in collaboration of two research units: RITS team, INRIA France and MICA Institute, Vietnam and funded by Vietnamese government scholarship program 911.

RITS (Robotics for Intelligent Transportation Systems) team is a multidisciplinary project team at INRIA, working on Robotics for Intelligent Transportation Systems. The team focuses on enabling advanced intelligent robotics systems for autonomous and sustainable mobility. One notable application is Intelligent Vehicles (IVs) which can navigate autonomously in different environments.

MICA (Multimedia, Information Communication and Application) International Research Institute is established in Vietnam by CNRS, Grenoble INP and Hanoi University of Science and Technology. One of its research interests is indoor localization in smart environments using wireless sensors networks. The main objective of this research is to enable indoor navigation for targets such as humans or robots.

With the increasing demand for urban space, more and more multistory carparks are needed. Although these carparks help to utilize urban space more efficient, they also introduce a new problem. Reports in (Belloche 2015; Gantelet and Lefauconnier 2006) suggest the average searching time for a free slot in a carpark in Paris or Lyon is 20 minutes and can be as high as 40 minutes for some districts. This leads to approximately 70 million hours of searching each year, equivalently 700 million euros loss for France alone. In addition, carparks uses are exceeding their original purposes. Demanding features such as electric charger, online booking of parking spaces, dynamic guidance or mobile payment etc. turn a carpark into a competitive smart environment. Furthermore, 20 most populous cities in France must engage an open data approach from October 1st, 2018 in accordance with the law for a digital Republic ("Loi Du 7 Octobre 2016 Pour Une République Numérique" 2016). This introduces a great chance to invent a new way to calculate traffic flow, develop intelligent services such as intelligent car parks ("Parking at the Service of Connected Urban Mobility and a Sustainable City - The Urban Mobility Blog" 2018).

Several solutions are developed such as automated carpark system (Skyline Inc. 2018; "Parkmatic - Multi Parking" 2018); smart car park guidance and management ("Parking Solutions - Solutions - OneSITU" 2018). Automated carpark system (Figure 1.1) is a complex, costly mechanical system that automatically collects vehicles and put them in specific places.

This solution requires a complete rebuild of a carpark. Although, a smart car park guidance and management system does not require such a high investment, it asks for various sensors and computing systems to guide users to a free parking lot from software level (Figure 1.2). These systems are either too costly or do not entirely eliminate time wasting issue. This is the motivation for intelligent vehicles to push toward fully autonomous navigation in an indoor situation such as a carpark to completely remove the time-wasting issue and enhance effectiveness and safety of car parking. With the centre role of car park in the transport chain, solving such problem would definitely benefit the traffic flow of the whole system. This solution will not only address the time-wasting issue but also enhance the parking space efficiency. According to report from the Audi's Urban Futures Initiative program, the autonomous vehicles solution could save up to 62% of parking space by 2030 (Nourinejad, Bahrami, and Roorda 2018). This is equivalent to 100 million Dollars for a single district of the testing area in the program.

The dream of having an intelligent vehicle navigating autonomously in different environments, has been realized step by step during the last ten years. One of those steps is the challenging task of locating a vehicle position in different circumstances, conditions and environments. The lack of Global Positioning System (GPS) appears to be a significant concern for any localization system. While outdoor, GPS-aided localization for intelligent vehicles has been widely studied in recent years, indoor, GPS-denied localization is yet to be fully addressed.

Figure 1.1 Parkmatic – Automated Parking System ("Parkmatic - Multi Parking" 2018)

From both theoretical and practical perspectives, the problem of navigation for intelligent vehicles in GPS-denied environment deserves a complete solution. This thesis will focus on solving a crucial part of it namely localization. The scope and objectives of the thesis will be presented in the following section.

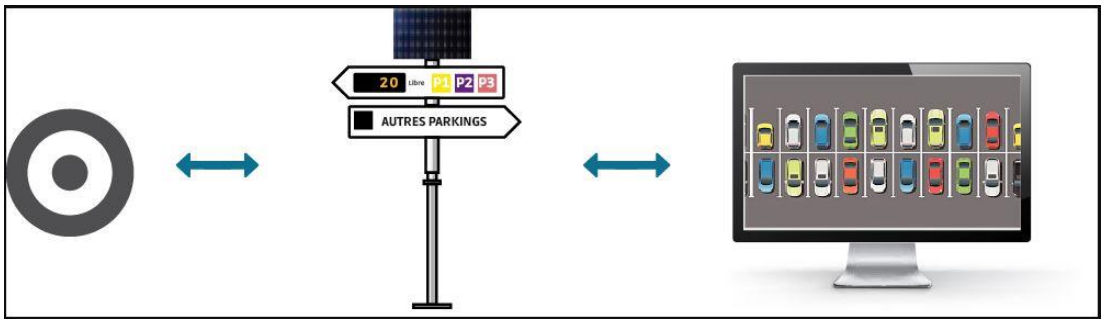

Figure 1.2 OneSITU – Parking Management System ("Parking Solutions - Solutions - OneSITU" 2018)

1.2 Scope

Autonomous navigation for an intelligent vehicle is a considerable task consisting of multiples sub-tasks. Rather than trying to find a complete solution at once, it is essential to identify each of these sub-tasks and deal with them separately. The thesis will identify one of these sub-tasks as follows.

In this thesis, the targeted environments are the one without GPS signal such as: indoor carpark. The targeted environment can also be extended to places with poor GPS signal and low movement speed such as industrial factory, university campus or outdoor carpark. Throughout this thesis, the term GPS-denied environment will be defined as an environment with poor or no GPS signal and GPS-aided environment refers to the one with good reception of GPS signal.

At the same time, by targeting environment such as carpark, university campus, the average movement speed of vehicles is expected to be around 3m/s (Belloche 2015). This is due to the nature of these environments conditions as well as speed regulation applied. In fact, in recent demonstrations of companies like Audi, BMW, etc. for autonomous carpark navigation systems, vehicles are operated at around 10km/h. Understanding the vehicle's dynamics in the localization problem will help to accurately identify advantages/ disadvantages of different positioning methods.

There are two levels of localization: global localization and local localization. In global localization, the vehicle will be localized within World Geodetic Coordinate System ("World Geodetic System (WGS84) - GIS Geography" 2018). This is the coordinate system used by global positioning systems such as GPS, GLONASS, and GALILEO etc. The coordinate system gives a global, absolute pose for different local coordinates to refer to. It is also useful in extracting semantic information of the surrounding environment. Figure 1.3 provides a general definition of the latest standard WGS84 for World Geodetic System. In this level of localization,

the main objectives are to offer semantic data as well as a global reference frame thus localization accuracy is not necessary to be in centimetres. On the other hand, local localization refers to a local coordinate localization where accuracy level is supposed to be high. This level of localization is responsible for accurate navigation and real-time obstacle avoidance. In intelligent vehicles navigation, both levels of localization are required to accomplish the task of navigation in different environment setups.

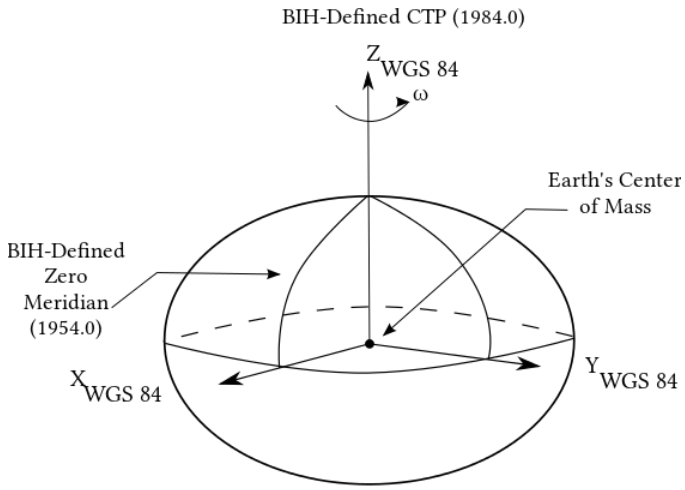

Figure 1.3 World Geodetic Coordinate System WGS84 (Malys et al. 2015)

With multiple sensors running on different local coordinates, it is critical to have a global frame to express those sensors outputs together. In the GPS-denied environment, the lack of GPS signal not only omits the essential global coordinate reference but also introduces a significant gap in the transition phase between GPS-aided and GPS-denied environments. This thesis aims to provide a global localization level method for GPS-denied environment. The proposed solution should be able to replicate GPS signal behaviour for the indoor environment.

Also, a fusion framework is proposed so that other local localization techniques can be fused into the global frame. This allows the system to achieve both local and global levels of localization. In addition, this framework should be generic that it could be potentially applied for both GPS-aided and GPS-denied environments thus allows seamless navigation transition between these two environments.

With respect to the primary target of carpark environment, the system must comply with the following requirements:

- Availability: The system should be easily deployable on existing infrastructure of a carpark with limited requirements of changes in structures, hardware or software.
- Scalability: The system should be extensible and scalable in large scale.

- Universality: there should be no specific hardware/ firmware changes other than off-shelf devices. This removes the need for dedicated sensors to be mounted in different carparks in order for the system to work.
- Accuracy: While ideally the system should be accurate in order of centimetres, in terms of global localization for carpark situation, it is not necessary to be so. Methods such as Laser-SLAM (Simultaneous Localization and Mapping) or vision based localization can deal well with local accuracy. Still, the system accuracy should be able to identify vehicle positioning within a parking plot. According to French standard "Norme NF P 91-100" ("Norme Francaise, Parcs de Stationnement a Usage Privatif" 1996), the minimum width for a parking spot is 1.80m. This should be the upper bound of the system accuracy. The final fusion localization system in this thesis is expected to be within 0.5m of mean localization error. Ideally, the localization error of a fully autonomous vehicle is under 0.2m (Ziegler et al. 2014).

1.3 Main Contributions

The thesis has two main contributions. First, a novel Wi-Fi Ensemble Fingerprinting Localization System (WEFLS) for GPS-denied environment to replace the need of GPS signal. Second, a framework for the fusion of multiple localization methods such as: GPS based, IMU based, WEFLS based, laser-SLAM based.

There are currently no de facto standards for GPS-denied environment positioning systems design as a global solution similar to the one used in the GPS-aided environment (e.g. GPS, GLONASS, etc.). Regarding intelligent vehicle navigation in the carpark, several solutions are proposed including: laser-SLAM with static map matching (Wahl et al. 2015), Embedded LIDAR sensors in the environment (Ibisch et al. 2013), 3D map matching using vision sensors (Bojja et al. 2013) or detection of parking lot using vision sensors (Houben et al. 2013) etc. While these studies may allow up to 10cm of localization precision, they also come with high cost or requirements such as: costly setup of sensors, complex environment map required, and no global coordinate transformation addressed. An in-depth review of these studies will be presented in chapter 2.

First, this thesis will present a novel method for GPS-denied environment localization using wireless sensors networks, more specifically a Wi-Fi fingerprinting localization system. The method makes use of existing Wi-Fi infrastructure (Wi-Fi Access Points – APs, Wi-Fi receiver) to determine the target position based on an offline mapping phase. The main argument of this

method is that the combination of Wi-Fi signal strengths from multiple static APs in the environment for one position is unique. By learning these unique features for several key positions in the environment, one can estimate its location just by scanning Wi-Fi signals strengths.

Although Wi-Fi fingerprinting localization system is already a popular approach for indoor localization, so far it only targets pedestrian walking speed. The advantages of this method are its availability, scalability and universal characteristics where off the shelf hardware like Wi-Fi receivers and Wi-Fi access points are used without any modification. These sensors are also expected to be widely available nowadays in urban area. One main concern of this method is the low sampling frequency of Wi-Fi scan. In general, the time to complete a scan of Wi-Fi signals in a particular environment is around 1 second (1Hz). At 1.0 to 1.6m/s of human walking speed (Harkema, Behrman, and Barbeau 2012), this sampling frequency is adequate to deliver real-time localization results. However, as the thesis aims to target intelligent vehicles in the carpark at 3m/s, the classic approach of the Wi-Fi fingerprinting method is insufficient. Thus, an original approach using ensemble neural network on Wi-Fi fingerprinting method is proposed in this thesis.

Secondly, a complete localization solution must be a fusion of multiple techniques. This allows global as well as local levels of localization to function together. At the same time, having redundancy in the system boosts accuracy and reliability. In this thesis, a flexible fusion framework for multiple localization sensors is proposed. This fusion framework will not only deal with the GPS-denied environment but could be potentially used in the GPS-aided environment and provide a smooth transition between the two areas.

1.4 Thesis Overview

Following this introduction, the thesis has 5 more chapters presented as follows:

- Chapter 2: A brief overview of intelligent vehicles localization, particularly, localization in the GPS-denied environment. The two categories of localization methods: absolute localization and relative localization are reviewed and discussed.
- Chapter 3: A summary of Wireless Sensors Networks and its strategies for localization. Two main strategies of this approach are range-based and range-free localization. This chapter will provide discussion to highlight the motivation of using WSNs in intelligent localization for GPS-denied environment.

- Chapter 4: The core algorithm of the preferred WSNs localization strategy is presented. The Wi-Fi fingerprinting localization method is introduced with critical improvement to adapt to intelligent vehicle dynamics.
- Chapter 5: To enhance localization accuracy as well as frequency, a data fusion model is proposed using Gaussian Mixture Model and Particle Filter. This strategy is also capable of providing a smooth transition from the GPS-aided environment to GPS-denied environment. The model is then verified by fusing Wi-Fi Fingerprinting localization with IMU and PML-SLAM.
- Chapter 6: A conclusion of the thesis. It also highlights possible future work for this thesis and discusses multiple perspectives regarding the results obtained.

2. INTELLIGENT VEHICLES LOCALIZATION

Résumé

Dans ce chapitre, quelques techniques générales pour la localisation de véhicules intelligents sont examinées. En outre, une étude des solutions existantes pour la localisation de véhicules intelligents dans des environnements sans GPS est présentée.

En général, les techniques de localisation IV peuvent être divisées en deux catégories: la localisation globale et la localisation locale. Souvent, la catégorie de localisation globale est une méthode de localisation basée sur GNSS. Ces méthodes utilisent les signaux satellites pour déterminer les informations de position 3D du récepteur dans une référence globale (telle que WGS84). Le terme GPS fait référence au système de positionnement global qui est régi par les États-Unis d'Amérique. Il existe d'autres systèmes mondiaux de navigation par satellite (GNSS) tels que GLONASS (Russie), Galileo (Europe) et Beidou (Chine). Pour simplifier le problème, la thèse se concentrera sur les performances du GPS en tant que représentant d'autres GNSS. Le principe de calcul de la position du récepteur est basé sur la connaissance des positions des satellites, puis sur la déduction des «pseudo-distances» respectives entre ces satellites et le récepteur, comme illustré à la figure 2.2. Ici, le terme "pseudo-distance" se réfère à la distance calculée entre les satellites et le récepteur mobile. Étant donné que les satellites se déplacent constamment, cette distance n’est pas une valeur fixe. Pour calculer la position 3D d'un récepteur, il faut au moins quatre satellites. Vous trouverez un aperçu du système GPS dans (Hofmann-Wellenhof, Lichtenegger et Wasle 2018).

Il existe deux niveaux de services GPS, à savoir le service de positionnement standard (SPS) et le service de positionnement précis (PPS). Alors que SPS est accessible aux utilisateurs publics, les PPS de haute précision ne sont accessibles qu'aux utilisateurs autorisés (personnel militaire,

agents de l'État). Le tableau 1 et le tableau 2 récapitulent les performances SPS et PPS. En général, SPS fournit une erreur de localisation maximale de 7,8 m dans 95% des cas, et le système PPS offre une meilleure précision avec une erreur de localisation maximale de 5,9 m dans 95% des heures. temps. En outre, la précision verticale devrait être inférieure à la précision horizontale dans toutes les mesures GPS. Dans le meilleur des cas, une solution DGPS de haute précision appelée GPS cinématique en temps réel (RTK GPS) peut offrir une précision de quelques centimètres. Cependant, le procédé nécessite des stations de base dédiées, des capteurs, des signaux GPS continus et un prix excessif pour le déploiement et la maintenance. Cela rend le RTK non adapté à la plupart des applications urbaines («Real Time Kinematics - Navipedia» 2018).

À l'instar des États-Unis, l'Union européenne a également mis au point un système de positionnement global appelé Galileo, destiné à fournir un système de positionnement global indépendant de haute précision aux pays européens. Le système est censé aider les pays de l'UE à ne pas compter sur le chinois BeiDou, le russe GLONASS ou, plus important encore, sur le GPS américain. Dans de bonnes conditions, telles que des satellites pleinement fonctionnels (jusqu'à 30 unités), une vision claire du récepteur aux satellites, etc., le libre accès libre pour la navigation du système Galileo à la frontière de l'UE devrait être d'environ 4 mètres de précision («Galileo Introduction générale - Navipedia "2018). Le GLONASS développé par la Russie dans les années 1980 est un autre système qui mérite d'être mentionné. En 2010, le GLONASS couvrait l'ensemble du territoire russe, puis après octobre 2011, la couverture mondiale est atteinte. L'évolution de la précision de positionnement du GLONASS est illustrée à la figure 2.5. Jusqu'à présent, sous un ciel statique, la précision du GLONASS pour l'accès public était de 2,8 mètres. Vous trouverez une comparaison rapide des différents systèmes de localisation globale dans le tableau 3.

Une méthode de localisation locale notable est la localisation au laser. En utilisant une technique de télémètre basée sur les rayons laser, le capteur estime avec précision la distance aux autres objets de l'environnement. Le LiDAR (James Eddy 2017) (détection de la lumière et télémétrie) est une forme importante de capteur laser qui déclenche des faisceaux laser en continu dans l'environnement. Cela aide à estimer la distance aux obstacles environnants et permet de cartographier l'environnement à haute résolution. Lorsqu'il s'agit de capteur laser, la majorité de ses algorithmes de localisation impliquent la résolution totale ou partielle d'un problème de localisation et de cartographie simultanées (Smith et Cheeseman 2018), (Durrant-Whyte et Bailey 2006), (Dellaert et al. 2018) . L'objectif du SLAM est d'estimer la trajectoire

du véhicule (ou de le poser en mode SLAM en ligne) et en même temps de cartographier l'environnement voisin à partir des entrées des capteurs du véhicule. Une représentation graphique du problème SLAM complet et du problème SLAM en ligne est présentée aux figures 2.6a et 2.6b, respectivement. Dans le problème du SLAM complet, l'algorithme est supposé estimer la trajectoire entière du véhicule, formulée par une liste de ses poses sur le pas de temps k: x_k avec des capteurs lisant z_k, une entrée de commande u_k et construisant en même temps la carte m environnement. Cette tâche exigeante devient de plus en plus complexe avec le temps et il est difficile d'être gérée en temps réel. L'idée du SLAM en ligne, censé être fait en temps réel, est ensuite introduite. Le SLAM en ligne estimera uniquement la pose du véhicule actuel, ce qui réduira efficacement la complexité du problème. Vous trouverez un aperçu de la tendance actuelle du SLAM dans (Bresson et al. 2017). Compte tenu de la précision des capteurs laser et du potentiel du SLAM, la combinaison de LiDAR-SLAM devient rapidement l'une des clés pour des véhicules totalement autonomes. Au fil des ans, les techniques d'estimation dans SLAM peuvent être classées en approches basées sur les filtres et en approches basées sur l'optimisation.

L'idée de base des approches basées sur les filtres provient du filtrage bayésien et comprend deux étapes: la prévision et l'observation. Lors de la première étape, une prédiction de la pose et de la carte du véhicule est effectuée à l'aide d'un modèle dynamique des véhicules. Le modèle pour faire correspondre une observation à la carte s'appelle un modèle d'observation. Les deux branches principales de cette approche sont les filtres étendus de Kalman et les filtres à particules SLAM.

Le SLAM basé sur l'optimisation (M. Liu et al. 2012) est également un algorithme en deux étapes itératives. La première étape identifie les contraintes du problème en fonction des données du capteur. Cela se fait en faisant correspondre les nouvelles observations à la carte. La deuxième étape calcule la pose du véhicule et la carte en fonction des contraintes identifiées. Les techniques basées sur la vision pour SLAM sont plus susceptibles d'utiliser cette approche, les techniques basées sur le laser sont également incluses dans la classe d'algorithme Graph-SLAM.

Une autre approche notable pour la localisation de véhicules est la technique basée sur des capteurs visuels. En utilisant un système de vision et des algorithmes de traitement d'image, un véhicule peut se localiser correctement dans un environnement pré-mappé. Cette approche est sensible aux conditions d'éclairage, ce qui en fait un candidat idéal pour la localisation à l'intérieur. La plupart des approches de localisation basées sur des caméras s'inscrivent dans des

types de méthodes basées sur l'appariement de cartes. Dans ces approches, une carte détaillée de l'environnement est construite dans une phase hors ligne. Sur la base de l'entrée de caméra de phase en ligne et de la carte hors ligne, l'emplacement du véhicule est calculé. Semblable au laser SLAM, le SLAM visuel est une approche populaire pour la localisation de véhicules intelligents. Le concept SLAM reste le même que dans le SLAM laser, mais dans ce cas, un ensemble de caméras est monté sur le véhicule pour capturer non seulement des images mais également pour mesurer la profondeur de la scène.

Le calcul à mort est un processus d'estimation de la pose actuelle d'un véhicule à l'aide d'une pose préalablement déterminée et du modèle dynamique du véhicule. À l'origine, il s'agissait d'une approche développée pour les applications marines et qui est maintenant utilisée dans divers domaines tels que la navigation aérienne, le suivi des piétons ou la navigation autonome par robot. L'algorithme de calcul à rebours utilise différentes configurations de capteurs. Le calcul à mort avec unités de mesure inertielle (IMU) est largement utilisé dans la navigation de véhicules spatiaux, de navires de mer ou de véhicules terrestres. IMU a généralement des gyroscopes à trois axes et des accélérateurs pour mesurer la vitesse angulaire et la vitesse de déplacement de l'objet attaché.

L'un des inconvénients du GPS est sa disponibilité dans les scénarios urbains. Le plus souvent, les signaux GPS sont perdus ou mal reçus dans un tunnel, un parking ou lorsque le récepteur est entouré de bâtiments, obstruant ainsi la visibilité directe des satellites. Les signaux GPS standard souffrent également de l'effet de trajets multiples qui pourrait entraîner une erreur de localisation supplémentaire de 8 m (Kos, Markezic et Pokrajcic 2010). Néanmoins, le GPS (et les autres GNSS) joue un rôle essentiel dans la localisation, en particulier à l'échelle mondiale, car il s'agit du seul système de positionnement qui affiche directement dans le repère global. Sans ces coordonnées de référence globales, chaque véhicule intelligent fonctionnera selon ses propres coordonnées locales. Aucune communication ni coopération n'est possible.

Au cours des dernières années, la communauté de recherche sur les véhicules intelligents a développé plusieurs systèmes dédiés à la localisation dans les zones interdites de GPS en général et les parkings en particulier. En raison du manque de signaux GPS, la plupart des solutions de localisation dans ce domaine se situent au niveau de la localisation locale. En fonction du choix du système de coordonnées de référence, ces travaux peuvent être classés en deux classes: méthodes de localisation absolue (ou basées sur une carte) et méthodes de localisation relative (autocentrées, sans carte). Les travaux récents des deux classes seront étudiés dans les sections suivantes.

Dans l'approche du positionnement absolu, il est nécessaire qu'une carte de l'environnement soit connue au préalable par le véhicule. Cette carte comprend deux composants principaux: les objets statiques qui contribuent à la structure de la carte (route, murs, portes, etc.) et les objets dynamiques qui constituent des obstacles dans l'environnement (autres véhicules, piétons, etc. .) Selon la solution, la carte peut contenir les deux ou uniquement des objets statiques.

Contrairement à la localisation absolue, la localisation relative ne nécessite pas une carte détaillée de l'environnement. L'approche vise à estimer la position du véhicule par rapport aux objets locaux environnants tels que les autres véhicules, le marquage des voies, etc.

Parmi ces deux approches, la méthode cartographique semble beaucoup plus précise. Un système bien défini peut localiser des véhicules avec une précision allant jusqu'à 0,1 m. Toutefois, pour ceux qui disposent d'une carte détaillée de l'environnement, la résolution et la précision des informations cartographiques ont une influence considérable sur l'erreur de localisation. Malheureusement, plus la résolution est élevée, plus la solution est complexe et moins évolutive. Ainsi, une nouvelle solution pour ce scénario est requise.

2.1 Overview of Intelligent Vehicles Localization

Localization is a task of determining an object's pose (e.g. coordinate, heading angle) or the spatial relationship among objects. This is an essential task for an autonomous navigation a vehicle has to achieve (Eskandarian 2012). Only by knowing precisely the location of itself in either a local or a global map, then action such as path planning or obstacles avoidance can be carried out. Often, this task is accomplished through a set of dedicated sensors (on vehicle sensors or environment sensors). The process of combining these sensors inputs to infer the vehicle's position is called sensor fusion.

There are two levels of localization for intelligent vehicles: global level and local level. The global level localization often results in the vehicle's pose in the global coordinates frame (e.g. WGS84, NAVD88, ETRS89, etc.) and offers a broad view of vehicle's location and context. The accuracy of this localization level is not required to be in the order of centimetres. Instead, a raw but stable estimation of the vehicle's absolute location is sufficient. One example of this level of localization is GNSS-based localization methods. The local level of localization is usually expressed in an arbitrary local reference coordinate frame. This level of localization is responsible for accurately determining the spatial relationship of the vehicle with other objects in the environment. Some notable methods for this level of localization are laser-SLAM, camera-based map matching, dead-reckoning, etc.

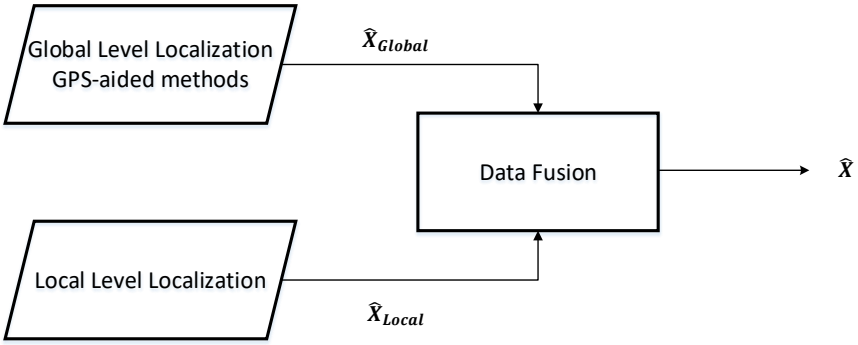

Figure 2.1 Fusion of localization systems

In an ideal intelligent vehicle, a localization system should be a fusion of both levels of localization as in Figure 2.1. The global level of localization returns the estimated pose $\hat{\boldsymbol{X}}_{\boldsymbol{Global}}$ in the global coordinates frame while the local level often output estimation $\hat{\boldsymbol{X}}_{\boldsymbol{Local}}$ in a local coordinates frame. The two estimations are then fused to deliver the final absolute pose of the vehicle. In practice, most localization systems consist of a GPS-like system combined to another local positioning method such as a SLAM based system. The final localization estimation is often expressed in the global coordinate standard.

In this chapter, a quick review of localization methods for intelligent vehicles is presented. Both local and global levels of localization methods are studied and more specifically, those that are dedicated to the GPS-denied environment.

2.2 GPS-based Localization

The GPS-based localization method is a class of localization methods that makes use of satellite signals to determine 3D position information of the receiver in a global reference (such as WGS84). The term GPS refers to Global Positioning System which is governed by the United States of America. There are others Global Navigation Satellite Systems (GNSS) such as GLONASS (Russia), Galileo (Europe), and Beidou (China). To simplify the problem, the thesis will focus on GPS performance as a representative for other GNSSs.

The principle of computing the receiver location is based on knowing the positions of the satellites then deducing the respective “pseudo-ranges” from those satellites to the receiver as in Figure 2.2. Here, the term “pseudo-range” refers to the distance calculated from satellites to the mobile receiver. Since satellites are constantly moving, this distance is not a fixed value. To calculate the 3D position of a receiver, at least four satellites are required. An overview of the GPS system can be found in (Hofmann-Wellenhof, Lichtenegger, and Wasle 2018).

There are two level of GPS services namely Standard Positioning Service (SPS) and Precise Positioning Service (PPS). While SPS is accessible by public users, high precision PPS is only accessible by authorized users (military personnel, government agents). Summary of SPS and PPS performance are shown in Table 1 and Table 2.

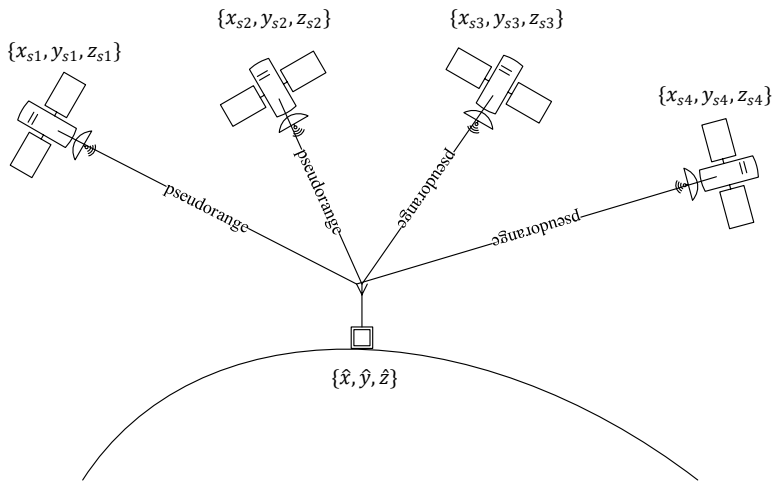

Figure 2.2 GPS principle

Table 1 Service performance standard for SPS (Department Of Defense 2008; "GPS Performances - Navipedia" 2018)

GPS Performance Standard Metric		*SPS User Performance*	*SPS Signal in Space Performance*
Global Accuracy	All-in-View Horizontal 95%	<100 m	< 9 m
	All-in-View Vertical 95%	<156 m	< 15 m
Worst Site Accuracy	All-in-View Horizontal 95%	<100 m	< 17 m
	All-in-View Vertical 95%	<156 m	< 37 m
User Range Error (URE)		N/A	<7.8 m 95% of time
Time Transfer Accuracy		N/A	<40 ns 95% of time
Geometry (PDOP ≤ 6)		> 95.86% global	> 98% global
		> 83.9% worst site	> 88% worst site
Constellation Availability		N/A	>98% Probability of 21 Healthy Satellites

In general, SPS provides 7.8m of maximum localization error in 95% of the time and PPS offers a better accuracy with 5.9m of maximum localization error in 95% of the time. Also, vertical accuracy is expected to be lower than horizontal accuracy in all GPS measurements.

Table 2 Service performance standard for PPS ("GPS Performances - Navipedia" 2018; GPS Directorate 2007)

GPS Performance Standard Metric		*SPS User Performance*	*SPS Signal in Space Performance*
Global Accuracy	All-in-View Horizontal 95%	<36 m	< 13 m
	All-in-View Vertical 95%	<77 m	< 22m
User Range Error (URE)		N/A	<5.9 m 95% of time
Time Transfer Accuracy		N/A	<40 ns 95% of time
Geometry (PDOP ≤ 6)		> 95.7% global	> 98% global
Constellation Availability		N/A	>98% Probability of 21 Healthy Satellites

There are ways to further improve GPS accuracy with a technique called Differential GPS (DGPS). The technique enhances GPS position using an accurately-surveyed position known as the reference station. Nowadays, most commercial GPS units offer DGPS data to some extent using world-wide available reference stations. Depending on the location as well as the distance to a reference station, DGPS accuracy is in the order of 1m (1 sigma) for users ("Differential GNSS - Navipedia" 2018) . The study presented by (Kuter and Kuter 2010) shows that an estimated Root Mean Squared Errors (RMSE) of GPS and DGPS are roughly 6.413m and 2.587m respectively. In the best case scenario, a highly accurate DGPS solution known as Real Time Kinematic GPS (RTK GPS) can deliver up to few centimetres of accuracy. However, the method requires dedicated base stations, sensors, continuous GPS signals and an excessive price for deploying and maintaining. This makes the RTK not suitable for most urban application ("Real Time Kinematics - Navipedia" 2018).

Similar to the US, the European Union also develop a global positioning system called Galileo to provide an independent high precision global positioning system for the European nations. The system is supposed to help the EU countries not to rely on China's BeiDou, Russian GLONASS or more significantly, the United States GPS. Under good conditions such as fully function satellites (up to 30 units), clear vision from receiver to satellites, etc. the free open access for navigation of the Galileo system within the EU border is expected to be around 4 meter of precision ("Galileo General Introduction - Navipedia" 2018). However, the much expected feature of the Galileo system lies in the commercial service. Its architecture is demonstrated in Figure 2.3. With this paid service, the global positioning accuracy is expected to be at decimetres (Ignacio, Irma, and Guillermo 2015). To achieve this level of accuracy, the system will either make use of the Real-time Kinematic concept (RTK) or the precise point positioning (PPP). While the RTK is almost instantly return high precision positioning result,

PPP requires 15-30 minutes of the initialization. Experiments results with the high precision commercial positioning service are shown in Figure 2.4.

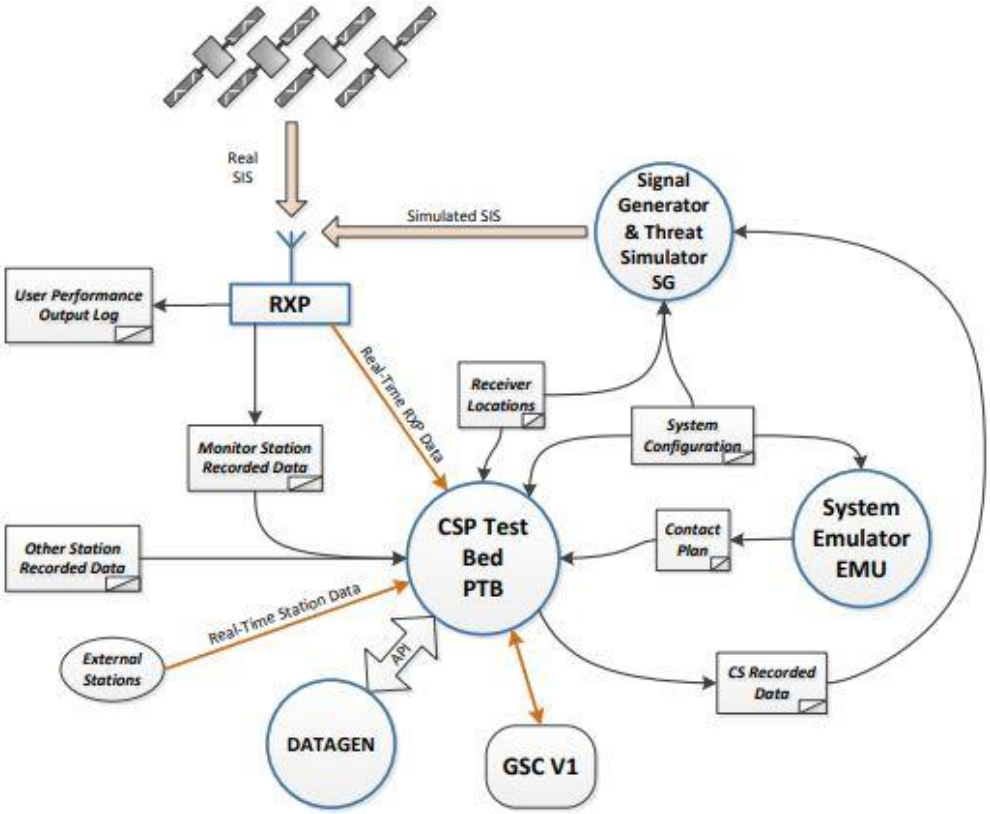

Figure 2.3 The Galileo satellites navigation system commercial service architecture (Fernández-Hernández et al. 2018)

Another worth to mention global positioning system is the GLONASS developed by Russia in 1980s. By 2010, the GLONASS has covered the entire Russia territory then after October 2011, the global coverage is achieved. The evolution of the GLONASS positioning accuracy is shown in Figure 2.5. Up to now, under static sky, the GLONASS accuracy for public access is as good as 2.8 meters.

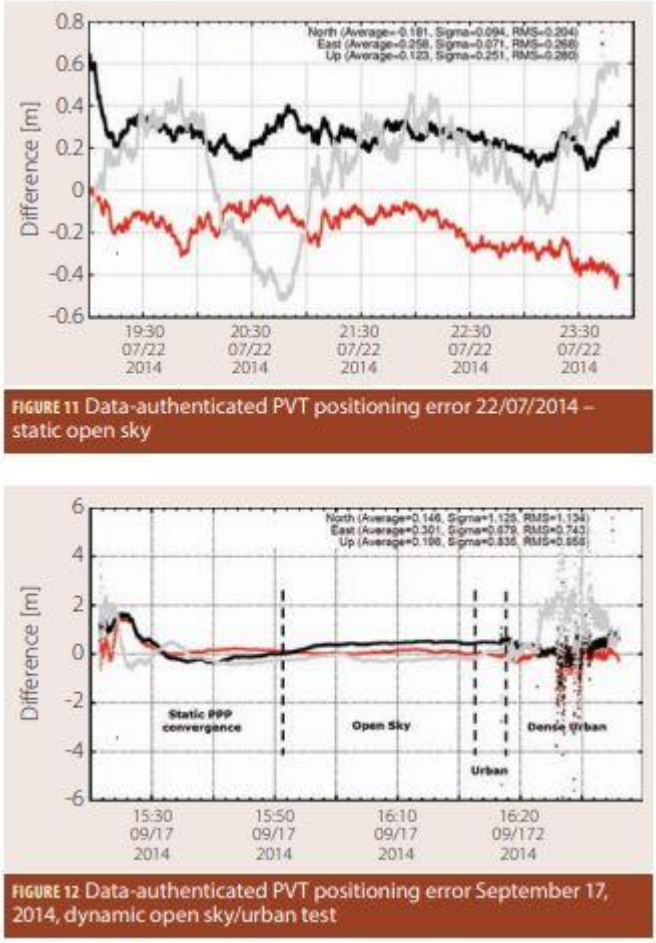

Figure 2.4 The kinematic high precision positioning results of Galileo (Ignacio, Irma, and Guillermo 2015)

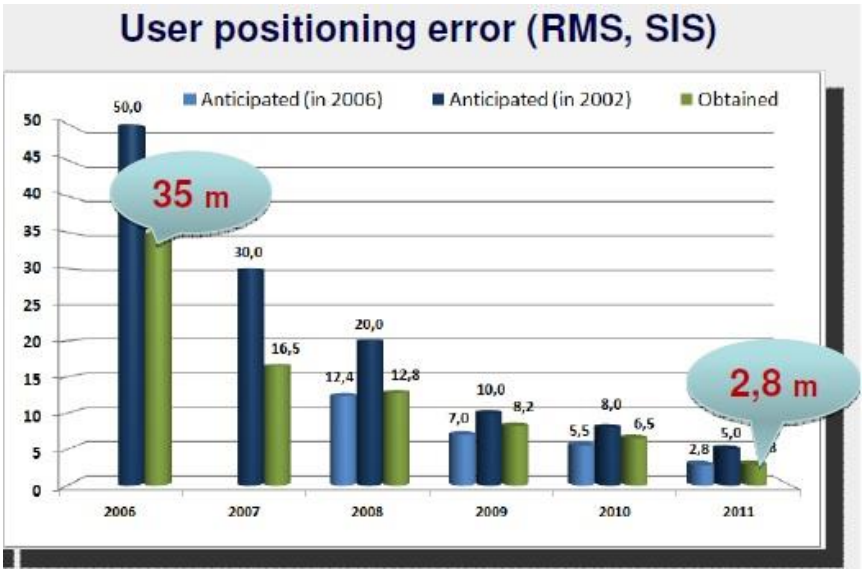

Figure 2.5 The GLONASS accuracy evolution ("GLONASS Performances - Navipedia" 2018)

A quick comparison of different global localization system can be found in Table 3.

Table 3 Comparison between global positioning systems (Hofmann-Wellenhof, Lichtenegger, and Wasle 2018)

System	*BeiDou*	*Galileo*	*GLONASS*	*GPS*
Owner	China	EU	Russia	United States
Coverage	Regional, Global by 2020	Global by 2020	Global	Global
Satellites	5 (+ 30)	24 by design 14 operational	24 by design 24 operational	24 by design 31 operational
Precision	10m Public 0.1m Private	4m Public 0.01m Private	4 – 7m	2- 4m Public 0.01m Private

2.3 Laser-based Localization

Laser-based localization methods are usually assigned to the local localization category. Using a rangefinder technique based on laser beams, the sensor accurately estimates the distance to other objects in the environment. An important form of laser sensor setup is LiDAR (James Eddy 2017) (Light Detection and Ranging) which fires continuously laser beams to the environment. This helps to estimate the distance to surrounding obstacles and allows to perform a mapping of the environment at a high resolution.

When it comes to laser sensor, the majority of its localization algorithms involve solving entirely or partially a Simultaneous Localization and Mapping (SLAM) problem (Smith and Cheeseman 2018), (Durrant-Whyte and Bailey 2006), (Dellaert et al. 2018).The SLAM objective is to estimate the vehicle's trajectory (or pose in online SLAM) and at the same time to map the neighbouring environment given inputs from the vehicle's sensors. A graphical representation of the full SLAM and online SLAM problem is shown in Figure 2.6a and Figure 2.6b respectively.

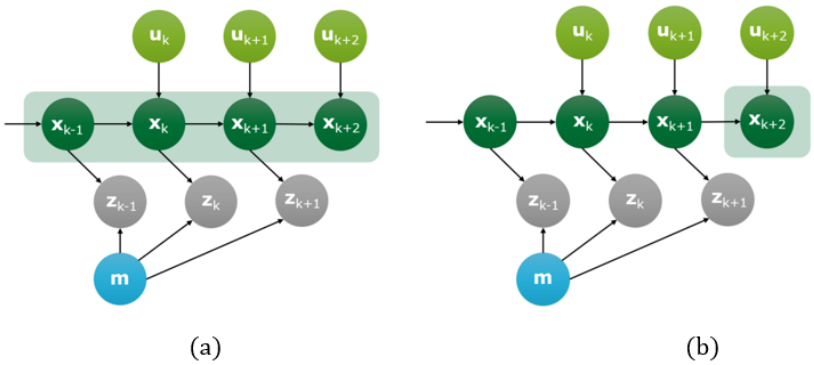

Figure 2.6 Graphical representation of (a) Full SLAM problem; (b) Online SLAM problem (Bresson et al. 2017)

In the full SLAM problem, the algorithm is supposed to estimate the whole trajectory of the vehicle formulated by a list of its poses over time step k: x_k given sensors reading z_k, control input u_k and at the same time building the map m of the environment. This demanding task becomes more and more complex over time and it is difficult to be handled in real time. The idea of online SLAM, which is supposed to be done in real time, is then introduced. Online SLAM will only estimate the current vehicle's pose thus effectively reduce the complexity of the problem. An overview of the current trend in SLAM can be found in (Bresson et al. 2017). Given the accuracy of laser sensors and the potential of SLAM, the combination of LiDAR-SLAM quickly becomes one of the keys towards fully autonomous vehicles. Over the years, the techniques of estimation in SLAM can be categorized into *filter-based* approaches and *optimization-based* approaches.

2.3.1 Filter-based Laser SLAM

The core idea of filter-based approaches comes from Bayesian filtering and consists of two steps: prediction and observation. In the first step, a prediction of the vehicle's pose and map state is made using a dynamic model of the vehicles with control inputs u_k. Having this prediction, a correction is made based on the current observation from sensors inputs z_k. The model to match an observation with the map is called an observation model. Two major branches in this approach are *Extended Kalman Filter* and *Particle Filter* based SLAM.

Extended Kalman Filter (EKF) (Fujii 2018) is a non-linear filter that adds a linearization step for a non-linear model. The linearization is performed around the current estimation state by a first-order of Taylor expansion. The result of this filtering method is converged as long as the linearization process is made around the true state. However, in practice, estimated states can fall well outside of true values uncertainty. This causes consistency issues for EKF-SLAM (Julier and Uhlmann 2001),(Bar-Shalom, Li, and Kirubarajan 2001). Still, with a well-designed estimation model, the EKF-SLAM is proved to be a success in a constrained situation such as urban environments. This makes EFK-SLAM one of the most widely studied solution (Xie et al. 2011; Elfes 2013; Weiss, Schiele, and Dietmayer 2007).

Since EKF-SLAM estimates a vehicle pose based on a map of landmarks, when the number of landmarks increases, the complexity of EFK-SLAM increases exponentially. Thus, FastSLAM is introduced with an idea of using *Particle Filter* as a tool to reduce complexity and consequently allow SLAM to run in real time. In particle filter, two states of the filter are: *Selection* where *N* independent particles are sampled with the same distribution and *Prediction*

where with each particle, a likelihood function is calculated as the score of how likely this particle is the true state. Thus, by limiting the solution space within *N* particles, the complexity of Particle Filter (PF) SLAM is then $O(N\log L)$ where L is number of landmarks in the map. In contrast, the complexity of EKF-SLAM is $O(L^2)$. When the number of landmarks increases, the advantage of PF-SLAM becomes more and more significant. Works in (Hahnel et al. 2018; Mohan and MadhavaKrishna 2010; Montemerlo et al. 2018) demonstrates FastSLAM approach which can work in a large scale environment and (Reineking and Clemens 2013; Trehard et al. 2014) implements FastSLAM using evidential theory instead of a classical probabilistic model. Results of the approach using evidential SLAM and particle filter is shown in Figure 2.7.

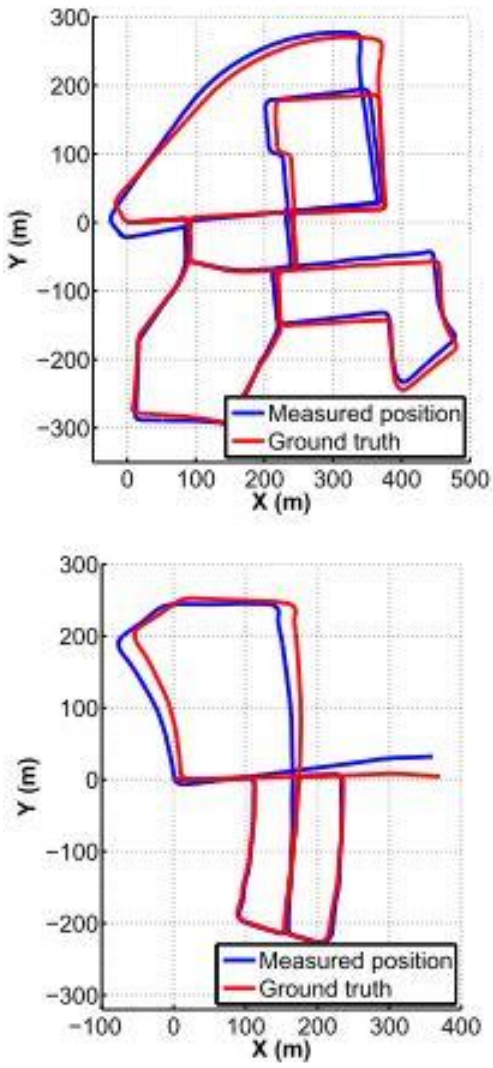

Figure 2.7 Particle Filter based Evidential SLAM (Trehard et al. 2014)

2.3.2 Optimization-based Laser SLAM

Optimization-based SLAM (M. Liu et al. 2012) is also a two iterative steps algorithm. The first step identifies constraints of the problem based on sensor data. This is done by matching between new observations and the map. The second step computes the vehicle pose and the map given the identified constraints. Vision-based techniques for SLAM are more likely to use this approach, laser-based techniques are also included within Graph-SLAM algorithm class.

Graph-SLAM is a graphical representation of Bayesian SLAM. Based on this representation, a matrix of the relationship between landmarks and vehicles' poses can be built and act as an optimization framework. An example of Graph-SLAM can be found in (Pierzchała, Giguère, and Astrup 2018) where a combination of Velodyne VLP 16, GPS, IMU and Stereo Camera are used to solve SLAM problem in a large scale of a forest. The map resulted from this work were evaluated using the relative distance between trees which is around 2.38cm of error (Figure 2.8).

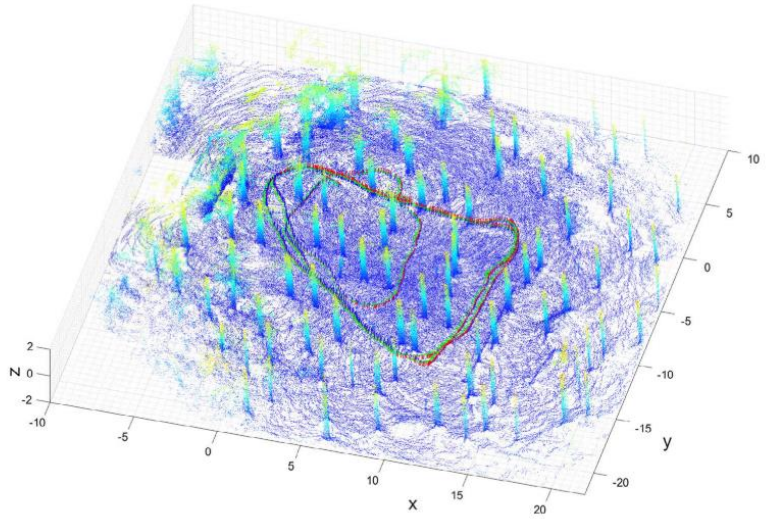

Figure 2.8 GraphSLAM visualization of large scale forest mapping (Pierzchała, Giguère, and Astrup 2018)

Another work is mentioned in (Carlson, Thorpe, and Browning 2010) where an attempt to map a large scale urban environment using SLAM and GPS reference is made. Demonstrated results are in Figure 2.9.

Figure 2.9 GPS-aided SLAM for large scale uban mapping (Carlson, Thorpe, and Browning 2010)

While promising results were shown in studies for this method, it is worth to mention that without absolute correction such as GPS, camera-based landmark detection or a pre-defined map, it is not possible for SLAM to achieve this high precision in mapping and localization.

2.4 Vision-based Localization

Another notable approach for vehicle localization is visual sensors based technique. Using a vision system and image processing algorithms, a vehicle can correctly localize itself within a pre-mapped environment. This approach is sensitive to lighting conditions making it a suitable candidate for indoor localization.

Most of camera-based localization approaches fall into map-matching based method types. In these approaches, a detailed map of the environment is built in an offline phase. Based on online phase camera input and the offline map, the location of the vehicle is calculated. The study in (Borges et al. 2010) shows a combination of laser-edged map and vision images matching method for industrial vehicles. The system first needs an edge-filtered map of the environment from a 3D point cloud of laser sensors in the offline phase as showed in Figure 2.10. It then processes to detect edge in online phase camera input for map-matching and consequently vehicle localizing. (Figure 2.11). Depending on weather and lighting conditions, the solution reaches an average localization accuracy of 0.875m for the best scenarios and 1.390m for the worst.

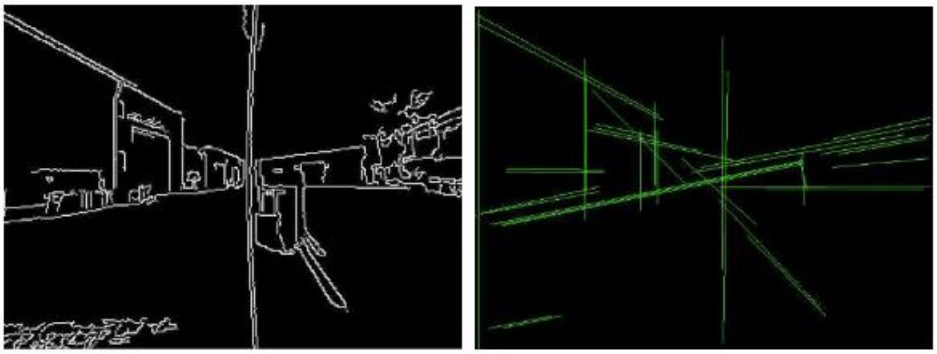

(a) Original edge-filtered image. (b) Edge-filtered image after straight line detection via Hough transform.

Figure 2.10 Edge-filtered map of the environment (Borges et al. 2010)

(a) Fish-eye image. (b) Image after undistortion, overlaid with edge model (in green). (c) Edge image after undistortion, overlaid with edge model (in green).

Figure 2.11 Camera image to edge image transformation (Borges et al. 2010)

Similar to Laser SLAM, visual SLAM is a popular approach for intelligent vehicles localization. The SLAM concept remains the same as in the laser SLAM but in this case a set of cameras is mounted on the vehicle to capture not only images but also to measure the depth of the scene. An interesting research work proposed by (Shi et al. 2012) consists of a fusion of GPS and aided visual SLAM methods, which does not use any additional sensor. The system however consists of six calibrated fish eyes cameras with a dual-frequency GPS receiver. In an offline mapping phase, the GPS observation is supported by CORS RTK technology which has an accuracy within 0.02m. Based on this map, the online localization method yields an accurate position with an average error under 0.067m. Note that this paper uses only 8 checkpoints as an evaluation ground truth and no lighting condition is mentioned.

2.5 Dead-Reckoning

Dead-reckoning is a process of estimating the current pose of a vehicle using a previously determined pose and the vehicle's dynamic model. Initially, it was an approach developed for

marine applications and has now been used in a variety of fields such as air navigation, pedestrian tracking or autonomous robot navigation.

The dead-reckoning algorithm makes use of different sensor configurations. Dead-reckoning with Inertial Measurement Units (IMU) is widely used in the navigation of spacecraft, marine ships or landline vehicles. IMU typically has three-axis gyroscopes and accelerators to measure angular and displacement velocity of the attached object.

Depending on the precision of sensors inside the IMU (gyroscopes and accelerators), the dead-reckoning can incrementally estimate the local pose of the vehicle using a pre-defined dynamic model. This, however, results in the accumulated error over time as inaccuracy in each measurement adds up. It is almost impossible to correct this error by the system itself as there is no absolute reference source. An attempt to fix this problem using dual drive system and modelling of expected accumulated error is found in (Borenstein 1995), yet the result is limited. Consequently, almost all dead-reckoning solutions are now used in fusion with other localization techniques such as GPS (Fouque et al. 2008), laser-SLAM (Akai et al. 2017) or vision-based (Vivacqua et al. 2018). The idea is to incorporate an absolute reference to regularly correct the accumulated error results from the dead-reckoning process. An example of a solution to correct dead-reckoning using static map can be found in (Fouque et al. 2008). The result of this solution is shown in Figure 2.12. It can be seen in the figure that even with correction from static map and some GPS injection, the dead-reckoning still has a large accumulated error over time (around 22m).

In conclusion, the general accuracy estimation of this method is large. It heavily depends on the precision of IMU components, the dynamic model of the vehicle as well as any possible correction applied. A carefully designed dead-reckoning process using high precision sensors could be extremely accurate in a close range. This makes dead-reckoning a preferable solution for indoor localization (Z. Liu et al. 2017; Huijie Chen, Li, and Wang 2018).

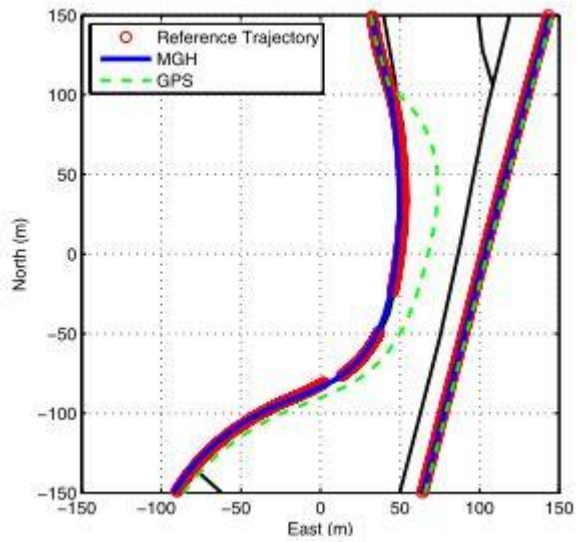

Figure 2.12 Dead-reckoning and static map (Fouque et al. 2008)

2.6 Intelligent Vehicles Localization in GPS-denied Environments

One of the drawbacks of GPS is its availability in urban scenarios. More often, GPS signals are lost or poorly received in a tunnel, a carpark or when the receiver is surrounded by buildings thus obstructs line-of-sight to satellites. The standard GPS signals also suffer from the multi-path effect which could result in additional 8m of error in localization (Kos, Markezic, and Pokrajcic 2010). Still, GPS (and other GNSSs) plays a vital role in localization especially at the global scale as it is the only positioning system that directly outputs in the global coordinate frame. Without this global reference coordinates, each intelligent vehicle will work on its own local coordinates hence no communication or cooperation is possible.

In the last few years, the research community in Intelligent Vehicles has been developing several dedicated systems for localization in GPS-denied areas in general and carparks in particular. Due to the lack of GPS signals, most of the solutions for localization in this domain fall into the local localization level. Depending on the choice of the reference coordinate system, these works can be categorized into two classes: absolute localization (or map-based) methods and relative localization (self-centric, without a map) methods. The two classes' recent works will be studied in the following sections.

2.6.1 Absolute Localization

In the absolute positioning approach, it is required that a map of the environment is known beforehand by the vehicle. In this map, there are two main components: static objects which contribute to the structure of the map (e.g. road, walls, doors, etc.), and dynamic objects which

are moving obstacles in the environment (e.g. other vehicles, pedestrian, etc.). Depending on the solution, the map may contain both or just static objects.

A FastSLAM approach can be found in (Wahl et al. 2015) where a *Rao-Blackwellized* particle filter laser-SLAM is implemented. As described in Section 2.3, a full SLAM can be stated as in Eq.2.1, given x_t the vehicle's state at time t, m is the map built in SLAM process, z_t sensors reading at t and u_t is control inputs. In this solution, the static map (i.e. map with only static objects) of the environment is included and denoted as s. Thus, the full SLAM problem with a static map can be formulized as in Eq. 2.2.

$$p(x_{1:t}|z_{1:t}, u_{1:t}) \qquad 2.1$$

$$p(x_{1:t}, m|s, z_{1:t}, u_{1:t}) \qquad 2.2$$

Consequently, the graphical model of SLAM can now be represented as in Figure 2.13. Notice that the static map only influences the SLAM map directly.

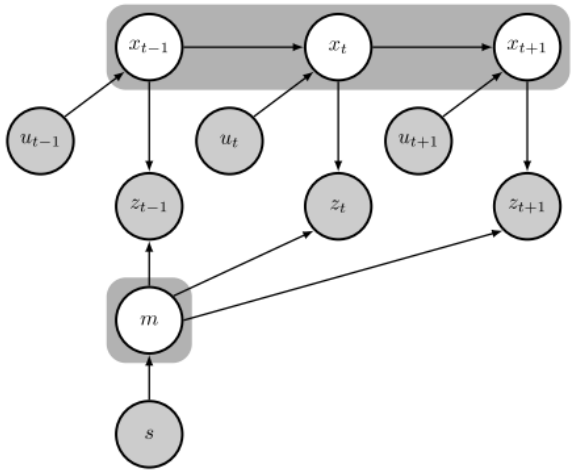

Figure 2.13 Graphical representation of SLAM with a static map (Wahl et al. 2015)

By adding static map s to classical SLAM, the posterior over maps can be computed using products of all cells (given an occupancy grid representation of map is selected) as show in Eq.2.3.

$$p(m|z_{1:t}, u_{1:t}, x_{1:t}, s) = \prod_i p(m_i|z_{1:t}, u_{1:t}, x_{1:t}, s_i) \qquad 2.3$$

Using information from a static map, the posterior of each cell can be estimated in Eq. 2.4.

$$p(m_i|z_{1:t}, u_{1:t}, x_{1:t}, s_i) = \begin{cases} 1, & s_i \ occupied \\ p(m_i|z_{1:t}, u_{1:t}, x_{1:t}), & s_i \ unknown \end{cases} \qquad 2.4$$

Given a static map with a resolution of 0.125m each cell, a parking garage of 80 $\times$ 35m is tested in this paper. A 0.19m in position error and 2.3°in orientation error are reported. This

solution, however, encountered issues with dynamic objects that obstruct the view to static map components and scalability potential since a high-resolution static map is required as it directly influences position error estimation.

A similar solution of laser-based FastSLAM can be found in (Groh et al. 2014). In this solution, a static map of static (e.g. walls, doors, column, etc.) and semi-static objects (objects that are supposed to be static for a short period of time e.g. parked car). The posterior of each cell in the map is then calculated as in Eq.2.5 follows:

$$p(m_i|z_{1:t}, u_{1:t}, x_{1:t}, s_i) = \begin{cases} 1, & s_i\ occupied \\ p(semin - static), & s_i\ unknown \\ p(m_i|z_{1:t}, u_{1:t}, x_{1:t}), & s_i\ others \end{cases} \qquad 2.5$$

This solution is tested with a 0.05m resolution map and returns a 0.33m of position error as well as 1.03° of orientation error. Despite a marked improvement in the orientation error compared to the previous study, this solution requires higher map resolution but shows a higher position error.

Instead of having LiDAR sensors **on vehicles**, a study in (Ibisch et al. 2013) adds LiDAR sensors **to the environment** in order to correctly track the vehicle inside a carpark. There are two phases: a training phase and an online tracking phase.

In the training phase, each LiDAR sensor will be trained with an obstacle-free environment and match with a 2D map.

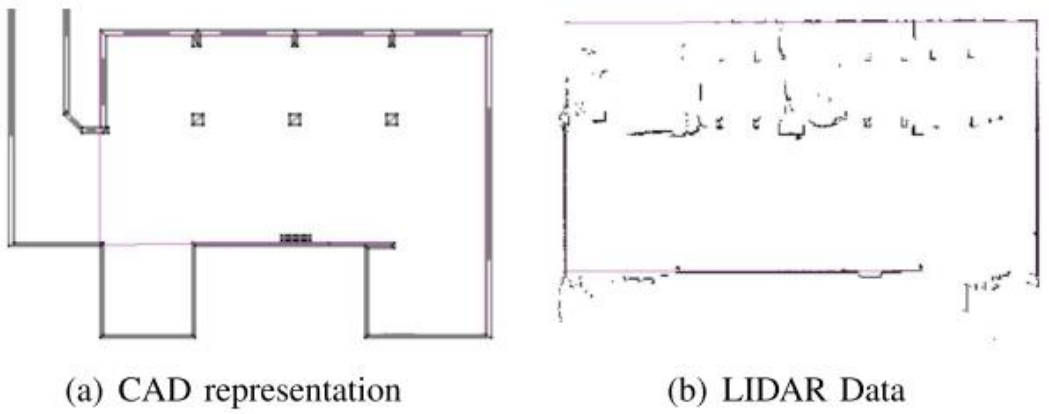

Figure 2.14 2D map and LiDAR reading of the obstacle-free environment (Ibisch et al. 2013)

This training phase helps to isolate moving vehicles from the environment along with avoiding duplication of tracking from multiple LiDARs. Having this trained phase, in online tracking phase, an extended Kalman Filter with a physical motion model is employed. This localization

system returns a 0.121m of combined position and orientation error. Although the system achieves a significant accuracy in localization, it is however expensive for large scale deployment as well as a potential difficulty in vehicle tracking in a crowded environment.

A dead-reckoning based map matching method for carpark is presented in (Bojja et al. 2013). The system flowchart is illustrated in Figure 2.16. The core idea of this paper is to use a detailed 3D structural map of the environment and process map-matching with particle filter and collision detection. The collision detection in this context is defined as the intersection/ overlapping of a particle (corresponding to a vehicle's possible position) with the 3D structure of the garage thus effectively results in the weight of each particle. The resulting localization is limited to 1.5m of accuracy partially due to inaccurate 3D mapping and dead-reckoning sensors' noise.

Research in (Schwesinger et al. 2016) demonstrates a fully autonomous vehicle in carpark. The vehicle is equipped with four monocular fisheye cameras, two stereo cameras and stock ultrasonic sensors (Figure 2.15). The method has an offline 3D mapping phase using cameras sensors for the entire environment and an online visual localization using grid map and map matching using both thresholds of the distance in image-space and the descriptor distance. In addition, a semantic mapping of the environment is required. This includes: a road-map graph which gives details about positions of lanes, way direction and intersections; the location of parking spaces; the speed profile allowed in the carpark. The system is tested and successfully automatically parked a vehicle within 0.1m of lateral and 0.15m of longitudinal localization accuracy.

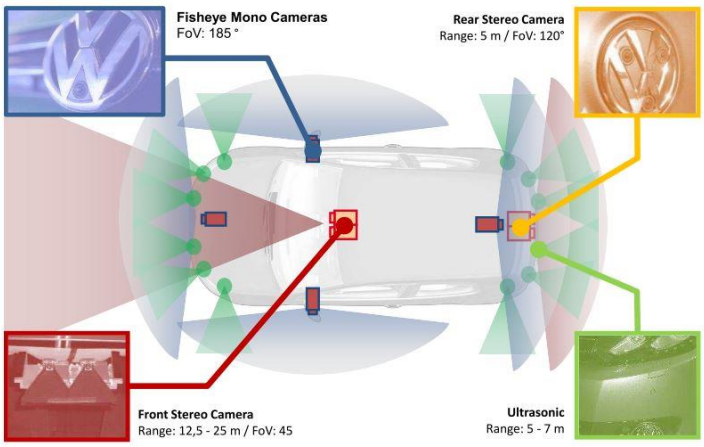

Figure 2.15 Sensor setup for camera-based carpark localization (Schwesinger et al. 2016)

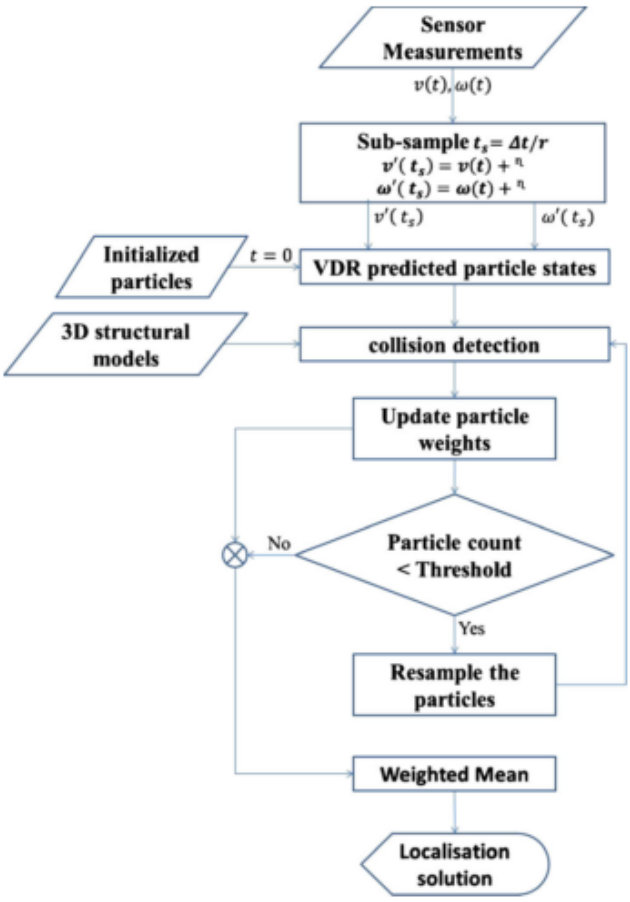

Figure 2.16 Flow chart of 3D map-matching based on particle filter (Bojja et al. 2013)

2.6.2 Relative Localization

In contrast to absolute localization, relative localization does not require an extensive map of the environment. The approach aims to estimate the vehicle position relative to its surrounding local objects such as other vehicles, lane marking, etc.

A free parking slot searching strategy using four fisheye cameras are shown in (Houben et al. 2013). Although the method focuses on detecting free parking lots, it also highlights the technique of localizing vehicles relatively to others objects. A general scheme is illustrated in Figure 2.17 where blue dotted lines show camera cover range and green stars mark parking lots spaces.

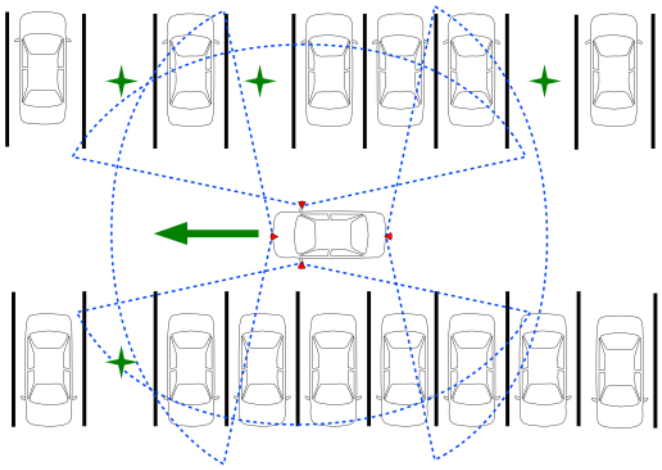

Figure 2.17 Fisheye-based parking lot searching (Houben et al. 2013)

Using pre-learned parking lot markings information such as standard width, parking lot structure as well as a database of training images for occupancy parking lots, the algorithm successfully locates the vehicle position relative to parking lots within 0.25m of accuracy.

An attempt of a relatively localizing vehicle using an inter-vehicular network is discussed in (Drawil and Basir 2010). This work uses radio ranging sensors (e.g. ultrasonic, radar, etc.) to estimate the distance to surrounding vehicles and share this information with other vehicles in the same cluster. Based on this one-hop information, each vehicle tries to create a map of the relative positions of its neighbours. This map then allows vehicles to avoid collisions and travel within its local frame. The reported root-mean-squared error is around 3m.

Inter-vehicular network between GPS-aided and GPS-denied area vehicles is studied in (De Ponte Müller, Diaz, and Rashdan 2017). This study introduces a novel way of communicating with a relative location between GPS-aided and GPS-denied area vehicles. By exchanging not only location but also Road Infrastructure Objects (RIOs), the network of vehicles has successfully improved localization of each compared to standard GPS accuracy. While this approach does not require a detailed map of the environment, it does require that the precise locations of RIOs are known. The estimated accuracy of this method is roughly 2.5m given a dense distribution of RIOs and other vehicles.

2.7 Discussion

Although more and more researches are covering the scenario of GPS-denied environment, there is yet no answer for a globally accepted solution for this scenario. More importantly, there is not yet a standard for the localization in such specific environments.

In every demanding system, the trade-off between accuracy and complexity is almost guaranteed to happen. A high accuracy level system can only be achieved with a dedicated and sophisticated scheme. The optimized solution for this compromise depends heavily on practical conditions. This also holds true for the localization issue, more specifically the GPS-denied environment localization problem.

In general, a global localization system can be as accurate as centimetre level of error. The RTK-GPS is a perfect example of this. However, the requirements of continuous GPS signals and availability of reference stations are never reached in real life conditions, thus this method is not suitable for a large scale deployment.

For GPS-denied environment, approaches without a detailed map of the environment often lead to several meters of localization error. This is only suitable for a navigation guidance system rather than an autonomous navigation system. In contrast, for those with a detailed map of the environment, the resolution and precision of map information severely influence the localization error. Unfortunately, the higher the resolution the map is, the more complex and less scalable the solution is. To address this balance, a fusion approach of two localization levels is proposed.

As mentioned in Section 0, there are two levels of localization: global localization and local localization. A solution for the GPS-denied environment can be described as in Figure 2.18.

- A global localization system acts as a reference framework for other localization techniques; it also allows seamless transition between the GPS-denied and the GPS-aided localization. This system is not necessary to be highly accurate. A standard GPS accuracy as mentioned in Table 1 is acceptable.
- A local localization system acts as a precise local positioning system. It is responsible for local navigation.

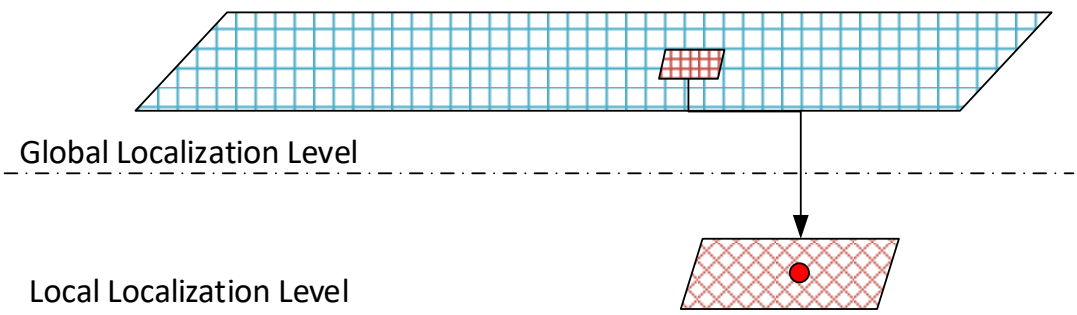

Figure 2.18 Two levels of localization system

The advantages of this approach are its scalability and accuracy characteristics. Each level of localization has a reasonable expectation of accuracy (low accuracy in broad view and high accuracy in local view). Also the existence of both level allows the system to scale and work seamlessly with other existed localization systems. Even though the complexity level of this fusion approach is not entirely reduced, the two levels fusion system is relatively straight forward and provides an opportunity of reducing global map resolution.

3. WIRELESS SENSOR NETWORKS LOCALIZATION

Résumé

Les réseaux de capteurs sans fil (WSN) font référence à un groupe de capteurs dispersés et dédiés dans l'espace pour surveiller et enregistrer les conditions physiques de l'environnement et organiser les données collectées à un emplacement central. Le GNSS, qui est une partie cruciale de ITS, est un exemple parfait de WSN pour des applications ITS. Le GNSS en général ou le GPS en particulier ont établi une norme pour le système de navigation global des véhicules intelligents. Malgré ses faiblesses dans les zones obstruées, l'impact du GPS est toujours important. En outre, le concept de localisation dans le GPS suggère une application possible des réseaux à grande vitesse (WSN) pour couvrir également ces zones obstruées. Ce chapitre examinera la stratégie de localisation des véhicules intelligents en particulier des réseaux intelligents WSN.

Il existe différents types de capteurs sans fil ainsi que des formes de réseaux pour les tâches de localisation à l'aide de WSN. Les capteurs sont infrarouges, ultrasoniques, unités de mesure inertielle (IMU), antenne Wi-Fi, etc. Les exemples de réseaux peuvent être le réseau satellite de GPS, le réseau cellulaire GSM, les réseaux Wi-Fi ou des réseaux plus spécifiques tels que Zigbee ou Bluetooth. Malgré les différences de types de capteurs et de formes de réseaux, les stratégies de localisation à l'aide de WSN peuvent être classées en deux classes: approches basées sur les gammes et approches sans plages.

Les approches basées sur la distance pour la localisation des WSN sont un groupe de méthodes qui estiment l'emplacement de l'objet d'intérêt en fonction de mesures de distance déduites des sorties de capteurs sans fil. Ces approches comportent deux étapes: les mesures de distance et l'estimation de la position. Souvent, des capteurs dotés de fonctions de mesure de distance telles

que les ultrasons, les UMI, les lasers, etc. peuvent directement être utilisés pour déduire la distance entre des objets d'intérêt et d'autres objets de l'environnement et permettre ainsi une estimation de la localisation possible. Cependant, il existe d'autres capteurs qui peuvent déduire indirectement la distance aux IO, tels que les signaux satellites, les signaux cellulaires, les signaux Wi-Fi, etc.), Algorithme Heure d'arrivée (TOA), décalage horaire (TDOA), ou angle d'arrivée (AOA), etc.

En revanche, les approches par fourchette de frais n'estiment pas la distance entre les OI et les OOI pour calculer la position. Ces méthodes utilisent des fonctionnalités de réseau et de capteurs telles que le graphe de connectivité réseau, la consommation d'énergie des capteurs et leur transmission ou la relation géométrique d'un réseau, etc. La plupart du temps, ces approches comportent deux étapes: l'extraction de caractéristiques et la reconnaissance de caractéristiques. Les algorithmes remarquables pour cette classe sont le saut de vecteur de distance (DV hop), le test de point approximatif de triangulation (APIT), l'empreinte digitale et l'algorithme de centroïde.

Le tableau 4 présente une comparaison rapide de ces approches.

3.1 Introduction

Wireless Sensors Networks (WSNs) refer to a group of spatially dispersed and dedicated sensors for monitoring and recording the physical conditions of the environment and organizing the collected data at a central location ("Wireless Sensors Networks" 2018). Before the era of the Internet of Things (IoT) wireless sensors networks have already been used in a variety of scenarios such as: weather monitoring system, disaster prevention, localization and tracking, etc. As devices become cheaper and smaller, the application domain of WSNs spreads wider. One of which concerns Intelligent Transportation System (ITS).

The GNSS, which is a crucial part of ITS, is a perfect example of WSNs for ITS applications. The GNSS in general or GPS in particular has set a standard for the global navigation system of intelligent vehicles. Despite its weaknesses in obstructed areas, the impact of GPS is still large. In addition, the concept of localization in GPS suggests a possible application of WSNs to cover those obstructed areas as well. This chapter will take a look at WSNs strategy for localization in general and intelligent vehicles localization in particular.

3.2 Localization Strategies Overview

There are various types of wireless sensors as well as forms of networks for localization task using WSNs. The sensors are infrared, ultrasonic, Inertial Measurement Units (IMU), Wi-Fi antenna, etc. and Networks examples could be the Satellites network of GPS, the GSM cellular network, Wi-Fi networks or more specific networks such as Zigbee, or Bluetooth. Despite differences in sensors types and networks forms, the strategies of localization using WSNs can be categorized into two classes: *Range-based* and *Range-free* approaches.

Range-based approaches for WSNs localization are a group of methods that estimate the location of the object of interest based on distance measurements inferred from wireless sensors outputs. These approaches have two stages: distance measurements and position estimation. Often, sensors with distance measuring feature such as ultrasonic, IMU, lasers, etc. which can directly be used to infer the distance from/to objects of interest (OOIs) to other objects in the environment and thus possible location estimation can be calculated. However, there are other sensors that can indirectly infer the distance to OOIs such as Satellites signals, cellular signals, Wi-Fi signals, etc. The distance computation from these sensors outputs is based on a signal propagation model using Received Signal Strength Indicator (RSSI), Time of Arrival (TOA), Time Difference of Arrival (TDOA), or Angle of Arrival (AOA) algorithm, etc.

Range-fee approaches, in contrary, do not estimate the distance to/from OOIs in order to calculate position. Those methods use network and sensors features such as network connectivity graph, sensors power consumption and transmission or geometric relationship of network etc. Most of the time, these approaches have two steps: feature extractions and feature recognition. Notable algorithms for this class are distance vector hop (DV hop), approximate point-in-triangulation test (APIT), fingerprinting and centroid algorithm.

3.3 Range-based Approach

3.3.1 Time of Arrival

Time of arrival (TOA) refers to the time for radio signal travel from the transmitter to a receiver. It is sometimes called Time of Flight. One of the first studies of this method is mentioned in (Caffery 2000). Due to the known constant speed of radio signal in the air, the distance between two nodes (transmitter and receiver) can be calculated if the time for radio signal to travel is also known. There are two schemes for measuring this elapsed time: *one-way scheme* and *two-way scheme*.

In the one-way scheme, only time delay between transmitter sending and receiver receiving of signal is measured. Assume that a signal is sent from the transmitter at t_1 and the receiver gets the message at t_2 then simple TOA is:

$$\tau = t_2 - t_1 \qquad 3.1$$

However, there is also the time of encoding and decoding message in both nodes, thus a better TOA can be written as in Eq. 3.2 with t_{dc} is decoding / encoding time. Although this method is not complicated, it strictly asks for clock synchronization between two nodes.

$$\tau = t_2 + t_{dc} - t_1 \qquad 3.2$$

In the two-way scheme, the transmission back and forth between two nodes are considered. The time of propagating radio signals from a transmitter to a receiver and returning from the receiver to the transmitter are taken into account. Illustration of a two-way scheme is showed in Figure 3.1.

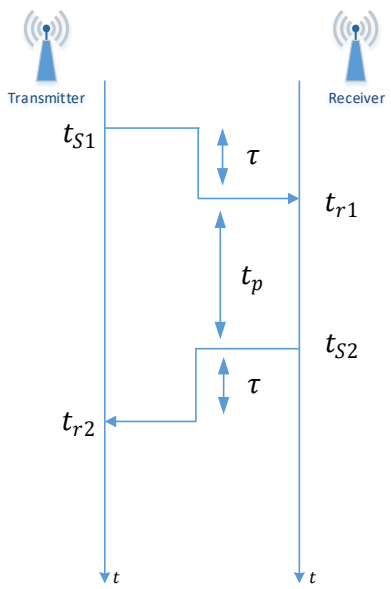

Figure 3.1 Two-way scheme of TOA

Here, the transmitter sends a message at t_{s1}. The message reaches the receiver at t_{r1} including the decoding time. The receiver takes t_p to process the message and write back to transmitter at t_{s2}. Finally, the message is received at transmitter including decoding time t_{r2}. The TOA in this case will be calculated as:

$$\tau = \frac{1}{2}(t_{s1} - t_{r2} - t_p) \qquad 3.3$$

As indicated in Eq.3.3, the TOA τ does not depend on the clock of receiver so no synchronization is required between two nodes. However, the accuracy of this estimation relies on the estimation of the processing time t_p.

An alternative method of TOA is TDOA (Time Difference of Arrival) (Venkatraman, Caffery, and You 2004) as it does not use the absolute time but rather the time difference between events in the network. Many radiofrequency localization techniques use TOA or TDOA including the GPS. A study in accuracy of those networks can be found in (Kaune 2012). The results are depending on the transmission environment as well as the quality of the devices.

3.3.2 Angle of Arrival

The angle of arrival (AOA) technique was initially designed for objects detection and localization in radar system and adopted as a localization technique for other systems (Yin et al. 2016). Significantly different from TOA, the AOA technique requires specifically an array of antennas (not a single antenna). Given a single source of transmission, the delay of receiving signals between each receiver's antennas will be used to calculate angle information. Generally, as indicated in (Boushaba, Hafid, and Benslimane 2009), the angle of arrival is defined as the direction of a signal which is received from a transmitter. To calculate this angle θ_l, let $r_i(t)$ be the time of receiving signal in the antenna i^{th}. As the signal moves in an empty space evenly and the distance Δ between antennas in the receiver is known, the different travel path can be calculated as:

$$S = \Delta \times sin(\theta_l) \qquad 3.4$$

Plus, this distance can also be calculated as:

$$S = \vartheta_{signal} \times (r_i(t) - r_{i-1}(t)) \qquad 3.5$$

Thus, the angle of arrival can be written as:

$$\theta_l = sin^{-1} \frac{\vartheta_{signal} \times (r_i(t) - r_{i-1}(t))}{\Delta} \qquad 3.6$$

Here, we assume that given a significant distance between the transmitter and array of antennas in the receiver in comparison to the wavelength of the signal, incoming signal are parallel. The illustration of the method is in Figure 3.2.

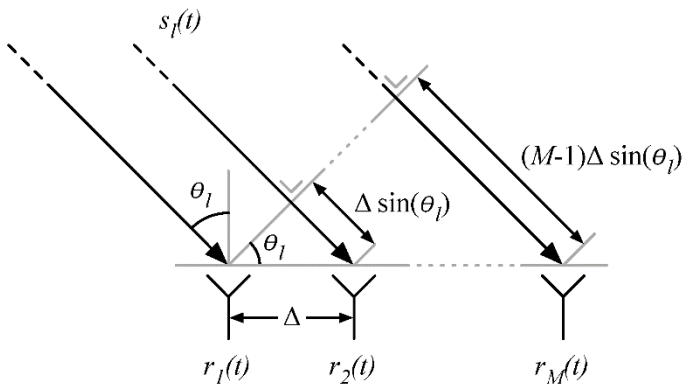

Figure 3.2 Angle of Arrival (AOA) localization method (Yin et al. 2016)

By calculating multiples AOA of different transmitters, the position of the receiver can be calculated from three or more transmitters using triangulation concept or estimated confidence zone as in Figure 3.3.

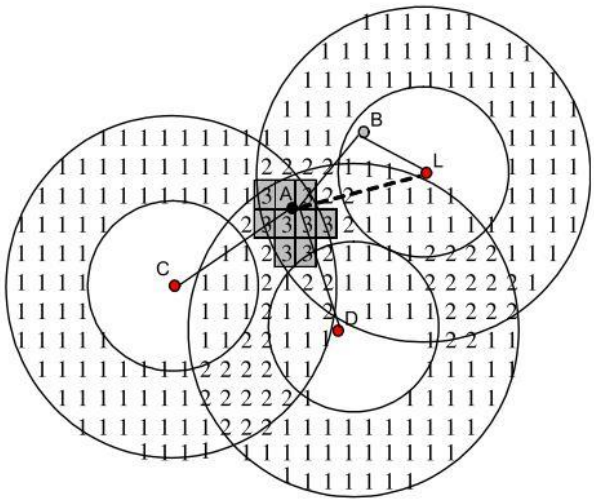

Figure 3.3 Angel of Arrival confidence zone

Using the estimated angle of arrival, the direct line-of-sight between known transmitters to the receiver can be computed. The length of this line represents a radius of the circle which takes the receiver as the centre point. Having three or more areas like this allows us to compute the confidence score for each grid cell. Apparently, area with most overlapping cells from all circles will get higher score and thus is likely the position of the receiver.

A notable localization system which employs this technique is called ArrayTrack (Xiong and Jamieson 2013). Using only 6 access points in a large office floor, the localization accuracy can be as good as 0.5m for 90% of confidence. The summary of localization error for Array Track can be found in Figure 3.4

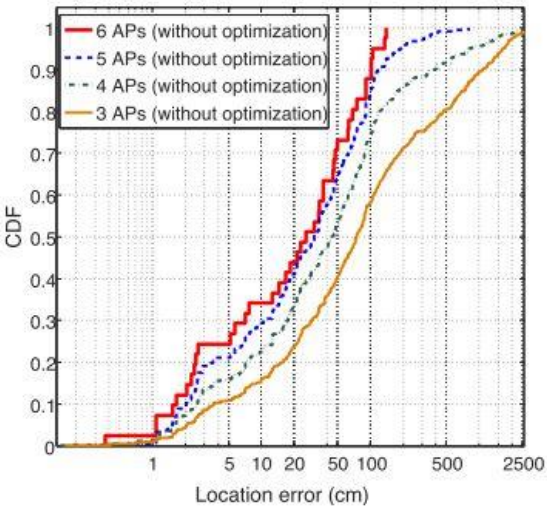

Figure 3.4 Array Track localization error

3.3.3 Received Signal Strength Indicator

The received signal strength indicator (RSSI) based localization is also featured in range-free approaches. In range-based approaches, most of the solutions are using a propagation model of the signal to calculate the distance from a transmitter to a receiver and then a triangulation method is applied for positioning determination.

One widely accepted propagation models is a log-normal model as follows (Dao et al. 2014):

$$RSSI = RSSI_0 - 10n\ log(\frac{r}{r_0}) \qquad 3.7$$

Where $RSSI_0$ is the known signal power at the reference distance r_0; and RSSI is the received signal power at an unknown distance r.

However, while traveling in the environment, radio signal suffers from multiple sources of noise such as the attenuation when signals crossing walls, the interference from other radio signals and the multipath effect (Giger, Member, and Barnett 1981; Kos, Markezic, and Pokrajcic 2010). Thus, there are several improvements that can be applied to Eq.3.7.

First, a different antenna at the receiver has a different gain constant. This results in a significant loss of the received power compared to the transmitted power. The attenuation of the antenna can be modelled as:

$$P_{atena_gain} = -10\ log(\frac{G_{transmit}G_{receive}\lambda^2_{transmit}}{(4\pi)^2 r_0^2}) \qquad 3.8$$

Where $G_{transmit}$ is the antenna gain factor at the transmitter, $G_{receive}$ is the antenna gain of the receiver and $\lambda_{transmit}$ is the wavelength of propagation signal.

Second, during the propagation of signals, there are obstacles such as walls, doors, etc. Depending on the size, material and position of the obstacles, power loss occurs. Figure 3.5 illustrates one case of obstacles interrupting a signal propagation. In this case, the power loss can be computed as:

$$P_{obstacles} = k_d \sum_{i=1}^{n} \frac{d_i}{\cos \beta_i} \qquad 3.9$$

Where k_d is the attenuation factor of obstacles' materials, d_i is the thickness of obstacles and β_i is the angle between line-of-sight of transmitter-receiver and the obstacle's surface.

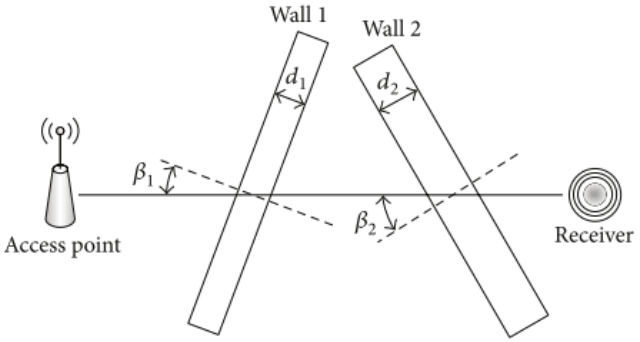

Figure 3.5 Signal propagation through obstacles (Dao et al. 2014)

Finally, the environment noise is considered as a random variable χ and the final equation of signal propagation becomes:

$$RSSI = RSSI_0 + 10\, log\left(\frac{G_{transmit} G_{receive} \lambda_{transmit}^2}{(4\pi)^2 r_0^2}\right) - 10n\ log\left(\frac{r}{r_0}\right) - k_d \sum_{i=1}^{n} \frac{d_i}{\cos \beta_i} + \chi \qquad 3.10$$

With this method, given a sufficient data of the environment factors (i.e. attenuations of antennas, obstacles' materials, a map of the structures and position of each sensors), could be as accurate as 2.6m (Nguyen et al. 2014; Guan and Ploetz 2017). It is also prone to multiple sources of noises such as multipath, interference from other radio sources that cannot be modelled mathematically.

3.4 Range-free approach

3.4.1 Distance Vector Hop

The distance vector hop (DV hop) (Niculescu and Badri Nath 2001) is a three steps localization process as described below:

- Given a network of sensors, each node is a landmark with a known location. An information table for each node of this network is built keeping a vector of $(x_i,\ y_i\ , h_i)$ where (x_i, y_i) is the coordinate of the ith node and h_i is the minimum hop count value from the ith landmark to the current node of the table.
- The average distance of one hop for a landmark in the network is calculated by mean sum of all hop distances corresponding to that landmark.

$$\bar{h}_i = \frac{\sum_j \sqrt{(x_i - x_j)^2 + (y_i - y_j)^2}}{\sum_i h_i} \qquad 3.11$$

- Finally, to localize an unknown node, the unknown node will send a message to the other nodes in the networks. The number of hops for each known nodes is recorded. This implies the estimated distance from a known node in the network to the unknown node using the average distance calculated in the above step. With distances estimations from all nodes in the network to the unknown node are now computed, the localization method can use trilateration, linear least squares, etc. to find the position of a target node in the network by simply sending message throughout the network.

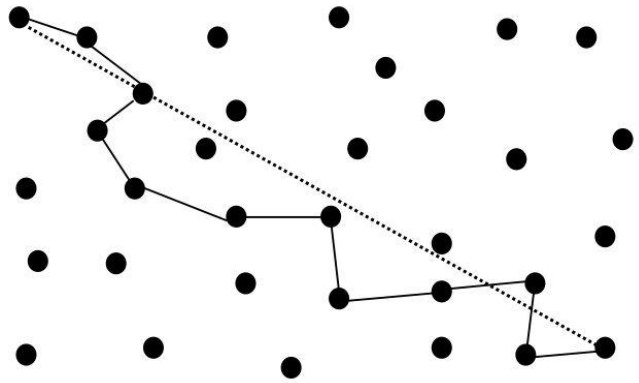

Figure 3.6 DV-Hop distance

The advantages of this method are its simplicity, robustness and noise-free characteristics. It is however, giving only rough estimation of the location with a high margin of error. As shown in Figure 3.6, while the dotted line is the actual distance between two nodes, the black line is considered as the DV-hop distance in this algorithm. This estimation introduces error as the number of hops increase. Still, the method is a good choice for a location indicator system. With a dense structure of network nodes, the accuracy of this method can be up to 5.1m (Agashe, Agashe, and Patil 2012).

3.4.2 Approximate Point-in-Triangulation Test

Approximate Point-in-Triangulation Test (APIT) is a range-free method that uses heuristic search to find the most likely position of an unknown node within a network of nodes with known coordinates. It is first proposed in (S. He et al. 2015). The idea is fairly straightforward as follows:

- Randomly pick-up three known nodes in the network, then test if the unknown node is covered within the triangle formed by those three nodes. The test is performed with the key idea is should the unknown node is within the triangle, any move to any direction of the unknown node must bring it closer to one edge of the triangle and further to the rest.
- Repeat the test multiple times until the intersection of selected triangle areas are small enough. The unknown node position is taken as the centroid of overlapped area

The concept of this method is shown in Figure 3.7

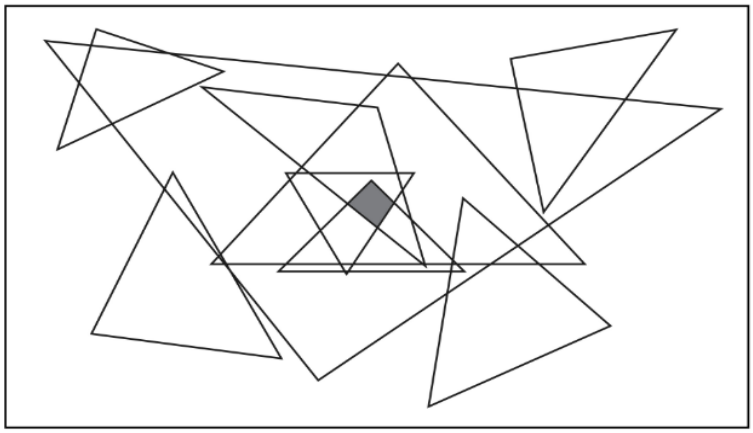

Figure 3.7 Approximate point-in-triangulation test (F. Liu and Tan 2012)

3.4.3 Fingerprinting Localization

The fingerprinting localization method is a popular method for WSNs localization given its simplicity, easy to deploy and scalable characteristics. With a well-designed algorithm and dedicated hardware, the accuracy of this method can be up to 0.6m of error (Kotaru et al. 2015; Kotaru et al., n.d.; Wang et al. 2017).

The main idea of the method is: given a network of radio transmitters, at any position in the environment covered by the network, the combination of RSSIs recorded by a receiver listening to all transmitters is unique. In other words, given a network of n nodes in the environment, a receiver perform signal scan of all available transmitters. This results in a combination of

signals strengths and transmitters ID (most commonly transmitter's MAC address) which is unique for any location in the environment. In Figure 3.8, the receiver is scanning for RSSI from a total of 5 transmitters in the environment, each with a different MAC address. Consequently, the unique feature vector of this location $\{x, y\}$ will be written as:

$$\{(MAC_1, RSSI_1), (MAC_2, RSSI_2), .., (MAC_5, RSSI_5)\} \rightarrow \{x, y\} \qquad 3.12$$

By building a database of multiple locations' feature vectors in the environment, a localization process later can simply be carried out with a classification algorithm of real-time RSSIs scan. Each location with feature vectors registered in the database will be called *a fingerprint*.

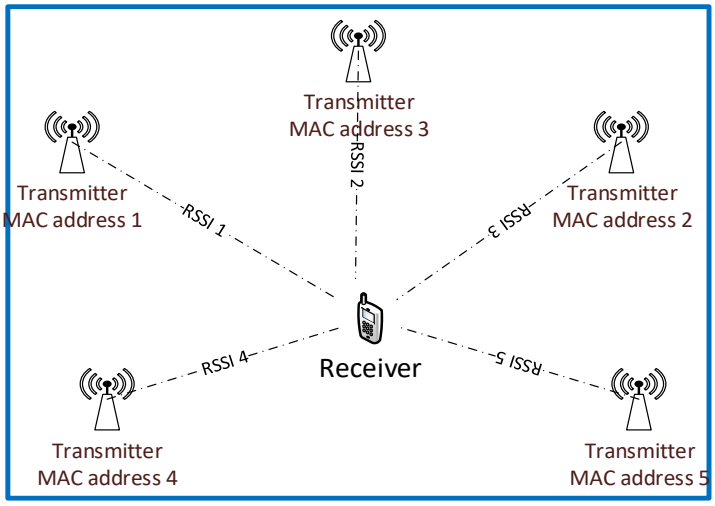

Figure 3.8 Fingerprinting localization concept

There are several advantages of this method. Database building of feature vectors is a relatively simple process. It does not require the receiver to actually connect to the transmitter and exchange messages. There is also no need of transmitters' positions information to be known. One can simply perform standard scanning action from the receiver and store the information received. Any commercial off-the-shelf device should be able to perform such task which makes deploying this solution feasible and scalable.

On the other hand, this method suffers from noise and changes in the environment setup. Any major change of the environment is likely to decrease localization accuracy. At the same time, depending on radio frequency of the transmitters and receivers, the initial assumption of unique feature for a unique position is likely to vary. Ultra-wideband radio frequency devices tend to perform much better than other signals such as Wi-Fi, cellular (Alarifi et al. 2016; "Infsoft Ultra-Wideband Technology for Indoor Positioning" 2018). However, unlike other classical radio devices, the ultra-wideband devices are not commonly available in the environment and has much shorter range of coverage.

3.4.4 Centroid Localization

The concept of centroid algorithm is based on the definition of a stable connection between nodes in a network. Assume that there are multiple nodes with known positions in a network, an unknown node enters the network and exchanges messages with all available nodes. A connection is defined as a stable link if the number of packets received by the unknown node from a known node exceeds a certain threshold h. If number of stable links is higher than 3, a polygon is formed by all known nodes in stable links. The centroid of that polygon is likely to be the position of the unknown node. An example of the centroid algorithm is illustrated in Figure 3.9. The red dot represents the centroid of a polygon formed by node1, node2 and node3 since those nodes have stable links to the unknown node.

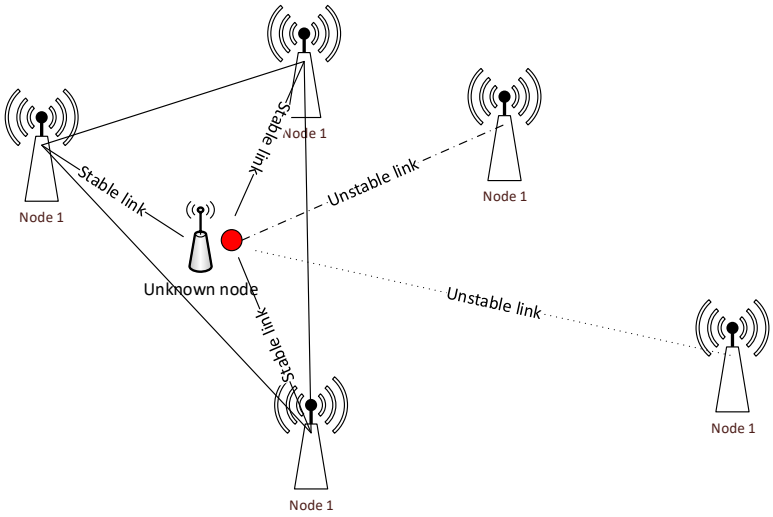

Figure 3.9 Centroid algorithm concept (Hongyang Chen et al. 2008)

As the number of nodes in the network increases, the accuracy of the localization algorithm is likely to increase. At the same time, the distribution of the nodes in the environment as well as the threshold definition of a stable link heavily influence the results. Reports in (Pivato, Palopoli, and Petri 2011; Blumenthal et al. 2007; Hongyang Chen et al. 2008) show a 3m of error maximum and a 90 percent of confidence of 0.8m of error in the best case scenario. While there is no distance measurement needed for the method, it does require to know all nodes' location in the network. The complexity of the algorithm increases exponentially as the number of stable links increase.

3.5 Discussion

For nearly two decades, from the early 2000s, the WSNs are extensively studied for different applications. This chapter presents a few notable approaches for WSNs in localization. Already,

it is clear that the potential of WSNs in localization is high. With a wide range of coverage, the availability of sensors and their increasing accuracy, WSNs become a preferred solution for both GPS-denied and GPS-aided environment.

However, in context of intelligent vehicles localization, there are very few studies in recent years. A study in (Moussawi 2012) presents a cooperative localization strategy of vehicles using WSNs. Using methods such as TOA, RSSI with Ultra-Wideband technology, the study achieves a RMSE localization accuracy of 2m. Another cooperative strategy is mentioned in (Garip et al. 2017) where vehicles are nodes within a WSNs. This system is able to identify a vehicle within 10m range. A WLAN-based localization system for the parking area is introduced in (Mauro et al. 2009) where a fingerprinting localization method is used. The accuracy of the method is around 7.3m. A university campus localization method of vehicles using wireless network is implemented in (Hernandez et al. 2017) results in 9.34m of localization accuracy.

As mentioned in Section 2.6, the balance between complexity and accuracy is essential for a true autonomy. Thus a two levels localization system is proposed. Studies in this chapter suggest that a WSN localization solution is suitable for a global localization layer for the following reasons:

- WSN solutions tend to have a wide coverage range due to radio signals characteristics. Depending on the sensors, it may or may not require Line-of-Sights (LoS). Unlike other sensors such as ultrasonic, cameras, lasers where LoS is extremely important. This makes WSNs a suitable candidate for obstructed areas global localization.
- WSN solutions often do not require much investment but still offer a relatively high accuracy of localization. The availability, performance of wireless sensors is increasing and so to theirs qualities. However, the accuracy of those solutions is still in order of a meter. Hence, it is not yet fit for local localization level.
- Due to signals transmission and messages exchange happening in a complex network, the localization rate for a WSN solution is more often low (around 1Hz). This is one of the main reasons why WSNs are not yet applied for intelligent vehicle navigation at high speed. Still, at a relatively low speed of navigation, it is feasible for a WSNs to keep track of an intelligent vehicle.

Given the arguments listed above, this thesis will propose and develop a WSN solution for a low-speed vehicle localization in GPS-denied area. This solution will be a global level localization system. Furthermore, with a fusion strategy with other sensors information such as

IMU or laser-based SLAM, the system is expected to achieve a significant localization accuracy.

4. WI-FI FINGERPRINTING LOCALIZATION

Résumé

En comparant différentes approches de localisation des WSN, une méthode de prise d'empreinte est choisie car elle satisfait aux quatre critères énoncés dans la section 1.2, à savoir la disponibilité, l'évolutivité, l'universalité et la précision.

Le concept général de la localisation d'empreintes digitales Wi-Fi est présenté à la section 3.4.3. Il existe deux phases pour cette méthode: une phase hors ligne et une phase en ligne.

Dans la phase hors ligne, une base de données d'empreintes digitales (FP) est construite. Comme défini dans la section 3.4.3, une empreinte digitale peut être n'importe quel emplacement de l'environnement ciblé avec des coordonnées connues. Chaque enregistrement dans la base de données d'empreintes digitales est un mappage des coordonnées d'une empreinte digitale et de tous les RSSI numérisés à cette position. Dans la Figure 4.1, chaque point bleu est une empreinte digitale (FP) avec des coordonnées connues. À un certain FP, les RSSI des cinq points d'accès (AP0, AP1, .., AP4) sont enregistrés et mis en correspondance avec ses coordonnées. Répétez cette procédure pour tous les PF de l'environnement pour établir la base de données d'empreintes digitales. Un enregistrement dans cette base de données est écrit comme dans Eq.4.1.

Dans la phase en ligne où l’estimation de la localisation est effectuée, le véhicule se déplacera dans l’environnement tout en recherchant les RSSI des points d’accès environnants. Une fonction de vraisemblance basée sur les données de la phase hors ligne est définie par Eq.4.3. En général, l'empreinte digitale avec le score de vraisemblance le plus élevé sera choisie comme emplacement estimé.

Récemment, plusieurs tentatives d'utilisation du concept d'empreinte digitale Wi-Fi ont été utilisées pour déterminer la position d'un véhicule. Certaines approches utilisent les smartphones des utilisateurs pour aider et guider le conducteur vers un parking. D'autres approches visent directement des véhicules intelligents avec des capteurs montés sur des véhicules. Selon le choix des capteurs (smartphone ou capteurs montés), la précision du système de localisation risque d'être affectée. Le chapitre présente quatre études notables. Ces études permettent d'atteindre environ 3-4 m d'erreur de localisation moyenne.

Après avoir examiné ces études, nous avons identifié deux problèmes majeurs concernant la méthode de localisation d'empreintes digitales Wi-Fi pour les véhicules: une fréquence d'échantillonnage faible du balayage Wi-Fi et une forte variance des forces du signal reçu. Pour résoudre ces problèmes, des modifications sont proposées aux phases hors ligne et en ligne. Dans la phase hors ligne, une base de données d'apprentissage hybride est mise en œuvre pour résoudre le problème de la vitesse de déplacement. De plus, un réseau de neurones d'ensemble (Dietterich 2000) pour la fonction de vraisemblance de phase en ligne est déployé pour résoudre le problème des signaux à forte variance.

La base de données hybride hors ligne est proposée avec une nouvelle définition d'empreinte digitale et un mélange d'analyses dynamiques et statiques. La distance entre deux lieux d'initiation et de fin de l'analyse est appelée une plage d'analyse. En fonction de la vitesse de déplacement de la cible, la plage de balayage peut également varier. Ainsi, une nouvelle définition d'empreinte digitale en tant que cercle est modélisée dans Eq.4.4. De plus, pour modéliser correctement les signaux reçus de la phase en ligne, en plus de la collecte classique de données statiques, des signaux sont également enregistrés pendant le déplacement des véhicules dans l'emplacement de l'empreinte digitale.

Dans la phase en ligne, une fonction de vraisemblance h est requise pour évaluer le vecteur RSSI d'entrée en temps réel. L'idée d'utiliser plusieurs modèles d'apprentissage pour améliorer les performances d'un seul est proposée dans (Krogh, Anders Jesper, 1995; Breiman, 1996; Hansen et Salamon, 1990). Dans certaines conditions, la combinaison d'estimateurs divers, non corrélés mais précis, devrait donner de meilleures performances qu'un seul. Cette section présente la stratégie d'ensemble visant à améliorer les résultats prévus (Eq.4.9 à Eq.4.13).

Les expériences relatives à la méthode proposée sont effectuées dans une place de parking ouverte du campus de l'INRIA Rocquencourt. En raison de la difficulté d'avoir un parking couvert pour les expériences, l'espace extérieur est utilisé. En même temps, ce parking extérieur

bénéficie d'un RTK-GPS précis pour la vérité du terrain. Cela permet une meilleure évaluation du système. La zone d'essai est illustrée à la figure 4.16. Il existe deux véhicules dans les expériences: un Cybercar bleu conçu comme un prototype pour les véhicules intelligents et une Citroën C1 rouge modifiée à des fins expérimentales.

Tout d'abord, une étude de la zone de test est réalisée pour comprendre les caractéristiques de la méthode. Les résultats de cette enquête suggèrent qu'il existe une forte corrélation entre la force moyenne du signal Wi-Fi et la précision du résultat de la localisation. Ainsi, avec une attente réaliste d'une bonne force de signal moyenne dans le scénario réel, la zone d'essai est alors définie. Dans la figure 4.23, les empreintes digitales sont marquées d'un cercle rouge. La distance moyenne entre deux empreintes digitales adjacentes est de 6,1 m, ce qui correspond à la limite supérieure de l'inter-distance entre les empreintes digitales décrite à la section 4.1. Avec cette distance, il ne faut que 25 empreintes digitales pour couvrir la zone de test. Pour chaque empreinte digitale, 60 analyses statiques et 20 analyses dynamiques sont enregistrées pour la base de données hors connexion. Un total de 156 points d'accès avec différentes adresses MAC est détecté sur 25 empreintes digitales. nous définissons ensuite un bon résultat de classification du réseau de neurones comme étant les empreintes digitales les plus proches de la vérité au sol en distance euclidienne. Comme mentionné dans l'équation 4.18, le résultat de Ensemble Neural Network est une liste des indices d'empreintes digitales et de leur confiance. Supposons que l'empreinte digitale de confiance la plus élevée est choisie comme résultat final de la classification. Un bon résultat de la classification doit satisfaire à l'Eq. 4.22. Pendant un an, avec plus de 60 expériences menées, la méthode proposée a surperformé toutes les solutions existantes et a une précision moyenne de 2,25 m.

4.1 Introduction

As discussed in Chapter 2, there is a need for a global positioning system of intelligent vehicles in the GPS-denied area. Given the characteristics of the WSN, Section 3.5 pointed out that it is a feasible solution for the quest. However, choosing an approach for such a system needs to be considered carefully. In the scope of the thesis, four criteria have been identified: availability, scalability, universality and accuracy. A quick comparison of WSNs localization approaches highlighted in Chapter 3 is shown in Table 4. Note that this comparison takes into account only approaches without any hardware modification.

Although such comparison may change depending on sensors type as well as the targeted environment, it gives an overview of these approaches under the four selected criteria. In the

carpark environment, a fingerprinting approach will be selected as it satisfies all of four criteria stated in Section 1.2 which are *availability*, *scalability*, *universality* and *accuracy*.

As Wi-Fi access points are readily available in most of urban areas, the *availability* of the Wi-Fi related localization system should be high. Also, these sensors are required for any Vehicle-to-Infrastructure (V2I) communications thus it further enhances the readiness of the system.

With a Wi-Fi fingerprinting approach, increasing the number of Wi-Fi access points (for a wider area) only affects the offline mapping phase. Furthermore, the Wi-Fi fingerprinting localization system, unlike the RSSI based, utilizes environment "access points". This means the systems does not need to know the precise location and the signal to distance characteristics of any access point. In addition, it is possible to divide the environment into several clusters (such as different buildings, floors, etc.) to deploy the fingerprinting system. Thus the *scalability* requirement of the system is satisfied.

Most of the Wi-Fi systems are currently using IEEE 802.11 standard ("IEEE 802.11: Wireless LAN Medium Access Control (MAC) and Physical Layer (PHY) Specifications" 2016). This enables a *universal* standard for the localization system based on Wi-Fi signals to work with.

Finally, as reported in Chapter 3, the *accuracy* of a carefully designed fingerprinting system could be as high as 0.6m (Kotaru et al., n.d.). This accuracy appears to be much higher than other solutions.

The general concept of Wi-Fi Fingerprinting localization is introduced in Section 3.4.3. There are two phases for this method: *an offline* and *an online* phase.

In the *offline* phase, a database of *fingerprints* (FPs) is built. As defined in Section 3.4.3, a *fingerprint* could be any location in the targeted environment with known coordinates. Each record in the database of *fingerprints* is a mapping of a *fingerprint* coordinates and all scanned RSSIs at that position. In Figure 4.1, each blue dot is a *fingerprint* (FP) with known coordinates. At a certain FP, RSSIs from all five access points (AP0, AP1, .., AP4) are recorded and mapped to its coordinates. Repeat this process for all FPs in the environment to establish the database of *fingerprints*. A record in this database is written as in Eq.4.1.

$$\{X_i, \rho_l\} = \{x_{i,1},\ x_{i,2},\ x_{i,3},\ \dots,\ x_{i,n},\ \rho_l\} \qquad 4.1$$

Here, $x_{i,j}$ is the Wi-Fi signal strength from the jth Wi-Fi access point (AP) that is recorded from the absolute coordinate ρ_l of FP_l in the ith scan. n is the total number of APs recorded in the environment and l is the total number of FPs in the environment.

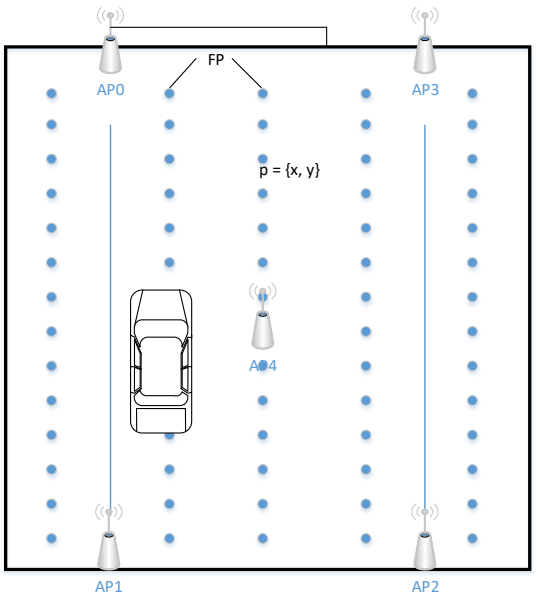

Figure 4.1 Fingerprints illustration

Table 4 Comparison of different WSNs localization techniques

Method	*Availability*	*Scalability*	*Universal*	*Accuracy*
TOA	Medium Requires connection between receiver and transmitters	Medium Requires map of Transmitters	High May require clock synchronization	~ 5m(Kaune 2012)
AOA	Medium Requires connection between receiver and transmitters	Medium Requires map of Transmitters	Medium multiple antennas receiver	~2.5m (Boushaba, Hafid, and Benslimane 2009)
RSSI (Range-based)	High	Low Requires maps of transmitters and the environment	High	2.6m (Dao et al. 2014)
DV-Hop	Medium Requires connection between receiver and transmitters	Medium Requires map of Transmitters	High	~5.1m (Agashe, Agashe, and Patil 2012)

APTIT	Medium Requires connection between receiver and transmitters	Low Requires map of Transmitters $O(N^2)$ – N number of network's nodes	High	>20m (F. Liu and Tan 2012)
Fingerprinting	High	Medium – high Requires map of fingerprints	High	~ 0.6m (Kotaru et al. 2015)
Centroid Algorithm	Medium Requires connection between receiver and transmitters	Low Requires map of Transmitters $O(N^2)$ – N number of network's nodes	High	~10.8m (Hongyang Chen et al. 2008)

The *offline* phase database *D* is then formulated as:

$$D = \begin{Bmatrix} x_{1,1}, x_{1,2}, x_{1,3}, \dots, x_{1,n}, \rho_1 \\ x_{2,1}, x_{2,2}, x_{2,3}, \dots, x_{2,n}, \rho_1 \\ x_{3,1}, x_{3,2}, x_{3,3}, \dots, x_{3,n}, \rho_2 \\ \vdots \\ x_{m,1}, x_{m,2}, x_{m,3}, \dots, x_{m,n}, \rho_l \end{Bmatrix} \qquad 4.2$$

In the *online* phase where localization estimation is carried out, the vehicle will move inside the environment while scanning for RSSIs from surrounding APs. A likelihood function based on data from offline phase is defined as:

$$h(X_t) = c_l \qquad 4.3$$

Where X_t the input vector of RSSIs scan at time *t* and c_l the likelihood score of X_t to be scanned at FP_l in the environment with regard to *D*. In general, the *fingerprint* with the highest likelihood score will be chosen as the estimated location.

Compared to other map building processes (such as camera-based map, LiDAR-based map, etc.) the Wi-Fi fingerprints map is fairly straightforward and simple. All FPs coordinates can be measured only once in a global coordinate frame. These measurements remain correct regardless of changes in the environment as there is no change in the global coordinates of the surveyed position. RSSIs vector however, will need to be updated if a major change occurs. Still, the cost of map updating in this case is much lower than other methods.

4.2 Related Works

Recently, there are several attempts to use the concept of Wi-Fi fingerprinting in determining position of a vehicle. Some approaches take advantages of users' smartphones to assist and guide driver to a parking lot. Other approaches directly aim for intelligent vehicles with sensors are mounted on vehicles. Depending on the choice of sensors (smartphone or mounted sensors), the accuracy of the localization system is likely to be affected. In this section, several notable studies are examined.

An early attempt can be found in (J. Liu et al. 2012) where the authors use handheld devices to determine vehicles' position. A classical Wi-Fi fingerprinting module is implemented on user's device to determine its position. A dead-reckoning module is built using inputs from smartphones' sensors such as accelerometer, compass, etc. The two modules are then combined to estimate the final position. An illustration of the system is shown in Figure 4.2. Despite the limitation of smartphones' sensors, the system has achieved a considerable accuracy. The reported RMSE is around 4m and 95% of the errors are under 6m. The whole system is reported to function at 1Hz. Thus the vehicle speed is not expected to be high. Since the authors only target giving location-based services such as: guidance to points of interest, location-based information or car finding, etc., this accuracy is relatively sufficient.

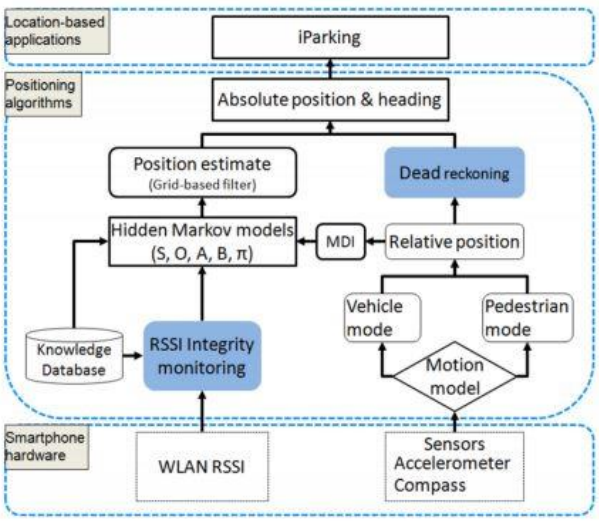

Figure 4.2 iParking system architecture (J. Liu et al. 2012)

An approach in (Wilfinger and Thesis 2015) presents a combination of fingerprinting for both Wi-Fi and Bluetooth Low Energy(BLE) devices. The study divides the environment into grid-based map and build a radio map for each intersection. A 4800m^2 carpark is used as a test bed. The distribution of BLE and Wi-Fi access points as well as the fingerprinting position (reference

points) are shown in Figure 4.3. A total of 60 BLE access points and 10 Wi-Fi access points are used. The BLE sensors are operated at 10Hz while the Wi-Fi scan is performed at a rate of 1Hz. Three databases of fingerprint for Wi-Fi, BLE and a combination both Wi-Fi and BLE are built to evaluate the accuracy of each method. The final result for localization is shown in Table 5. The vehicle speed in this research is around 10km/h (or 2.8m/s). The fingerprinting algorithm in this work is referred as a simple standard fingerprinting localization algorithm.

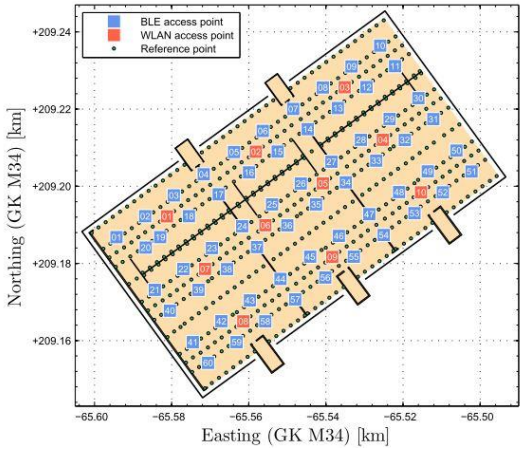

Figure 4.3 Thondorf carpark (Wilfinger and Thesis 2015)

The position error for a test run is shown in Figure 4.4. In this figure, the WLAN fingerprinting localization appears to be highly inaccurate. The BLE shows a much better result as the functioning rate and number of BLE units in the environment is significantly higher than those in WLAN. The combination result of both solutions shows a slightly improvement compared to the BLE method.

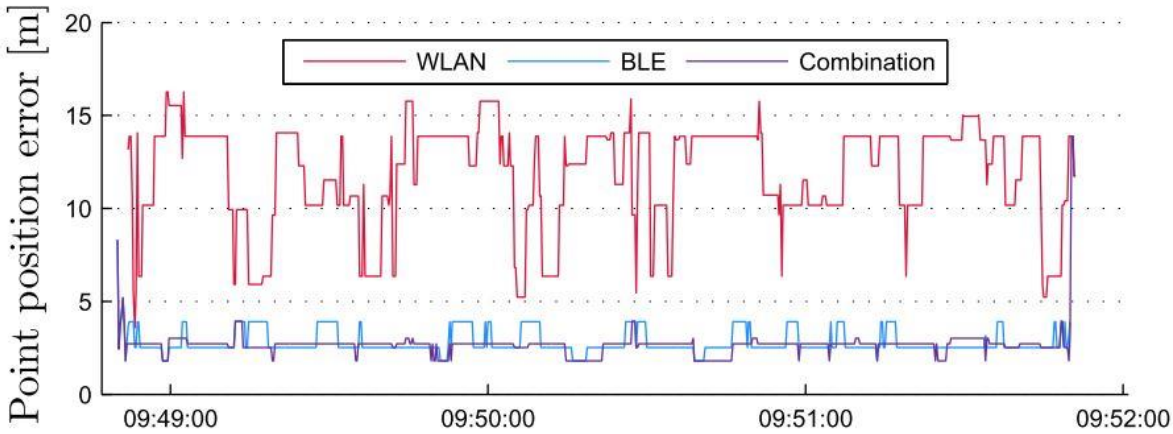

Figure 4.4 Time series for a test run (Wilfinger and Thesis 2015)

Table 5 Positioning Error using BLE and Wi-Fi fingerprinting (Wilfinger and Thesis 2015)

Type	#	*Mean Error*	*Standard Deviation*	*Below Mean Error*
WLAN	1	6.2 m	5.5 m	68.4%
	2	6.9 m	5.9 m	63.3%
	3	5.7 m	5.1 m	64.1%
BLE	1	4.8 m	3.7 m	61.9%
	2	4.5 m	3.5 m	64.8%
	3	6.2 m	5.5 m	65.8%
	4	6.3 m	4.9 m	61.3%
Combination	1	4.1 m	2.9 m	63.0%
	2	4.4 m	3.6 m	66.5%
	3	5.5 m	4.9 m	68.4%

Another smartphone-based positioning for vehicles in carpark can be found in (Gikas et al. 2016). This study makes use of a dedicated IMU, Wi-Fi positioning and RFID technology. In this solution, the vehicle will be equipped with an RFID device (tag or reader). A number of RFID readers are installed in the environment to detect any moving tag. A dedicated IMU provides input for a dead-reckoning algorithm. And by monitoring the number of Wi-Fi access points detected, an estimation of the vehicle current area is calculated. The testing site and sensors mount in the study is shown in Figure 4.5. The figure shows a large number of RFIDs readers is required as well as some Ultra-Wideband nodes. Finally, the estimated area of the vehicle is then derived accordingly to the RFID readers' locations in the environment. The study suggests that 70-80% of true positive is reached.

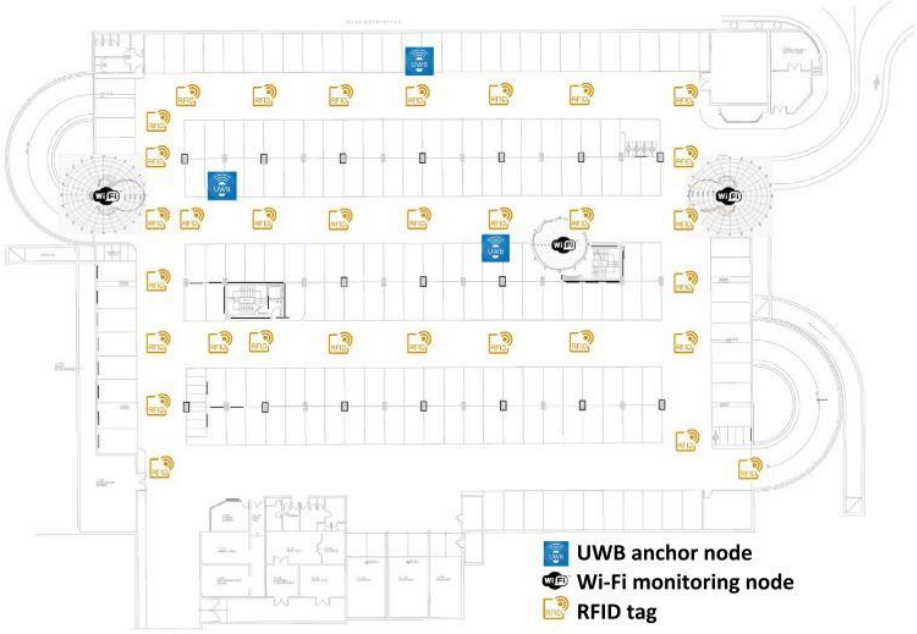

Figure 4.5 Sensors setup and testing environment (Gikas et al. 2016)

A recent study in (Hernandez et al. 2017) also exploits a possibility of using Wi-Fi fingerprinting localization for a smart vehicle in an university campus area. The study takes the campus of the Universidad Carlos III de Madrid with 30 points in the environment are chosen to be training position (Figure 4.6).

Figure 4.6 The Universidad Carlos II de Madrid campus (Hernandez et al. 2017)

Unlike other standard Wi-Fi fingerprinting approaches, this study treats the environment as a grid-based map with a resolution of 15cm. With this grid-based map, an attempt to localize the vehicle in an arbitrary position (which most of the time is different from training position) is made. A Support Vector Regression algorithm (SVR) is implemented to handle the continuous solution space. The flowchart of the system is shown in Figure 4.7

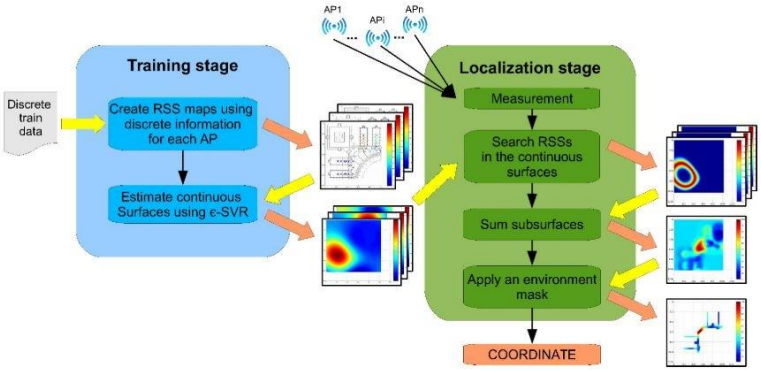

Figure 4.7 General architecture of the system (Hernandez et al. 2017)

The experiments are carried out with 175 Wi-Fi access points recorded, an intelligent vehicle operated at 4.86km/h speed moving through a path of 145m. Final results show an average localization error at best case is 6.18m.

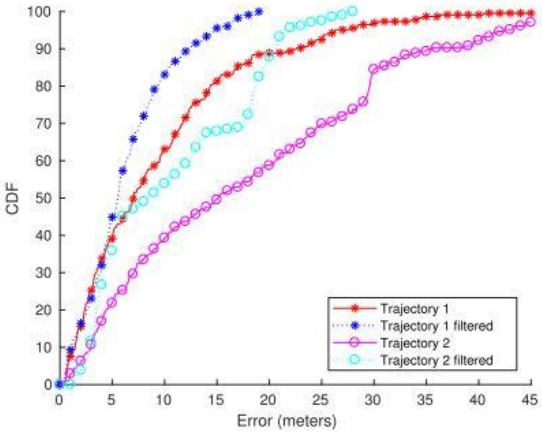

Figure 4.8 Cumulative Distribution of Error (Hernandez et al. 2017)

The latest research on the Wi-Fi fingerprinting for intelligent vehicle is presented in (Ang 2018). This research is particular interesting for their ambitious goal of replacing the GPS signal in urban area with the existing Wi-Fi infrastructure. Due to the obstruction in urban area, the GPS signal is expected to be poor. Thus, a Wi-Fi fingerprinting localization system is deployed in the crowded streets of Singapore in this research to improve the absolute localization. The research, however, uses a Nexus 5 android device to capture Wi-Fi signal instead of mounting sensors on the vehicle. The test run and area of experiment is shown in Figure 4.9. An early result is obtained with 80% of errors are under 15m.The cumulative distribution of error is shown in Figure 4.10. Although such result is still large, it shows promising sign of using the method in a complex environment such as urban area. Given that the authors use a phone instead of a dedicated Wi-Fi receiver for the experiments, there is still room for improvement.

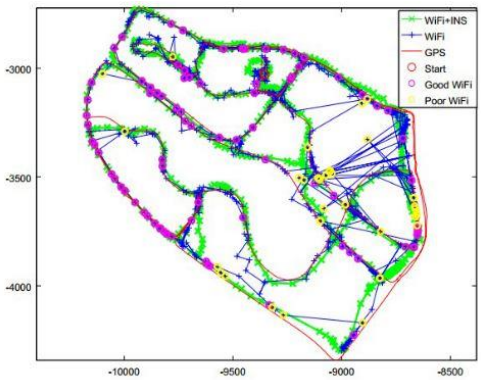

Figure 4.9 Wi-Fi localization in urban area (Ang 2018)

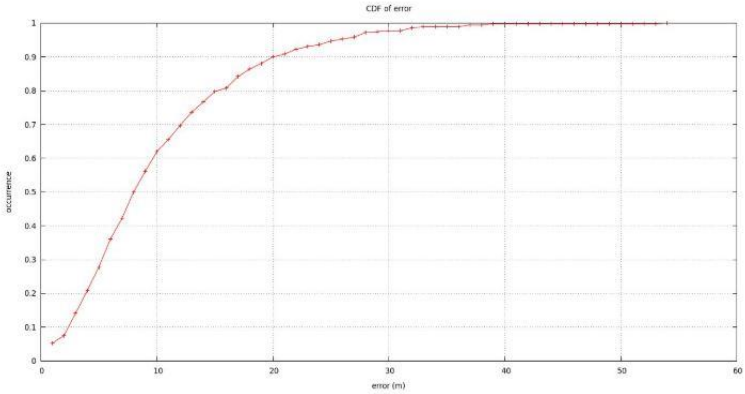

Figure 4.10 Cumulative distribution of error in urban area (Ang 2018)

4.3 Ensemble Approach for Wi-Fi Fingerprinting Localization of Intelligent Vehicles

There are two major issues for Wi-Fi fingerprinting localization when it comes to vehicles tracking:

- Low sampling frequency: the time to complete a scan of Wi-Fi signals in a particular environment depends on multiple factors but it is generally around 1 second. This means the Wi-Fi receiver performs at 1Hz of sampling frequency. For the human average walking speed of around 1.35m/s (Anderson and Pandy 2001), this low sampling frequency is neglected in the tracking problem. However, a vehicle in a carpark moves at 3-3.3m/s (Belloche 2015). With 1Hz of sampling frequency, the Wi-Fi fingerprinting localization system is only capable of giving a measurement every 3m. Since localizing a vehicle is a demanding task in terms of precision, this low sampling rate is inadequate.
- High variance in signal strengths: the Wi-Fi signal, as any other radio signal, is influenced by multiple factors in the environment such as other radio signals, heavy

metal obstacles, etc. this results in a high variance of RSSIs which in turn lowers the precision of the likelihood function. Also, in case of vehicles' movement, due to the higher speed of movement, this issue becomes much more significant in comparison to the pedestrians' movement.

To address these issues, changes in both *offline* and *online* phases are proposed. In the *offline* phase, a hybrid learning database is implemented to overcome the movement speed issue. Furthermore, an ensemble neural network(Dietterich 2000) for the *online* phase likelihood function is deployed to solve the high variance signals problem.

4.3.1 Hybrid Database Offline Phase

In the classical approach of Wi-Fi fingerprinting localization, the mapping $\{X_i, \rho_l\}$ in the offline phase is perceived as a representative *feature vector* X_i of the *fingerprint* ρ_l. The underlying assumption for this mapping is at a *fixed* location, its *feature vector* is unique. However, as this database is used for evaluating the *online* phase likelihood function, there is an issue with the online input data.

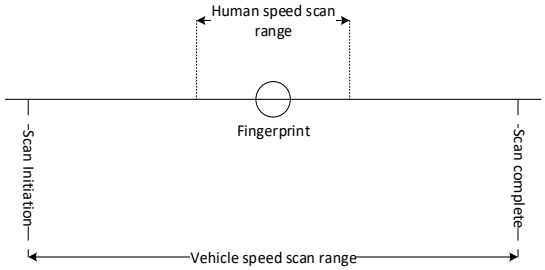

Figure 4.11 Online scan range for different speeds

Consider a scenario as in Figure 4.11, the fixed location fingerprint is defined in the *offline* phase and illustrated as the circle in the figure. With 1Hz of sampling frequency, a Wi-Fi scan is initiated at a certain position and terminated at a different one. The distance between two locations of scan initiation and termination is called a *scan range*. Depending on the movement speed of the target, the *scan range* can also vary. With an average of 1.35m/s for human walking speed, the scan range for a human walking case is also around 1.35m. Thus, a signal vector X_t in the online phase is the feature vector of a *path* but not a *fixed position*. By reducing this path to a fingerprint location in the likelihood function, an error of localization is introduced. When it comes to the targeted scenario in this thesis, a vehicle in a carpark has 3.3m/s average speed which results in an approximately 3.3m of scan range. This is a significant distance for the vehicle navigation task. Hence, a new hybrid database of offline phase database is proposed.

In the hybrid database, instead of only collecting feature vector data at a fixed position (i.e. a fingerprint), the vehicle will move around the fingerprint location and collect the Wi-Fi signals. This create a new mapping $\{X_i, \rho_l'\}$ where ρ_l' is expressed as:

$$\rho_l' \in (\rho - \Delta\rho, \rho + \Delta\rho) \qquad 4.4$$

Equation 4.4 models the new fingerprint as a circle which takes location of ρ as the center and Δρ as the radius. Having the new fingerprint definition, a mix of fixed location scans and moving vehicle scans is collected to be the new feature vectors of the area. Scans with vehicles moving is called *dynamic scan*. Others with vehicles at fixed place is called *static scan*. Note that an assumption of symmetrical distribution of error in both x-axis and y-axis is made. In the best case scenario for the new fingerprint concept, the center of the scan range will be exactly at the location of ρ. Therefore, the radius Δρ is determined as:

$$\Delta\rho = {}^{\bar{v}_{vehicle}}/_{2} \qquad 4.5$$

With $\bar{v}_{vehicle}$ is the average of the vehicle movement speed. In this case, $\bar{v}_{vehicle}$ is 3.3m/s and $\Delta\rho$ is approximately 1.6m/s.

Finally, a normalization of collected RSSIs in each scan is performed to reduce the numerical impact of signal strength feature. A detected access point will have RSSI in range [0,1) after normalization while an undetected access point (i.e. access point which is inside the environment but not detected at a certain fingerprint) is scored as -1. This further emphasizes the weight of detected AP compares to undetected one. The formal representation of a RSSI normalization process is shown in Eq.4.6.

$$x_i = \begin{cases} -1, & AP_i\ undetected \\ 1 - \dfrac{(-1) \times RSSI}{100}, & AP_i\ detected \end{cases} \qquad 4.6$$

Having a newly defined hybrid database, it is also important to identify the density of the fingerprint locations within the environment. The number of fingerprint locations l influences directly the complexity of the map building process as well as the accuracy of the localization system (Eq. 4.7). In order to determine l, there are two major factors to address: the behaviour of the likelihood function h in the online phase and the optimal distance between two fingerprints.

$$\begin{cases} l \sim Complexity \\ l \sim \dfrac{1}{error} \end{cases} \qquad 4.7$$

Firstly, if the function *h* is an approximation function for a *classification* task then the output of *h* should be discrete (labels). In this case, the number of data gathered for each label must be sufficiently high to correctly model the relation between the label and the feature vector. In contrast, if *h* is a function for a *regression* task then the output of *h* should be continuous (i.e. real coordinates). This regression task demands for large number of data spread evenly within the targeted environment to estimate continuous coordinates (see Eq. 4.8). In other words, the classification task asks for multiple data on each fixed position while the regression task needs multiple data in the entire environment. Therefore, theoretically, the number of fingerprints l in the classification task should be far less than in the regression task. With the aim for a less complexity map building process, a classification approach is chosen.

$$h(X) = \begin{cases} FP, & Classification \\ (x, y), & Regression \end{cases} \qquad 4.8$$

With a classification approach, the goal of *h* is to return the closest (in Euclidian distance) possible label given an observation of RSSIs. This results in an accuracy constraint: the further the distance between two adjacent positions of Fingerprints the lower the absolute localization accuracy. In Figure 4.12, the green dot is the real position (ground truth), the two blue circles are adjacent fingerprints and the distance between two fingerprints is d_{FP}. The best classification result in this situation should be $h(X) = FP_n$. Obviously, as d_{FP} increases, the localization error ε may increase as well.

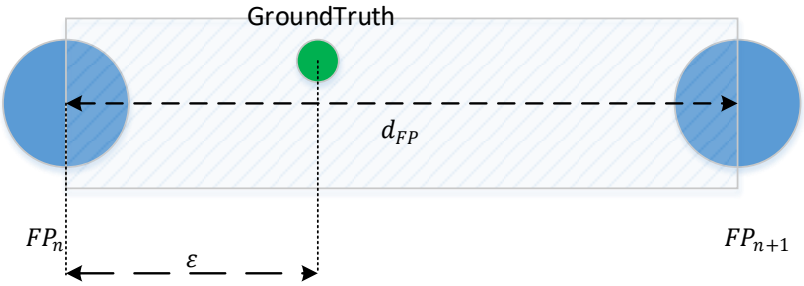

Figure 4.12 Distance between two adjacent fingerprints

Since the sampling frequency is 1Hz or one Wi-Fi scan each second, the lower bound for d_{FP} should be a *scan range* as mentioned previously which is likely to be 3.3m. A lower value than this distance is not optimal since one Wi-Fi scan would not be able to complete between two fingerprint locations. The upper bound is related to the desired localization accuracy as well as practical conditions of the environment such as the distribution of access points, the scale of the environment, etc. In this thesis, with an expectation of standard GPS accuracy level, the distance between two fingerprints is chosen to be between one *scan range* to two *scan range*

(3.3 – 6.6m). This is reasonable for the balance between localization accuracy and complexity of map building process since the fingerprints inter-distance is directly related to the number of fingerprints l in the environment. As suggested in Eq.4.7, a low l will help to reduce the complexity of the system. However, a small l will also affect the system accuracy as well. Assume that all fingerprints are distributed relatively evenly in the environment, then an optima l will be achieved with an optimal fingerprints inter-distance. With the lower-bound of the inter-distance argued to be at one *scan range* above, the upper-bound with regard to the GPS accuracy (~ 5-6m – Section 2.2) should not be more than 6 meters. A higher inter-distance than 6m will increase significantly the localization error (illustrated in Figure 4.12) and consequently degrade the system performance in comparison with the GPS.

4.3.2 Wi-Fi Ensemble Neural Network

In the *online* phase, a likelihood function *h* is required for evaluating the real-time input RSSIs vector. As discussed in previous section, a classification approach will be chosen for the task. Previous works in this phase often make use of classical statistical model such as KNN (K-nearest neighbours) (S. Chen, Li, and Long 2017; Zhou, Lu, Chen, et al. 2017), Random Forest (Hernández, Alonso, and Ocaña 2017; Wietrzykowski, Nowicki, and Skrzypczyński 2017; Guo et al. 2018), SVM (Support Vector Machine) (Zhou, Lu, Zhao, et al. 2017; Bhatt, Babu, and Chudgar 2017) etc. There are also approaches from the deep learning method such as (Zhang et al. 2016; Wang et al. 2017). However, these studies are mostly used for pedestrian's localization based on smartphone. In case of pedestrians, there is a fundamental difference in terms of movement speed in comparison with vehicles' scenario. There are only few studies of vehicles mentioned in Section 3.5 where the accuracy level is limited to around 7-9m of mean error. One of the causes is pointed out in Section 4.3 which is the high variance of collected RSSIs. In this thesis, an ensemble neural network learning model is proposed to address the issue.

The idea of using multiple learning models to enhance performance of a single one is proposed in (Krogh, Anders Jesper 1995; Breiman 1996; Hansen and Salamon 1990). Under certain conditions, the combination of diverse, uncorrelated but accurate estimators should have better performance than one alone. There are three reasons for this: statistical, computational and representational (Dietterich 2000) (Figure 4.13).

Firstly, a learning algorithm can be presented as a search in the hypotheses space $\mathcal{H}$ to identify the best one. The statistical problem arises when the amount of training data is too small

compared to the size of $\mathcal{H}$. This is usually true in real life as it is impossible to cover all hypotheses of a Wi-Fi fingerprinting problem. Without sufficient data, the learning algorithm can find many different hypotheses with the same level of accuracy. By aggregating different, uncorrelated good estimators, it reduces the risk of choosing a "wrong" one. Assume *f* in Figure 4.13 is the true hypothesis and in statistical case, h1, h2, h3 and h4 are equally good estimators. An aggregation of those four may deliver a closer result to *f* than any of them.

Secondly, many learning algorithms suffer from local optimal which means that instead of finding a global optimal solution, it may get stuck in a local one. Assume that there are sufficient training data to cover most of $\mathcal{H}$, it is still very difficult to find a global optimal point computationally. Building multiple estimators from different starting locations in hypotheses space $\mathcal{H}$ may provide a better approximation of the true optimal solution. In Figure 4.13 of computational case, suppose h1, h2 and h3 are three estimators with different starting points in the hypotheses space. Having a random start, each of those estimators will converge at a different accuracy level. With a finite large number of estimators, there is a high possibility that some of them overcome the local optimal point. Thus an ensemble of those estimators should be more accurate than picking just one of them.

Finally, in many applications of machine learning, the true approximation function *h* cannot be represented by any of the hypothesis in $\mathcal{H}$. This is also true in case of Wi-Fi fingerprinting as the mapping $\mathrm{h}(\mathrm{X}) = FP$ is impossible to model with a finite training samples. Thus, by taking weighted sum of all estimators, it is possible that the outcome of the ensemble is closer to the true answer. In Figure 4.13, the hypotheses space does not cover the true answer *f*. More often, this is because of only a finite number of training data is collected. By aggregating h1, h2 and h3, it is possible that the output accuracy is enhanced.

A necessary and sufficient condition for an ensemble estimator to be more accurate than any of its individual is each individual estimator should be accurate and diverse (Hansen and Salamon 1990). An accurate estimator is the one that has an accuracy rate better than a random guessing on new input value. Two estimators are diverse if they make different errors on new data. Thus, in order to construct an ensemble of neural network, the thesis proposes to employ a bagging technique (**B**ootstrap **Agg**regat**ing**) (Breiman 1996). The formal explanation of applying this technique for ensemble neural network is following.

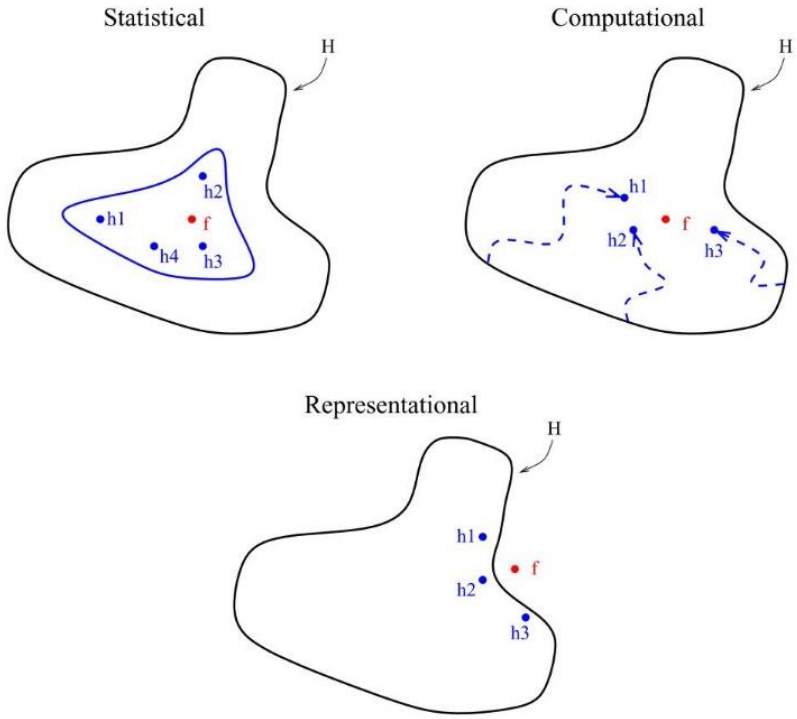

Figure 4.13 Ensemble of estimators motivation (Dietterich 2000)

Consider a classification problem with a pair $\{\boldsymbol{x}, y_j\}$ where $\boldsymbol{x}$ a feature vector and y_j denotes a response of a corresponding class, $y_j \in \{1, 2, .. m\}$. The target function is $P(y = j \mid \boldsymbol{x})$. Given a training database with the number of samples *n* and the number of classes *m*, an approximation function *h* is formed in Eq. 4.9.

$$g(\cdot) = h\left((x_1, y_1), (x_2, y_2), \dots, (x_n, y_m)\right) \qquad 4.9$$

Multiple bootstrap databases are formed by randomly sampling with replacement *K* times from the original data. Each database has equal size of *n* samples as in Eq. 4.10.

$$(\widehat{x_1}, \widehat{y_1}), (\widehat{x_2}, \widehat{y_2}), \dots, (\widehat{x_n}, \widehat{y_m}) \qquad 4.10$$

Compute *K* bootstrap estimators using the same approximation function *h* for neural network classification model with each of *K* bootstrap database as training data:

$$\hat{g}(\cdot) = h\left((\widehat{x_1}, \widehat{y_1}), (\widehat{x_2}, \widehat{y_2}), \dots, (\widehat{x_n}, \widehat{y_m})\right) \qquad 4.11$$

Aggregating all *K* estimators in 4.11 we have:

$$\widehat{g_{bagging}}(\cdot) = \frac{1}{K}\left(\sum_{i=1}^{K} \hat{g}_i(\cdot)\right) \qquad 4.12$$

Theoretically, as *K* goes to infinity, Eq. 4.12 can be written as

$$\widehat{g_{bagging}}(\cdot) = \boldsymbol{E}[\widehat{g}_i(\cdot)] \qquad 4.13$$

In practice, with a finite large *K*, the bagging estimator should come close to the expected global optimal.

With the strategy for ensemble, it is now important to discuss the structure of an individual neural network. A general fully connected architecture of a neural network with one hidden layer is shown in Figure 4.14. The number of inputs *nIn* is determined by the size of the feature vector $\boldsymbol{x}$. Here, the feature vector should have the size of total learned MAC address in the offline phase. Each neuron in the output layer is corresponding to a fingerprint. Thus, the number of outputs *nOut* is the number of chosen fingerprints in the environment. The number of neurons in the hidden layer, however, has no indicator. A two-third rule mentioned in (Heaton 2008) is applied as in Eq, 4.14. The network weight is randomly initialized within range of [0,1).

$$nHidden = \frac{2}{3}(nIn + nOut) \qquad 4.14$$

A soft-max activation function is employed for the classification task of the network. The general form of a soft-max activation function is:

$$P(y = j \mid \boldsymbol{x}) = \frac{e^{x^T w_j}}{\sum_{i=1}^{n} e^{x^T w_i}} \qquad 4.15$$

Where w_j is the weight of corresponding input in **x**.

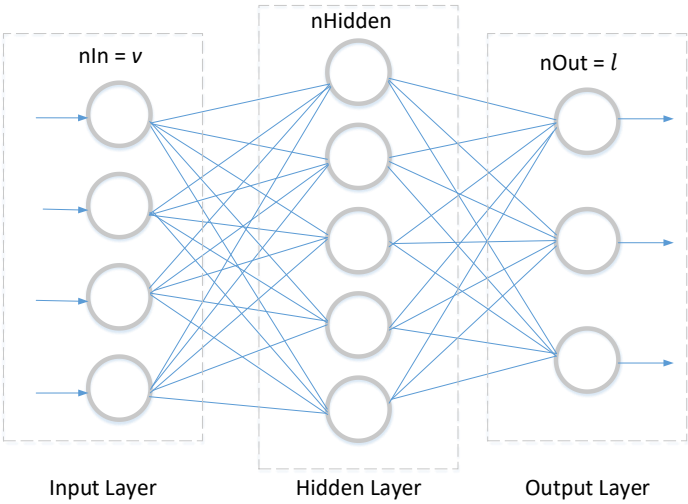

Figure 4.14 Fully connected neural network with 1 hidden layer

In case of Wi-Fi fingerprinting localization for intelligent vehicles, given the hybrid database proposed above, a bootstrap database is explained as in Figure 4.15. By randomly select with replacement each row of the original hybrid database, a new bootstrap database is constructed.

Since the original hybrid database is constructed with both *dynamic scan* and *static scan*, with a large *K*, bootstrap databases may include following possibilities: *dynamic-dominant*, *static-dominant*, *fingerprint-dominant*, *neutral* database.

A *dynamic-dominant* bootstrap database is a database with mostly dynamic scans. Estimators that learn those data should perform well on inputs from relatively high movement speed of the vehicle. On the other hand, a *static-dominant* bootstrap is constructed mostly static scans. These databases deliver better output for data from a low speed movement. A *fingerprint-dominant* bootstrap database has majority of the scans (both dynamic and static) for a single fingerprint only. Estimators with this type of dataset should be accurate only on the given fingerprint. Finally, a *neutral* bootstrap database possesses the similar characteristics of the original hybrid database with both dynamic and static scans for multiple fingerprints. These databases reflect a fair view of a subset of fingerprints in the environment.

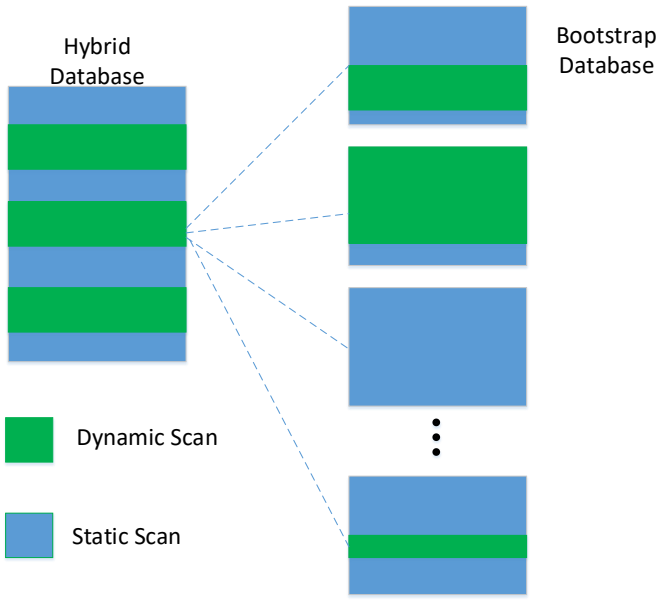

Figure 4.15 Boostrap hybrid database

Having those different perspectives on the original hybrid database, the set of estimators built upon those views with the same neural network structure should be diverse. This help eliminating noise from the database as well as reducing data variance. At the same time, each of those estimators perform better than a random guess. With the number of fingerprints l increases, the chance for a correct random guess $\frac{1}{l}$ decreases and becomes insignificant. Also, each of those estimators should be accurate with a particular input case. Hence, the diversity and accuracy conditions for each estimator are satisfied with a large l.

The Wi-Fi fingerprinting localization problem is now viewed as a standard supervised classification problem where a newly scan vector **x** of RSSIs in the online phase will be fed into each bootstrap estimator as in Eq. 4.16. The returned result of each classifier is a list of fingerprints IDs FP_i and its confidence $\hat{c}_i$. Note that l is the number of fingerprints in the entire environment.

$$\hat{g}(\boldsymbol{x}) = \{FP_i, \hat{c}_i | i = 1,2,..,l\} \qquad 4.16$$

The sum of all fingerprints' confidence should be equal to 1:

$$\sum_{i=1}^{l} \hat{c}_i = 1 \qquad 4.17$$

The final aggregated ensemble results is also a list as in 4.18

$$\widehat{g_{bagging}}(\boldsymbol{x}) = \{FP_i, c_i | i = 1,2,..,l\} \qquad 4.18$$

Where the bagging confidence is calculated as in Eq.4.19

$$c_i = \frac{\sum_{j=1}^{K} \hat{c}_{i,j}}{\sum_{i=1}^{l} \sum_{j=1}^{K} \hat{c}_{i,j}} \qquad 4.19$$

In general, the fingerprint with the highest confidence score will be selected as the final output. Consequently, its coordinates will be the localization result for the Wi-Fi fingerprinting localization.

4.4 Experiments and Results

Experiments for the proposed method are carried out in an open parking space of the INRIA Rocquencourt campus. Due to difficulties in having an indoor carpark for experiments, the outdoor space is utilized. At the same time, this outdoor carpark benefit from a precise RTK-GPS for localization ground truth. This allows a better evaluation of the system. The testing area is shown in Figure 4.16.

Figure 4.16 Testing area in INRIA Rocquencourt campus

There are two vehicles in the experiments: a blue Cybercar designed as a prototype for intelligent vehicles and a red Citroen C1 with modification for experimental purposes. The two vehicles are shown in Figure 4.17.

Figure 4.17 Blue Cybercar and Red Citroen C1

Both vehicles are equipped with a Wi-Fi receiver, a RTK-GPS receiver, an IMU system and two LiDAR sensors (front and back). The average movement speed across all experiments is around 2.5m/s to 3.0m/s.

4.4.1 Survey of the Wi-Fi Characteristics in the Experiment Area

A quick survey of the testing are is carried out to understand the Wi-Fi signal characteristics. The RSSI received from an access point is measured in dBm and generally in the range of (0, -100dBm]. Applying normalization in Eq. 4.6, the RSSI signal becomes:

$$x_i = \begin{cases} -1, & AP_i\ undetected \\ [0,1)\ , & AP_i\ detected \end{cases} \qquad 4.20$$

As the signal strength becomes extremely weak at approximately -100dBm, x_i goes to zero. Based on Eq.4.20, a heat map of Wi-Fi signal strength indicating the average signal strength in the environment is built as in Figure 4.18. Here, the darker the color, the lower the average Wi-Fi signal strength received from all reachable Wi-Fi access points. Note that only the road area is surveyed, the rest of the environment is in black as there is no recorded data.

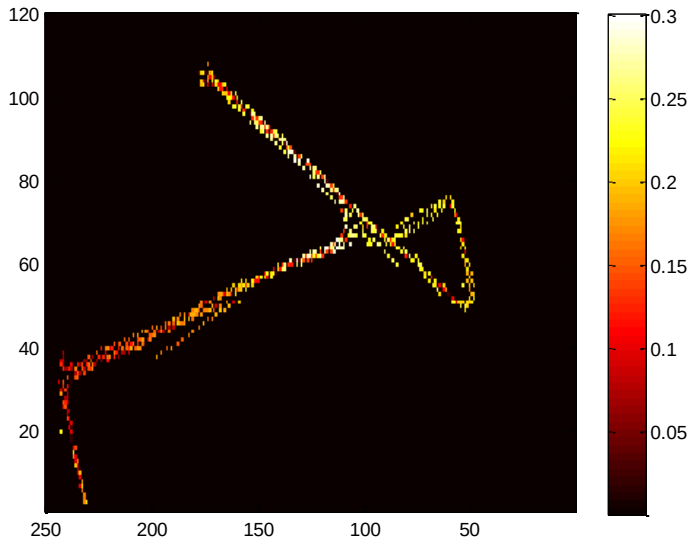

Figure 4.18 The Wi-Fi heat map of the testing area

There are thirteen reference points showed in Figure 4.19. At each of these locations, the number of detected access points (with distinct MAC addresses) is recorded in Figure 4.20. Having the idea of the surrounding environment, only few key reference points are chosen to survey. Area from reference point 1 to 9 is surrounded with buildings and a dense Wi-Fi access points' network thus the distances between these reference points are shorter. Other reference points from 10 to 13 are expected to have low signal quality due to the obstruction of trees, metal objects, etc. For instance, the reference point 11 has more than 20 detected access points but the average signal strength received from these access points is only around 0.15 (~ -85dbm). In contrast, reference points 4 and 5 have a low number of detected access points but the average signal strength around 0.2-0.25 (-75dbm to -80dbm). This is because the distance

of these reference points to buildings (with Wi-Fi access points) are high but there is no obstruction.

Figure 4.19 13 Reference points in the environment

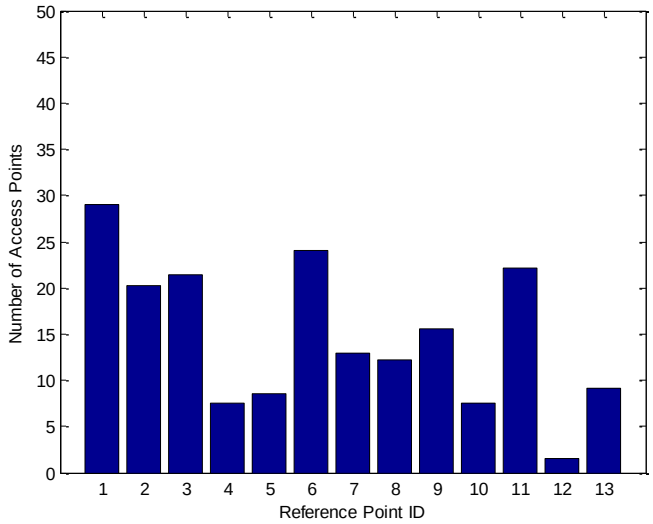

Figure 4.20Number of detected access points for each reference point

An ensemble neural network for localization in the area with only these thirteen reference points as fingerprints is used. For each fingerprint, 30 records of static scans and 20 records of dynamic scans were used as the offline database. Table 6 shows the localization error after 10 runs of the Cybercar which visits all fingerprints in each run.

Table 6 Wi-Fi fingerprinting localization using 13 fingerprints

Total Distance	*Mean error*	*RMS error*	*Maximum error*
1264	5.77m	6.85m	16.48m

A distribution of the localization errors for each fingerprint is illustrated in Figure 4.21. Interestingly, the result suggests a weak correlation between the number of access points

detected and the localization error. This is shown in fingerprints 5 and 10 as the localization accuracy is high despite the number of detected access points is low (compare to other fingerprints).

Still, the obtained result demonstrates a strong correlation between the average recorded Wi-Fi signal strength and the accuracy of the localization. It is further confirmed in Table 7. The average Wi-Fi signal strength here is computed from input RSSIs vector in the online phase of Wi-Fi fingerprinting localization. With a higher average signal strength, the localization result tends to be more accurate.

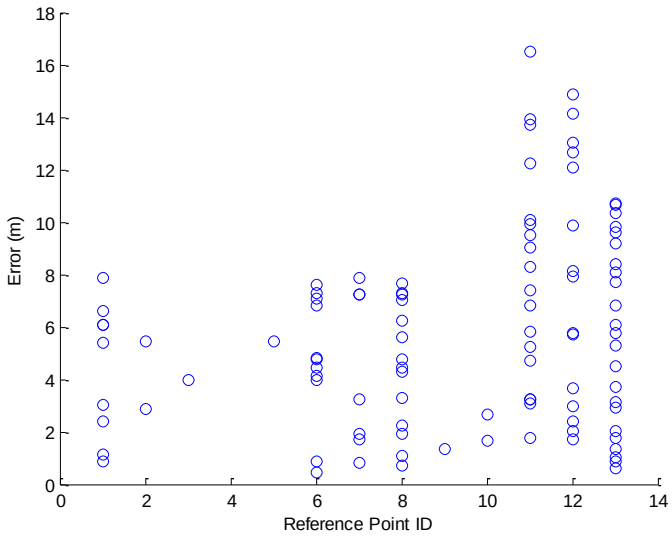

Figure 4.21 Distribution of localization error for each fingerprint

Table 7 Correlation between the average Wi-Fi signal strength and the localization error

Average Wi-Fi Signal Strength range(dBm)	*Average Localization Error (m)*	*Maximum Localization Error (m)*
(-100, -70]	6.85	16.48
[-80, -70]	4.76	13.02
[-75, -70]	3.89	7.05

Also, as illustrated in the Wi-Fi heat map Figure 4.18, the fingerprints 10, 11, 12 and 13 has a much lower average Wi-Fi signal strength compared to fingerprints 1-9. A cumulative distribution of the localization error excluding the results from fingerprints 10-12 is showed in Figure 4.22. At 90% of confidence, the localization error is under 7.5m.

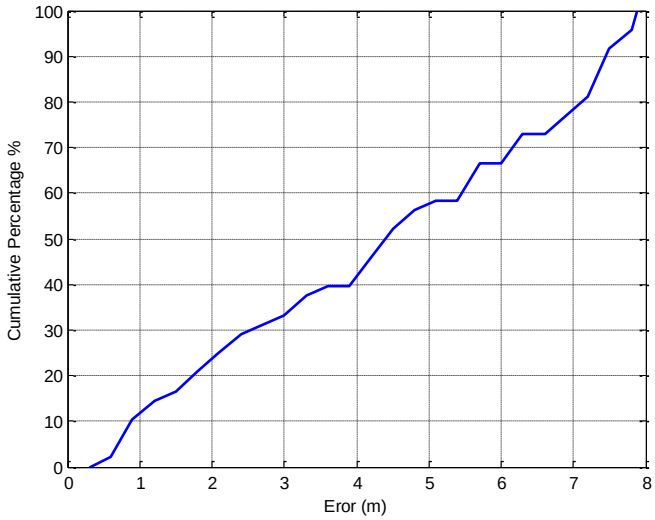

Figure 4.22 Cumulative distribution of the localization error for fingerprints 1-9

4.4.2 Wi-Fi localization Experiments

It is a realistic expectation to have a good average signal strength for the carpark area in the real life scenario. Thus, the experimental area is restricted to the area covered by fingerprints 1-9. Also, the number of fingerprints as well as the location of each should be chosen according to the argument in Section 4.3.1.

In Figure 4.23, fingerprint locations are marked with red circles. The average distance between two adjacent fingerprints is 6.1m as this is the upper-bound of the inter-distance between fingerprints discussed in Section 0. With this inter-distance, it takes only 25 fingerprints to cover the testing area.

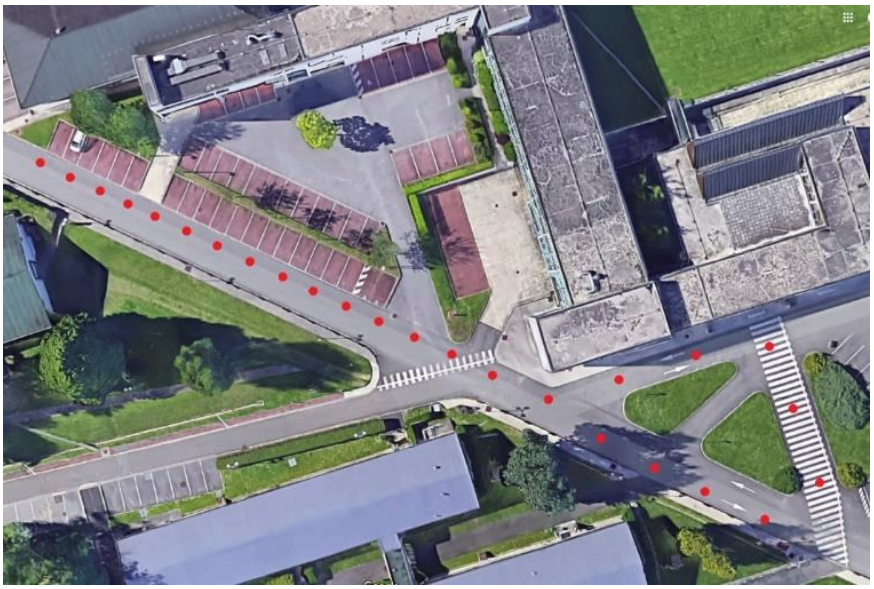

Figure 4.23 The experiment area with 25 fingerprints

For each fingerprint, 60 static scans and 20 dynamic scans are recorded for the offline database. A total 156 access points with different MAC addresses are detected across 25 fingerprints. By apply the rule in Eq.4.14, an individual neural network in the ensemble has the architecture as following:

$$nIn = 156; nOut = 25; nHidden = 120 \qquad 4.21$$

The number of individual neural networks is K = 50. For each network, a 10 random early-restarts in the training phase (Magdon-Ismail and Atiya 2000; Prechelt 2012) is applied in order to avoid local optimum.

A 10-fold cross-validation test with 80% data for the training set, 10% data for the validation set and 10% data for the test set is performed on the neural network structure with the hybrid training database. The average cross-entropy error is low at 0.428 which indicates a good generalization error of the network architecture.

One of the major issues with this classification approach is that in real life, there are inputs which do not match with any specific class (i.e a RSSIs vector collected in between two adjacent fingerprints). Theoretically, these inputs should not be classified into any class. However, as the Wi-Fi fingerprinting localization acts as a global level of localization system, it should give a good indication of absolute positioning of the vehicle. Thus, we then define a *good classification result* of the neural network as the closest fingerprints to the ground truth in Euclidean distance. As mentioned in Eq. 4.18, result from the Ensemble Neural Network is a list of fingerprints' indices and their corresponding confidence. Assume that the highest confidence fingerprint is chosen as the final classification result, it is a good classification result if:

$$dist\left(FP_{c_max}, Ground\ Truth\right) = min\{dist(FP_i, Ground\ Truth)\} \qquad 4.22$$

Here *dist* is the Euclidean distance function. Similarly, all other fingerprints can be examined. Table 8 shows the statistical of good classification rate if classification result is chosen from top 3 highest confidence fingerprints. Those results are obtained from 64 test runs in one year period with 9058 classification estimation.

In the classification approach for Wi-Fi fingerprinting localization, the fingerprint with the highest confidence score will be selected as the localization result. However, based on the statistic above, a threshold θ for the confidence score is set. The fingerprint with the highest confidence score is selected as the final result if only Eq.4.23 is satisfied.

$$c_{max} \geq \theta \qquad 4.23$$

A single run of localization experiment is shown in Figure 4.24. The red dot indicates a Wi-Fi localization result and the green one is the corresponding RTK-GPS ground truth. The threshold θ is set at 0.55. This threshold is set to ensure the significance of the highest score fingerprint compared to other fingerprints. If a classification result with a threshold below θ the result will not be acknowledged thus there is case where certain section of the moving path does not have a valid localization result.

Table 8 Top 3 highest confidence fingerprints as the classification result

Classification result among top highest confidence fingerprints	*Good classification rate*
1st	65.84%
1st – 2nd	72.63%
1st – 3rd	82.07%

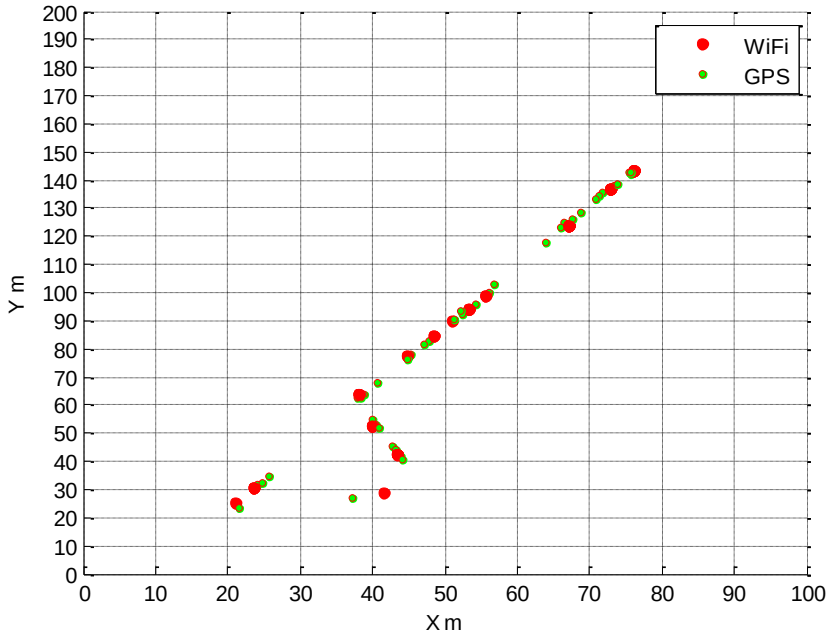

Figure 4.24 Localization result for 1 run

Table 9 Wi-Fi ensemble fingerprinting localization error

Method	*Maximum Error*	*Average Error*	*RMSQ Error*
Ensemble	6.84m	**2.25**m	**2.80**m
Single Neural Network	12.3m	5.9m	6.3m
Random Forest	**5.81**m	3.112m	3.32m
SVM (classification)	9.23m	4.01m	4.4m
SVM (Regression)	16m	9.34m	9.5m

A quick comparison of the Wi-Fi ensemble fingerprinting localization with other methods such as random forest, SVM, and Single Neural Network can be seen in Table 9. An improvement is observed compared to the survey results presented in previous section. With maximum error at 6.84m and average error of 2.25m, the performance of the Wi-Fi ensemble fingerprinting localization is equivalence to the performance of standard GPS mentioned in Table 1. Although a better maximum error is found in the random forest approach, ensemble method delivers a much better average localization error. Note that the random forest used in the experiment has 50 sub-trees which is equal to the number of individual neural networks in the ensemble method.

4.5 Discussion

This chapter presents a novel method of Wi-Fi fingerprinting localization using Ensemble Neural network for intelligent vehicles. To the best of the author knowledge, this is the first solution for localizing an intelligent vehicle using Wi-Fi signals. Other approaches are either for human walking or industrial robots. The only recent solution which applies for intelligent vehicle is mentioned in (Hernandez et al. 2017) has a much lower accuracy at 9.34m of average localization error.

Having defined the original Wi-Fi fingerprinting localization method, two significant changes are proposed in this thesis: an offline hybrid database and an online ensemble neural network for classification.

As discussed in Section 4.3.1, while the target of localization is moving, it is not always possible to characterize a fingerprint as one single position in the environment. In fact, depending on the target's movement speed, the distance that it moves to complete a Wi-Fi scan varies. This distance, defined as a *scan range*, has a critical impact on the offline phase map building complexity as well as the accuracy of the online phase localization. Based on the average movement speed of a car in a car park, this thesis defines a hybrid database with both dynamic and static fingerprints. Compared to the traditional static databases of fingerprints, this hybrid database is supposed to represent better the characteristics of the moving vehicle in a real life situation. This is justified in the improved localization accuracy from experiments with average error at only 2.25m. In addition, the author also discusses the optimal range for the inter-distance between two consecutive fingerprints in the environment. For a balance between complexity and accuracy of the problem, an inter-distance range from one *scan range* to two *scan ranges* is believed to be optimal.

Together with the hybrid database, an ensemble neural network is proposed to solve the problem of high variance and high noise in the Wi-Fi signal strength collecting process. At the start of this thesis, a thorough search of the relevant literature did not yield any significant study that uses the method for the Wi-Fi fingerprinting localization. Only recently studies from (Torres-Sospedra et al. 2016; Ta et al. 2016) which embrace the ensemble strategy for the Wi-Fi fingerprinting are found. These studies achieve a significant boost in accuracy of 3.39m for localization. However, these are studies for human localization using smartphone which has two fundamental differences with the vehicle localization problem: movement speed and hardware consistency. If the movement speed of a human is expected to be much lower than a vehicle, then the hardware (more specifically the Wi-Fi antenna) of a smartphone has a much lower consistency than a dedicated Wi-Fi antenna for a vehicle. Hence, it is difficult to make a direct comparison between the Wi-Fi fingerprinting localization performance for human using a smartphone and intelligent vehicles using a dedicated antenna. Therefore, in Section 4.3.2, the ensemble method is presented only for intelligent vehicles localization case using the hybrid database which is mentioned previously. A quick comparison with other solutions such as Random Forest, single neural network, SVM classification or SVM regression (Hernandez et al. 2017) shows that the ensemble neural network with hybrid database provides a higher accuracy than the other approaches.

With the fingerprints' coordinates measured in global coordinate framework (WGS84 standard), this solution can be directly compared to the outdoor performance of the Global Positioning System (GPS). With only 2.25m of average error, in an environment with high density and quality of Wi-Fi signals, this solution out-performs the GPS. Naturally, this is also true for the GPS-denied area. Hence, the Wi-Fi fingerprinting localization can provide a smooth transition for global localization from GPS-aided area to GPS-denied area.

Finally, with the Wi-Fi system is often readily available, this solution can be deployed quickly in urban area such as car park. Also, the mapping phase of the Wi-Fi fingerprinting localization is much simpler at low cost compared to other methods such as camera-based or Lidar-based. This is achieved because instead of building a continuous detailed map of the environment, the Wi-Fi fingerprinting localization system creates a discrete map of fingerprints to represent the environment. The characteristic benefits both the initial deployment process and the map correction later on.

5. FUSION STRATEGY FOR LOCALIZATION ENHANCEMENT

Résumé

Ce chapitre présente un cadre de fusion pour le système de localisation de parkings utilisant plusieurs capteurs, notamment: l'empreinte Wi-Fi, l'IMU et le laser-SLAM. Pour compléter le faible taux d'échantillonnage, la localisation absolue à partir des empreintes Wi-Fi, un filtre à particules modèle de mélange gaussien est utilisé. Avec les entrées haute fréquence de l'IMU ou du laser-SLAM, les particules du filtre à particules évoluent en temps réel. Une fois que l'observation du système de localisation d'empreintes digitales Wi-Fi est disponible, une correction à l'aide de la fonction d'évaluation du mélange gaussien est effectuée pour éliminer l'erreur accumulée.

Une contribution majeure de ce chapitre est la fonction de notation du mélange gaussien, qui permet au filtre à particules de récupérer d'une mauvaise position initiale et de mauvaises observations pendant le mouvement. Tout d'abord, comme indiqué à la section 5.6.1.1, une bonne estimation de la position de départ augmenterait considérablement le taux de convergence du filtre à particules. L'utilisation du mélange de quelques empreintes digitales supérieures comme position initiale permet non seulement à la particule de converger plus rapidement, mais élimine également toute condition nécessaire au démarrage du système de localisation (c'est-à-dire à partir d'une position connue). De plus, même avec une mauvaise position de départ, la fonction d'évaluation du mélange gaussien aide la particule à converger

rapidement. Ceci est montré dans les résultats d'expériences de cas de test où la position initiale est en dehors de la zone d'empreinte digitale. L'erreur de localisation est rapidement réduite lorsque le véhicule se rapproche d'une empreinte digitale. Deuxièmement, les observations du système de localisation d'empreintes digitales Wi-Fi ne donnent pas toujours une bonne estimation de la position réelle. Au lieu de cela, il s'agit d'un cas de test réel présenté dans la section 5.3.2, dans lequel le résultat de classification de confiance le plus élevé de la localisation d'empreintes digitales Wi-Fi n'est pas un bon résultat de classification. Cependant, la fonction de notation du modèle de mélange gaussien donne au filtre à particules une chance de surmonter une telle situation en prenant en compte les autres résultats de classification supérieurs qui devraient théoriquement rapprocher l'estimation de la position réelle.

Une autre proposition intéressante de ce chapitre concerne la stratégie visant à fusionner le SLAM laser en un système de coordonnées global sans recourir à un processus d'initialisation ou à une carte laser prédéfinie. Contrairement aux autres solutions mentionnées au chapitre 2, ce framework de fusion ne nécessite pas de position initiale soigneusement calibrée pour le SLAM laser ni de carte prédéfinie pour la formulation d'une matrice de transformation entre la coordonnée SLAM et la coordonnée globale. Au lieu de cela, tirant parti de la haute précision du SLAM dans l’estimation par pas local, le cadre de fusion incorpore le laser-SLAM en tant qu’IMU, ce qui réduit le besoin d’une matrice de transformation.

Au cours d'une année d'expériences, la fusion de la localisation des empreintes digitales IMU et Wi-Fi est testée avec différents critères tels que: la stabilité du filtre à particules, le nombre de particules et le comportement du système avec différentes positions de départ.

Pour comprendre la stabilité du filtre à particules conçu, le système de fusion est testé sous deux perspectives: plusieurs exécutions sur le même jeu de données et différents jeux de données. Dans la première perspective, un seul jeu de données est introduit indépendamment dans l'algorithme pour 100 itérations. L'erreur de localisation moyenne et son écart type sont calculés au-dessus des 100 itérations. Une erreur moyenne faible (environ 0,8 m dans tous les cas et 0,5 m pour une bonne position de départ), ainsi qu'un faible écart type (~ 0,22) indiquent que le filtre à particules est stable. Pour la deuxième perspective, un total de 84 expériences indépendantes ont été menées. Les résultats finaux donnent un résultat similaire avec une erreur moyenne et un écart type de 0,859 m et 0,232 pour tous les cas et de 0,588 m et 0,127 pour une bonne position initiale. Ainsi, il a été prouvé que le filtre à particules conçu est stable.

Le nombre de particules dans un filtre à particules (ou sa dimension) est également un paramètre important. Cela détermine les ressources nécessaires pour que l'algorithme s'exécute en temps réel. Pour apprendre ce paramètre, différents nombres de particules sont testés dans le même jeu de données. Enfin, avec seulement 2000 particules, la solution de fusion est capable d'obtenir un résultat optimal.

Différentes positions initiales pour les tests sont également étudiées pour comprendre la généralisation de l'algorithme. Il existe deux possibilités de lieu pour la position initiale: à l'intérieur ou à l'extérieur d'une zone d'empreinte digitale. Si la position initiale est dans une zone d'empreinte digitale, une bonne estimation initiale peut être attendue. Cela se traduit par une faible erreur de localisation moyenne de 0,588 m. Sinon, comme le filtre à particules a besoin de temps pour converger vers la position vraie, l'erreur de localisation moyenne dans ce cas est d'environ 0,859 m. Cette erreur moyenne élevée est principalement due à la grande erreur de positionnement initiale. En outre, il est raisonnable de s'attendre à ce que la position initiale d'un véhicule entrant dans un parc de stationnement soit relativement connue. Par conséquent, une bonne précision peut être attendue du système de fusion en général.

Bien que la vitesse de déplacement moyenne dans toutes les expériences soit d'environ 3,3 m / s, il est possible d'étendre le résultat de la thèse à une vitesse de déplacement supérieure. Pour ce faire, il faut trouver une solution permettant d'améliorer la fréquence d'échantillonnage de localisation des empreintes digitales Wi-Fi. Une solution potentielle consiste à utiliser plusieurs antennes Wi-Fi avec différents processeurs, chacun ayant un léger retard par rapport à l'autre. De cette manière, la fréquence d'échantillonnage du balayage Wi-Fi peut être augmentée proportionnellement au nombre d'antennes. Malheureusement, avec un temps limité, la thèse n'a pas pu être étendue pour couvrir l'idée.

Enfin, le cadre de fusion proposé permet non seulement de fusionner les empreintes Wi-Fi avec d'autres capteurs, mais il est également possible de combiner différentes stratégies telles que le GPS avec SLAM laser, le GPS avec système de localisation par caméra, etc. Cela étant dit, ce cadre peut être appliqué à plusieurs scénarios, mais pas uniquement à un sans GPS environnement ou à un parking privé.

5.1 Introduction

Up to this section, a global localization strategy for intelligent vehicles using Wi-Fi is presented. Chapter 4 proves that the Wi-Fi fingerprinting localization is capable of matching the standard GPS performance. However, at around 1Hz of sampling rate, both the Wi-Fi fingerprinting

system and the standard GPS are failing to track a moving vehicle at a relatively high speed. This problem is commonly solved by integrating other sources of location estimation into the system to smoothly increase the sampling rate as well as the positioning accuracy (N. E. El Faouzi, Leung, and Kurian 2011).

In fact, almost all localization systems are fusion systems of different sensors. For instance, approaches in (Carlson, Thorpe, and Browning 2010; Kim 2004; Amini et al. 2014; Schleicher et al. 2009) integrate the GPS absolute localization measurements into camera, laser or dead-reckoning localization system. These methods use the same tactics discussed in Chapter 2, with the GPS giving a raw global estimation while other sensors such as laser, camera, IMU, etc. offer local positioning. Results from the GPS and other sensors must be expressed in the same coordinate system to infer the final localization result. These methods often require an initialization process to find the transformation matrix between the sensors local coordinates system and the global one of the GPS.

Compare to a single sensor approach, a multiple sensors fusion localization system has advantages in terms of coverage range, adaptation and redundancy. Each sensor has a different coverage range. A laser sensor has the maximum measurement range from 20m up to 200m while most of cameras should have around 20-30m of effective range. In addition, under different environment conditions, sensors may not function properly. While the lighting conditions of the environment rarely influence the laser measurement accuracy, it has a major impact on the camera system performance. However, the camera system is superior when it comes to landmarks or objects detection and identification. Similarly, the GPS is globally accepted for the outdoor localization but is failed to perform in the indoor environment. Thus, a well-designed fusion system should theoretically adapt well to changes of the environment conditions (Kunz et al. 2015). Lastly, by having inputs from different sensor types, the system offers redundancy. Since each sensor has its own advantages and disadvantages, the combination of more than one sensor type's information may help to overcome each one's limitation.

In localization problem, there are several algorithms dedicated to sensors fusion such as Kalman filtering, grid-based Markov localization, Particle filtering or Neural Network etc. Those approaches can be split into three categories: Statistic based, Probabilistic based and Machine Learning based.

Statistical approaches often make use of weighted combination of sources. The weighting is based on statistical analysis of a recorded dataset (Han, Kamber, and Pei 2012). However, these approaches are not suitable when information from sensors are not exchangeable or when the performance of sensors are vastly different (N.-E. El Faouzi 1997).

Probability approaches use a distribution model to estimate weight of data. Methods such as Kalman filtering (Dongliang Huang and Leung 2004; Kalman 1960), Evidential theory (Trehard et al. 2014; Shafer 1976) or Particle filtering (Daum, Huang, and Noushin 2011; F.~Gustafsson 2010; Calvet, Czellar, and Ronchetti 2015) are some significant representatives of the category. They are widely used in recent solutions for localization.

Machine Learning approaches are quickly becoming a new popular solution as well. With algorithms such as neural networks, genetic algorithms and especially deep learning, these approaches deliver promising results (Moreira et al. 2019; Abdallah, Saab, and Kassas 2018). Those approaches rely on a huge database of training data to predict the true fusion parameters. They are commonly found in cameras system or WSNs (Zhang et al. 2016; Belagiannis et al. 2015; Iter, Kuck, and Zhuang 2016).

Table 10 Comparison of Algorithms for Nonlinear Filtering (Daum 2005)

	Extended Kalman Filter	*Unscented Kalman Filter*	*Particle Filter*	*Numerical Solution of Fokker-Planck Equation*	*Exact Nonlinear Recursive Filter*	*Batch or Non-recursive Filter*
Statistics propagated by the algorithm	Mean vector and covariance matrix	Mean vector and covariance matrix	Complete probability density conditioned on the measurement	Complete probability density conditioned on the measurement	Sufficient statistics	Mean vector and covariance matrix
Prediction of statistics from one measurement time to the next	Linear approximation of the measurement equations	Approximation of the multidimensional integrals using the "unscented transformation"	Monte Carlo Integration using importance sampling	Finite difference or other numerical solution of the Fokker-Planck PDE	Numerical integration of ODEs for the sufficient statistic in the exponential family of probability densities	Numerical integration
Correction of statistics at measurement time	Linear approximation of the measurement equations	Approximation of the multidimensional integrals using the "unscented transformation"	Monte Carlo sampling of the conditional density using both importance sampling & resampling	Bayes' rule	Bayes' rule for exponential family of probability densities	Numerical minimization of cost criterion

Accuracy of state vector estimate	Sometimes good but often poor compared with theoretically optimal accuracy	Often provides a significant improvement relative to the EKF, but sometimes it does not	Optimal performance for low dimensional problem but can be highly suboptimal for high dimensions as limited by real time computer speed	Optimal performance if designed carefully, but at the cost of enormous computational complexity for high dimensional problems	Significant improvement relative to the EKF for some applications	Significant improvement relative to the EKF for some applications
Computational complexity of real time algorithm	$O(d^3)$ for d-dimension state vectors	$O(d^3)$ for d-dimension state vectors	Overcomes dimensionality curse with a carefully designed PF	Suffers from the dimensionality for fixed grids	$O(d^3)$for most practical problem	$O(d^3)$for zero process noise, much higher if not.

In the scope of the thesis, it is not possible to explore each of those solutions mentioned above. However, since the problem of tracking and localization is often a non-linear problem with a huge solution space, machine learning approaches as well as classic Kalman filter do not always work. Statistical approaches suffer from noisy and biased data. A review of several non-linear filtering approaches can be found in (Daum 2005). Among them, particle filter appears to be a stand-out solution for nonlinear low dimensional problems. Thus, the particle filter, a non-linear filtering approach is chosen to be the fusion solution.

5.2 The Particle Filter

The Particle filter (Pitt and Shephard 1999) is a widely adopted framework for the localization and tracking problem. The general idea of the method is to use Monte Carlo algorithm for estimating the internal states in a dynamical system when there is a partial observation. Before the method became popular, the Kalman filter was used to solve this filtering problem. Often, Kalman filter provides optimal estimation for a linear Gaussian state-space model. However, when the linearity or Gaussian distribution is not guaranteed, other variants such as extended Kalman filter and unscented Kalman filter can be used. Still, for a highly non-linear and non-Gaussian problem, Kalman filters fail to deliver a reasonable estimation (Daum 2005).

Particle filter, on the other hand, offers an alternative approach to the problem. Instead of assuming the linearity of states as well as zero-mean Gaussian distribution of dynamic noise, the particle filter tries to predict the solution space with a propagation model on a discrete set of states known as particles. An importance sampling phase is applied each time based on observation to weight each of the particles and approximate the assumed distribution. In this way, the particle filter is able to deal with non-linear and non-Gaussian process. In general, a

particle filter has four main stages: Initialization, Prediction, Correction and Selection & Resampling as in Figure 5.1.

5.2.1 Initialization Step

In the *initialization step*, particles are generated randomly in the solution space. Consider N particles are generated in the solution space. N is also called the *dimension* of the particle filter. Without any *prior* knowledge about the environment, particles will be generated randomly (or rather uniformly) in the entire solution space. Consequently, every particle should have an equal weight $w_i = \frac{1}{N}$. However, if there is a partial observation available, particles can be spawned accordingly to reduce diversity.

5.2.2 Prediction Step

For a localization problem, the *prediction step* of particle filter usually embraces a motion model to move the particle cloud. Subject to the problem requirement, different motion models M are chosen to propagate particle $\boldsymbol{x}_i^t$ to $\boldsymbol{x}_i^{t+1}$.

$$\boldsymbol{x}_i^{t+1} = M(\boldsymbol{x}_i^t, v, \theta) \qquad 5.1$$

At this stage, there is no change in weight of each particle. More often, the vehicle's velocity v and heading angle θ are required for this step as in Eq.5.1.

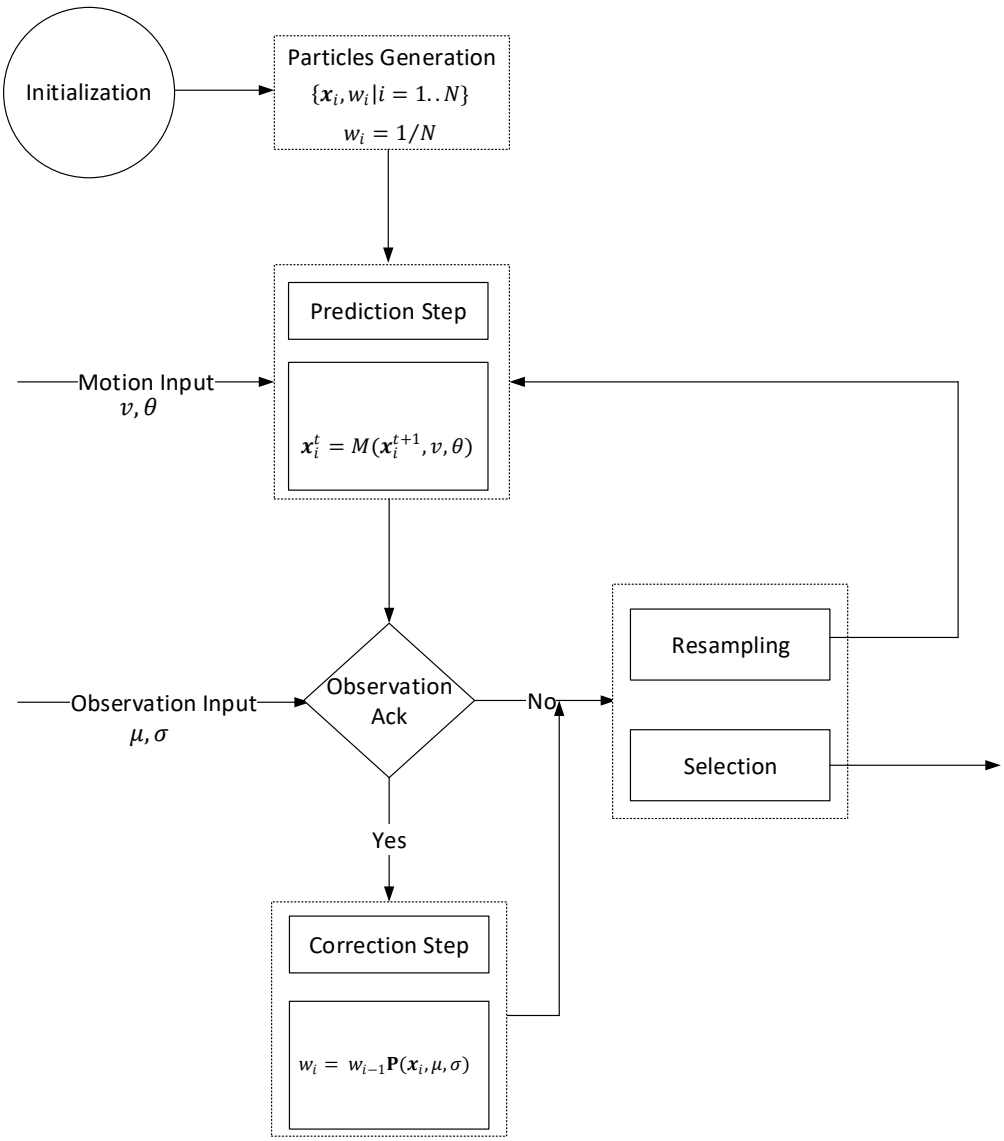

Figure 5.1 Particle Filter Flowchart

5.2.3 Correction Step

In case there is an observation available for the *correction step*, the correction will be carried out to update particles' weight based on the recorded observation. Here, a likelihood function is employed to be the scoring function for weight updating. For the Bootstrap particle filter version (Arulampalam et al. 2007), the particles' weight can be calculated directly from the likelihood function $\mathbf{P}(z^{\boldsymbol{t}}|\boldsymbol{x}^t)$ with z^t as the output vector (the estimated vehicle's state at time *t*) as following:

$$w_i^t \approx w_i^{t-1} \frac{\boldsymbol{P}(z^t|\boldsymbol{x}_i^t)\boldsymbol{P}(\boldsymbol{x}_i^t|\boldsymbol{x}_i^{t-1})}{q(\boldsymbol{x}_i^t|\boldsymbol{x}_i^{1:t-1}, z^t)} \qquad 5.2$$

Here, *q(.)* is the estimation of the *importance density*. *q(.)* denotes the chance for a particle at time *t* to be drawn randomly given the previous particles and the current state of the vehicle. Furthermore, with $q(\mathbf{x}_i^t|\mathbf{x}_i^{1:t-1}, z^t) \approx q(\boldsymbol{x}_i^t|\boldsymbol{x}_i^{t-1}, z^t)$, the Eq.5.2 can be written as:

$$w_i^t \approx w_i^{t-1} \frac{\boldsymbol{P}(z^t|\boldsymbol{x}_i^t)\boldsymbol{P}(\boldsymbol{x}_i^t|\boldsymbol{x}_i^{t-1})}{q(\boldsymbol{x}_i^t|\boldsymbol{x}_i^{t-1}, z^t)} \qquad 5.3$$

It is often convenient to choose the importance density *q(.)* to be the prior:

$$q(\boldsymbol{x}_i^t|\boldsymbol{x}_i^{t-1}, z^t) = \boldsymbol{P}(\boldsymbol{x}_i^t|\boldsymbol{x}_i^{t-1}) \qquad 5.4$$

Thus, substitute Eq. 5.4 for Eq.5.3, the weight of a particle can be calculated as:

$$w_i^t \approx w_i^{t-1}\boldsymbol{P}(z^t|\boldsymbol{x}_i^t) \qquad 5.5$$

Given that observation is available in this step, observation (μ, σ) is included in Eq. 5.5 with μ is the expected true position and σ is the standard deviation of the observation. Finally, particles 'weight is calculated as:

$$w_i^t \approx w_i^{t-1}\boldsymbol{P}(z^t|\boldsymbol{x}_i^t, \mu, \sigma) \qquad 5.6$$

Assume each particle is a potential pose of the target, substitute $z^t = x_i^t$ we have:

$$\boldsymbol{P}(x_i^t|\boldsymbol{x}_i^t, \mu, \sigma) = \boldsymbol{\mathcal{N}}(x_i^t, \mu, \sigma) \qquad 5.7$$

With $\mathcal{N}(\cdot)$ is the Guassian distribution function.

5.2.4 Selection & Resampling Step

Lastly, in the *selection & resampling step*, an estimation of the vehicle current location can be derived in multiple ways. This step includes two small steps: a required selection step and an optional resampling algorithm.

For the selection step, the goal is to find the final estimation for the vehicle position given a particles cloud and their weight. This could be done by picking the particle with the highest score:

$$\hat{\boldsymbol{x}}^t = \{\boldsymbol{x}_i^t | \, i = 1,2,..,N, w_i^t = max(w_1^t, w_2^t, .., w_N^t)\} \qquad 5.8$$

However, choosing only the highest score particle is potentially misleading since the entire particles cloud represents the likely distribution of the estimation around the ground-truth. Therefore, an expected value could be calculated to approximately reflect the estimation of the particle filter:

$$\hat{\boldsymbol{x}}^t = E[\boldsymbol{x}^t] = \sum_{i=1}^{N} \boldsymbol{x}_i^t w_i^t \qquad 5.9$$

Finally, a resampling process takes place to eliminate particles that have small weight and to concentrate more on particles with high weight. This resampling process also consisting of generating a new set of particles by resampling with replacement (bootstrap resampling). Those newly generated particles allow the particle filter to overcome the degeneracy issue (Doucet and Johansen 2011). The newly formed particles cloud will be fed into the *prediction step* for the next phase of position estimation. Still, repeated resampling in the absence of any actual sensory observation could lead to loss of diversity (the effective particles are randomly removed) and consequently fall into a local optimum (Drew Bagnell 2018). Thus, it is necessary to define when resampling is needed.

There are many different resampling algorithms for particle filter. However, four original approaches can be identified as: Multinomial resampling, Stratified resampling, Systematic resampling and Residual resampling. Other algorithms are built based on the idea of those algorithms. A comparison of those algorithms can be found in (Douc, Cappé, and Moulines 2005). As there is no clear winner among these, the multinomial resampling approach is adopted for this thesis.

The multinomial resampling (Efron and Tibshirani 1994) can be formally expressed as follows:

Generate *n* independent uniform random numbers in range (0,1]:

$$\{U_i \mid i = 1,2..n\} \in (0,1] \qquad 5.10$$

Select $\boldsymbol{x}_i$ according to the multinomial distribution:

$$\boldsymbol{x}_i = \boldsymbol{x}(F_w^{-1}(U_i)) \qquad 5.11$$

Here F_w^{-1} is the inverse of the cumulative distribution function associated with the normalized weight $\{w_i\}$ of particles. Thus, for $u \in \left(\sum_{j=1}^{i-1} w_j, \sum_{j=1}^{i} w_j\right)$ we have:

$$F_w^{-1}(u) = i \qquad 5.12$$

5.3 Gaussian Mixture Model Particle Filter

Given the definition of a particle filter above (more specifically a bootstrap particle filter), two significant changes are proposed to adapt to the problem in this thesis. Those changes are shown in Figure 5.2 below.

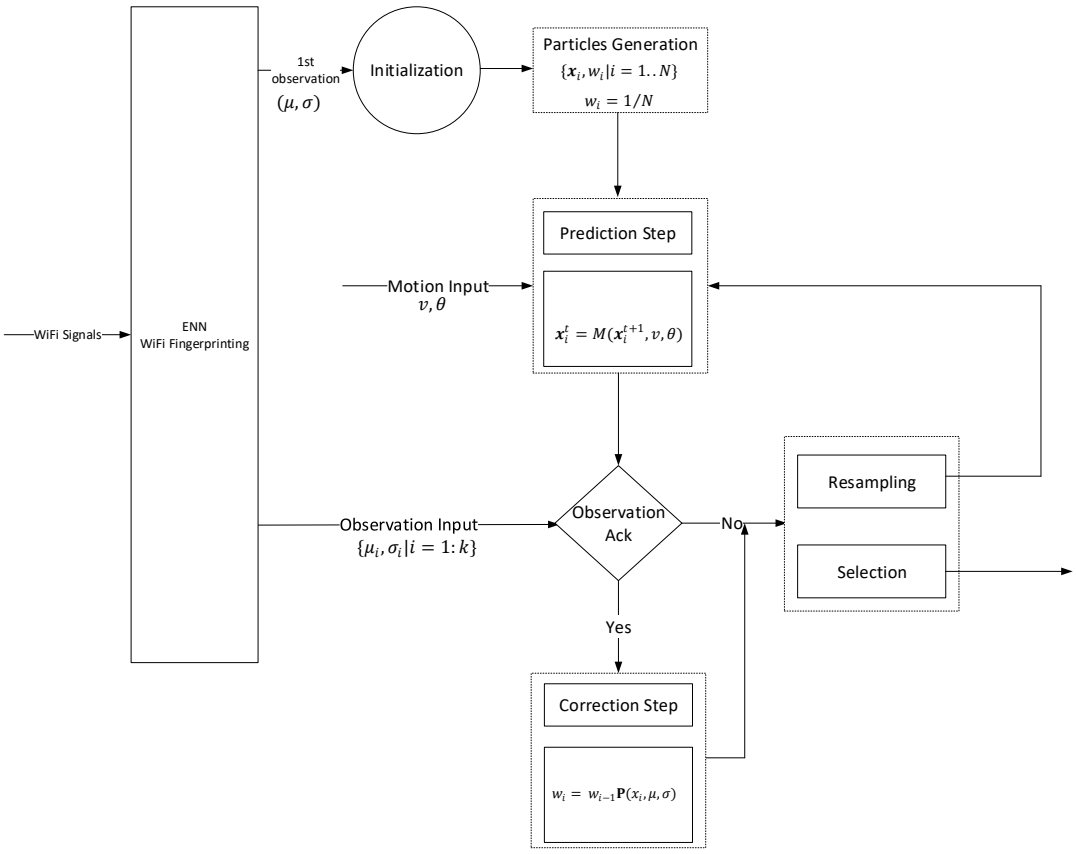

Figure 5.2 Particle filter and Wi-Fi fingerprinting flowchart

5.3.1 Initialization Step

Firstly, instead of randomly picking particles in the entire solution space in the initialization step, particles are now generated based on the first observation obtained from the Ensemble Neural Network (ENN) for Wi-Fi fingerprinting localization. As indicated in Chapter 4, the ENN will return a list of fingerprints and their corresponding confidence scores $\{FP_i, c_i \,|i = 1{:}\,m\}$. At this step, an aggregated sum of top k highest confidence fingerprints is calculated and assigned as the expected position. The standard deviation for this observation is calculated from the statistic of the Wi-Fi fingerprinting localization results in the previous chapter.

$$\mu = \sum_{i=1}^{k} FP^i c^i \qquad 5.13$$

$$\sigma = \sigma_{Wi-Fi} \qquad 5.14$$

Particles are then drawn around (μ, σ) with the Gaussian distribution. Using this initialization process, the particle filter will converge quicker due to the reduction of the solution space for particles generation and still maintain its correctness.

5.3.2 Correction Step

Secondly, a Gaussian mixture model is applied for the observation in the correction step. Similar to the initialization step, a top k highest confidence fingerprints will be taken into account for the correction. Eq.5.6 is then written as follows:

$$w_t^i = w_{t-1}^i \sum_{j=1}^{k} \frac{c^j}{\sum_{j=1}^{k} c^j} \boldsymbol{P}(\boldsymbol{x}_t^i | \sigma_t^j, \mu_t^j) \qquad 5.15$$

Here, μ_t^j is the jth highest confidence fingerprint FP^j and σ_t^j is related to the measured standard deviation of the Wi-Fi fingerprint as follows:

$$\sigma_t^j = 1 - \frac{c^j}{\sum_{j=1}^{k} c^j} \sigma_{Wi-Fi} \qquad 5.16$$

The underlying assumption in Eq.5.16 is as the confidence of the fingerprint becomes lower, its standard deviation should increase.

Assume that the mixture distribution follows a Gaussian distribution then Eq. 5.15 is:

$$w_t^i = w_{t-1}^i \sum_{j=1}^{k} \frac{c^j}{\sum_{j=1}^{k} c^j} \frac{1}{\sqrt{2\pi(\sigma_t^j)^2}} e^{-(x_t^i - \mu_t^j)/2(\sigma_t^j)^2} \qquad 5.17$$

The Gaussian mixture model is utilized to enhance the weighting function. Consider a case where three top fingerprints are chosen (k = 3). The normalized confidence scores for these fingerprints are 0.58, 0.277 and 0.143 respectively. An illustration of particle weight is shown in Figure 5.3. In this example, a 20m by 20m area is taken into account with each particle drawn in every 10cm cell with the same weight. Using the Gaussian mixture model scoring function in Eq.5.17, each particle's weight is calculated regarding the confidence score of each fingerprint. The final estimation is an aggregated sum of all particles with their weight as in Eq.5.18.

$$\boldsymbol{x}^t = \sum_{i=1}^{N} \boldsymbol{x}_i^t w_i^t \qquad 5.18$$

Unlike a single Gaussian model estimation approach where only the highest confidence fingerprint is chosen (k =1), the approach with Gaussian mixture model estimation allows the final estimation to be closer to the true position. This happens due to in single Gaussian estimation, if particles are generated uniformly over the entire solution space, then the final estimation should be at exactly the highest confidence fingerprint as in Figure 5.4. Thus, the Gaussian mixture model should deliver better estimation for particles' weight.

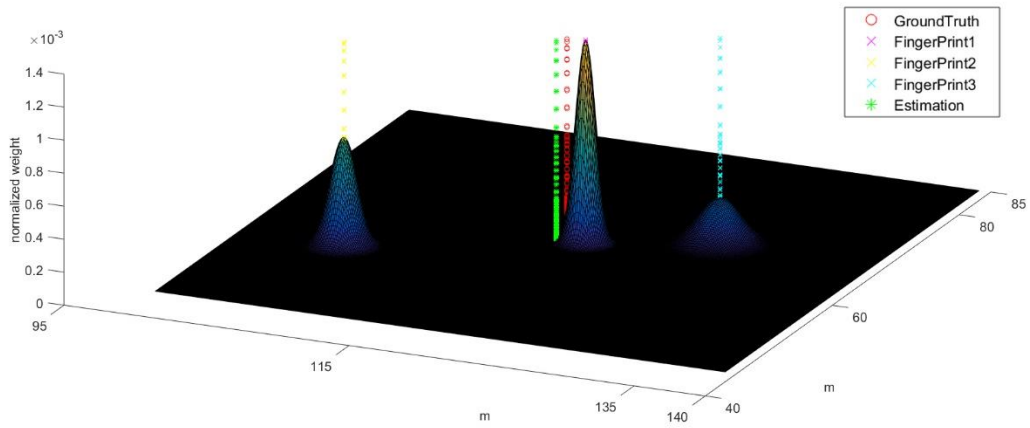

Figure 5.3 Gaussian Mixture Model Estimation

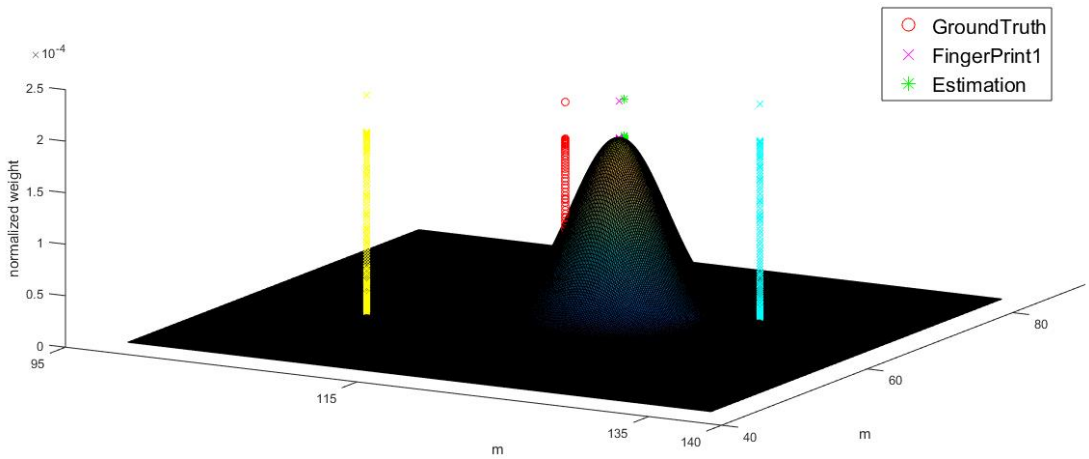

Figure 5.4 Single Gaussian Model Estimation

A real case scenario of the Gaussian Mixture Model in practice can be seen in Figure 5.5 and Figure 5.6. In the two figures, the fingerprints of the environment are shown in blues. The ground-truth and the estimated position are shown in green and yellow respectively. With three top highest confidence fingerprints are chosen for the Gaussian mixture model (k = 3), each of these fingerprints' confidence score is proportional to the red circle's size.

In Figure 5.5, the highest confidence fingerprint is also a *good classification* from the Ensemble Neural Networks (the closest to the ground-truth in terms of Euclidian distance – Section 4.4.2). The final estimation is carried out based on two factors: The propagated particles cloud from the previous step using the motion model and re-evaluation of the particles 'weights with new observations. With a good classification from the Ensemble Neural Networks, particles that are closer to the highest confidence fingerprint should also have higher weights. Suppose that the propagated particles cloud correctly covers the vehicle's true position (in the ideal case, the true

position is at the centre of the particles cloud) then the final estimation is expected to be accurate.

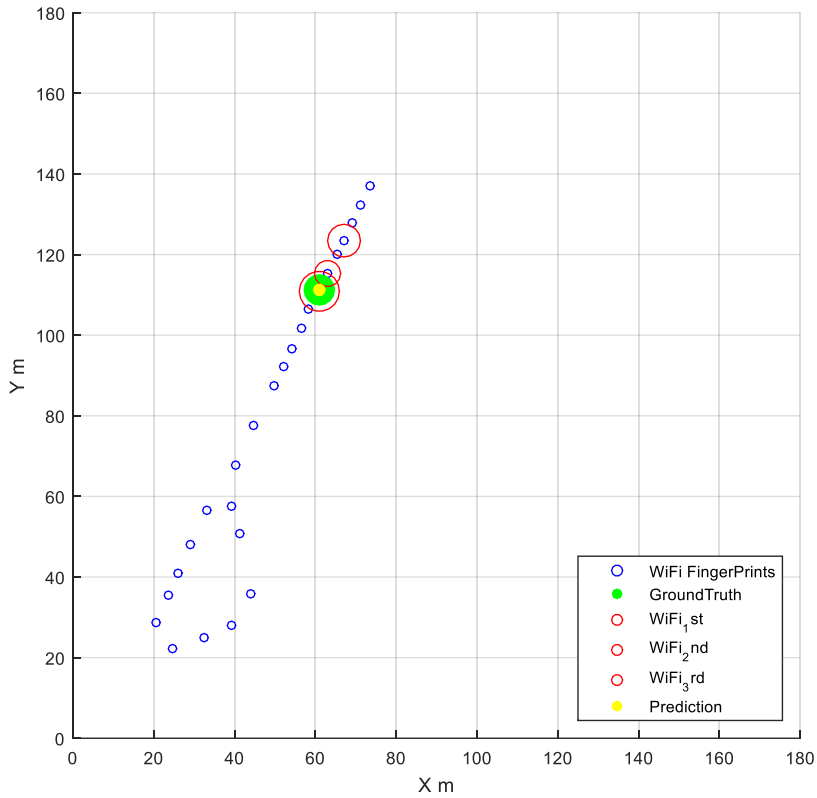

Figure 5.5 Gaussian Mixture Model in Practice 1

In contrast, Figure 5.6 shows a case where the highest confidence fingerprint is not a *good classification*. Instead, the second highest confidence fingerprint represents a *good classification* result here. If a single Gaussian model were adopted for only the highest confidence fingerprint, the estimated position would be pulled further away from the ground-truth as particles closer to the observation should have a higher weight. However, as the Gaussian mixture model approach is implemented, other observations should be able to negate the effect of the first observation.

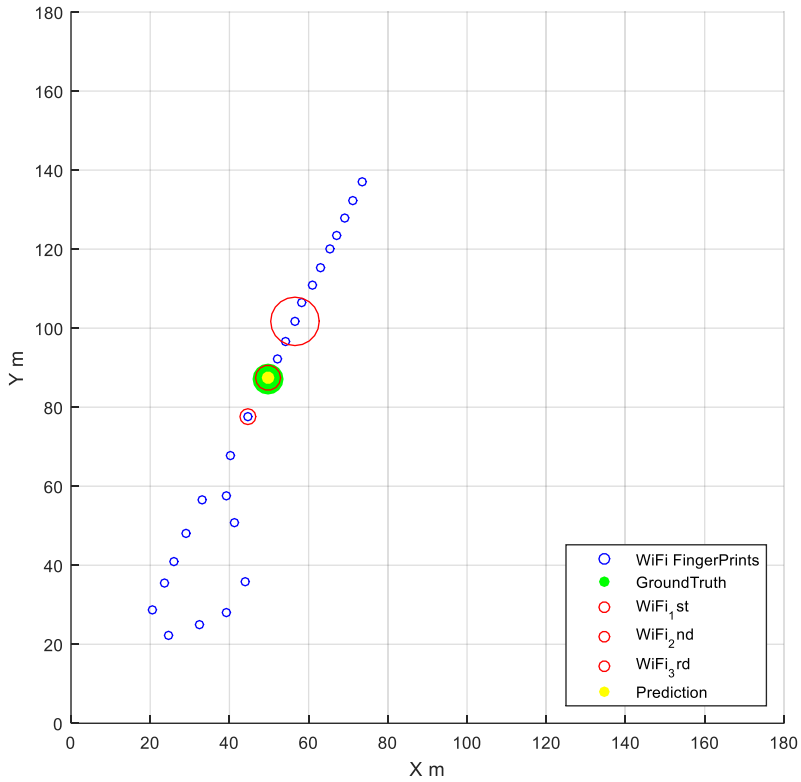

Figure 5.6 Gaussian Mixture Model in Practice 2

5.4 Fusion of Wi-Fi Fingerprinting and IMU

With the Gaussian mixture particle filter introduced above, it is important to discuss also the prediction phase where particles evolve. In the localization task, the main purpose of this phase is to move a particle from $\boldsymbol{x}_i^t$ to $\boldsymbol{x}_i^{t+1}$ using a motion model so that the distribution of particles at time t+1 still follows Eq.5.19:

$$P(\boldsymbol{x}_i^{t+1}|z^t) \approx w_i^{t+1} \qquad 5.19$$

Typically, an IMU (Inertial Measurement Unit) is used to provide necessary inputs for a motion model such as the vehicle velocity and its heading angle. The fusion strategy is shown in Figure 5.7.

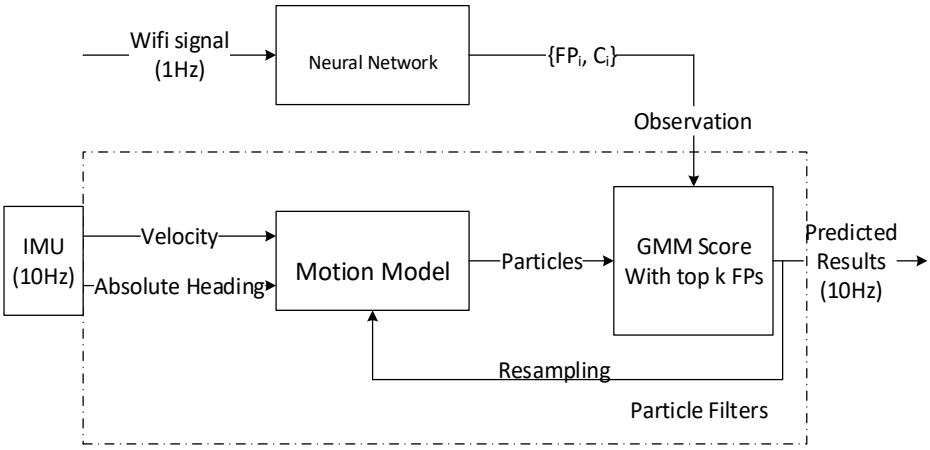

Figure 5.7 Gaussian Mixture Model Particle Filter with IMU and Wi-Fi fingerprinting

5.4.1 Inputs Synchronization

The fusion system above requires 3 different input signals: Wi-Fi signals for Wi-Fi fingerprinting localization, the estimated vehicle's current velocity and heading angle for the motion model. While the Wi-Fi signal is scanned at 1Hz frequency, the vehicle velocity and heading angle are available at 10Hz (from the IMU). Using the IMU input as the lead signal, the Wi-Fi signal will be synchronized using the condition in Eq.5.20:

$$\left|t_{wi-fi} - t_{IMU}\right| < \frac{1}{f_{IMU}} \qquad 5.20$$

Here, t_{IMU} represents the time of the latest IMU input sent to the system. Once IMU input received, the most recent Wi-Fi observation received time t_{wi-fi} is asserted with the above condition where f_{IMU} denotes the IMU sampling frequency. If the condition is met, the Wi-Fi observation is acknowledged and synchronized with the IMU input. Otherwise, only IMU input is recorded. As illustrated in Figure 5.8, in order to correctly predict the current movement of the vehicle, t_{wi-fi} must be chosen as the time of completion of a Wi-Fi scan.

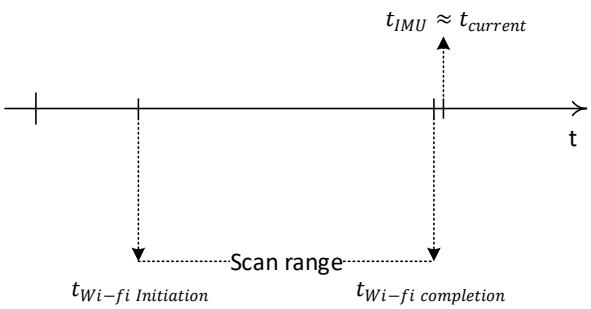

Figure 5.8 Input Synchronization Timestamp

5.4.2 Particles Propagation

One of the most notable advantages in this fusion strategy is the significant boost in the sampling frequency of the localization estimation compared to the Wi-Fi fingerprinting localization system. As the Wi-Fi fingerprinting localization suffers heavily from its low sampling frequency (1Hz) (refer to Chapter 4), not only delay in position estimation but also huge error in localization are expected. A much higher sampling frequency IMU (often from 10Hz to 100Hz) provides a decent fix. If there is no correction from Wi-Fi fingerprinting localization system is available, the particle filter with IMU will act as a dead-reckoning algorithm to deliver a position estimation. The correction from the Wi-Fi fingerprinting localization will be applied to eliminate the "drifting issue".

However, the low sampling frequency of Wi-Fi fingerprinting results in low correction rate of the particle filter. The rate between prediction and correction of the fusion solution is:

$$\gamma = \frac{f_{Wi-fi}}{f_{IMU}} \qquad 5.21$$

Often, the particle filter expects a rate of $\gamma \approx 1$. At every step, there should be an observation of the surrounding environment that allows the particle filter to update particles' weights. Without the correction step, the particles' weights will be propagated unchanged. Hence, no resampling required until a new observation is made.

5.4.3 Motion model

A constant acceleration motion model is employed for the prediction phase in the fusion with IMU. Given that the timing window between two consecutive IMU inputs is small, the acceleration of the vehicle can be assumed to be a constant. This leads to the following estimation of distance travelled:

$$d = \bar{v}\Delta t \qquad 5.22$$

Where d is the distance displacement (assumed to be linear in a short time), $\bar{v}$ is the average movement speed and Δt is the timing window. Since acceleration is a constant, the average speed $\bar{v}$ can be calculated as:

$$\bar{v} = \frac{v^{t-1} + v^{t}}{2} \qquad 5.23$$

With v^{t-1} is the known previous movement speed and v^{t} is the current vehicle movement speed (from the IMU).

For each particle $\boldsymbol{x}_i^t(x_i^t, y_i^t)$, with the absolute heading angle θ and the displacement distance d the coordinate is calculated as:

$$x_i^t = x_i^{t-1} + \bar{v}\Delta t cos(\theta) \qquad 5.24$$

And:

$$y_i^t = y_i^{t-1} + \bar{v}\Delta t sin(\theta) \qquad 5.25$$

However, the unbiased Gaussian noise of IMU measurement should be included as in:

$$\begin{pmatrix} \tilde{v} \\ \tilde{\theta} \end{pmatrix} \sim \mathcal{N}(\begin{pmatrix} v \\ \theta \end{pmatrix}, \begin{pmatrix} \sigma_v & 0 \\ 0 & \sigma_\theta \end{pmatrix}) \qquad 5.26$$

Thus, Eq.5.24 and Eq.5.25 can be rewritten as:

$$\begin{pmatrix} \hat{x}_i^t \\ \hat{y}_i^t \end{pmatrix} = \begin{pmatrix} x_i^{t-1} + \frac{\tilde{v}^{t-1} + \tilde{v}^t}{2}\Delta t\ cos(\tilde{\theta}) \\ y_i^{t-1} + \frac{\tilde{v}^{t-1} + \tilde{v}^t}{2}\Delta t\ sin(\tilde{\theta}) \end{pmatrix} \qquad 5.27$$

This demonstrates that for each particle $\boldsymbol{x}_i^{t-1}$, a newly predicted particle $\boldsymbol{x}_i^t$ is drawn using the IMU inputs $\tilde{v}, \tilde{\theta}$ with their respective Gaussian distribution $\mathcal{N}(v, \sigma_v)$, $\mathcal{N}(\theta, \sigma_\theta)$. The resulting particle cloud therefore closely follow the prior density $p(z^t | z^{t-1}, \tilde{v}, \tilde{\theta})$.

5.4.4 Selection & Resampling

Regarding the IMU fusion solution, the resampling step is skipped when there is no new observation recorded. Without new observation, resampling the particles will likely to introduce diversity loss problem. Moreover, when there is a new observation, the resampling step is only required when the number of *ineffective particles* (particles with their weight approaching zero) is large. A large number of approximately zero weight particles would contribute to a significant part to the approximation of the assumed distribution and therefore distorts the result. In order to determine when the resampling is needed, we define a Coefficient of Variation (CV) as follows:

$$CV = \frac{VAR(w_i)}{E^2[w_i]} \qquad 5.28$$

With

$$VAR(w_i) = \frac{1}{N}\sum_{i=1}^{N}\left(w_i - \frac{1}{N}\sum_{i=1}^{N} w_i\right)^2 \qquad 5.29$$

And

$$E^2[w_i] = (\frac{1}{N}\sum_{i=1}^{N} w_i)^2 \qquad 5.30$$

Hence, the CV can be written as:

$$CV = \frac{1}{N}\sum_{i=1}^{N}(N \cdot w_i - 1)^2 \qquad 5.31$$

Using this coefficient, the Effective Particle Size (EPS) can then be calculated as

$$EPS = \frac{N}{1 + CV} \qquad 5.32$$

This number describes how many particles that have an effective weight (not approximately zero). If more than half of the particles are effective, the resampling process is not required.

$$EPS < \frac{1}{2}N \qquad 5.33$$

5.5 Fusion of Wi-Fi Fingerprinting, IMU and Laser-SLAM

For intelligent vehicles, one of the most commonly elaborated localization fusion systems is a fusion of GPS and laser-based SLAM. The concept of localization using laser-based SLAM, which is discussed in Section 2.3, has two key steps: building the map of the environment using laser scans while simultaneously determining the relative position of the vehicle to the newly built map. Coupling this method with GPS signals brings not only the possibility of translating local localization results to global ones but also allows to provide an absolute correction for the drifting issue of SLAM (Bresson et al. 2016; Boucher, Ababsa, and Mallem 2013). Fusion solutions for SLAM and GPS can be found in (Kim 2004; Carlson, Thorpe, and Browning 2010; Pierzchała, Giguère, and Astrup 2018; Levinson, Montemerlo, and Thrun 2008; Trehard et al. 2014). Thus it is interesting to discuss a potential integration of the IMU, the Wi-Fi fingerprinting system with a laser-SLAM which: (1) Enables the GPS-denied environment global localization and mapping (2) Allows smooth transition between GPS-denied environment to GPS-aided one and (3) Enhances localization results. In general, there are two ways to fuse the laser-SLAM with an absolute localization system: (1) translate SLAM into global coordinate frame approach and (2) SLAM as a highly accurate pseudo-IMU.

In the first approach, the SLAM local coordinate system needs to be translated into a global coordinate frame. To do so, there is a need for a proper translation and rotation matrix between the local coordinate system of SLAM and the global coordinate system. This could be done by

using an algorithm such as Iterative Closest Points (ICP) (Besl and McKay 1992). Unfortunately, the ICP algorithm requires a proper initial value and the approximate registration of two laser point clouds to prevent the algorithm from failing into local optima (Y. He et al. 2017; Agamennoni et al. 2016). These conditions are difficult to achieve in the real life situation. Another way to establish the transformation matrix is to use the absolute static map of the environment as a reference. However, any bias in the static map will also be included in the transformation matrix as well. Furthermore, obtaining a highly accurate static map of the environment such as a carpark is a costly task as well.

An alternative approach for fusing laser-SLAM with an absolute localization system is to use laser-SLAM as a highly accurate IMU. Since laser-SLAM returns local estimation of distance displacement as well as heading changes with the accuracy up to centimetres, it is possible to calculate the temporal velocity and yaw rate. This approach, however, cannot fully exploit the benefit of the detailed environment map created by laser sensors in the SLAM algorithm.

In this thesis, both approaches for fusing laser-SLAM with the Wi-Fi fingerprinting localization system are examined. Since we want to eliminate the complex initialization as well as map building process of the environment using SLAM, the thesis will only deal with first time SLAM case. This means the vehicle is assumed to have no prior laser map of the environment nor a complex ICP calibration for the starting point. Thus, it is expected that most SLAM solutions will suffer from the drifting issue.

One part of this thesis work is to investigate the possible fusion of Wi-Fi localization and laser-based SLAM. To the best of the author's knowledge, there is no current attempt to fusion those two interesting methods together. Two representative approaches for laser-based SLAM are chosen for further analysis: the evidential-based C-SLAM (Trehard et al. 2014) and the probabilistic-based PML-SLAM (Alsayed et al. 2015). A quick review of the two SLAM algorithms will be presented in this section.

5.5.1 Evidential SLAM

From the beginning, a probabilistic background is chosen for the Simultaneous Localization and Mapping (SLAM) problem. However, a new approach using the evidential theory is studied in an attempt to overcome the limitation of the classical one. The main argument is for the online-SLAM (or other Maximum-Likelihood SLAMs), only the maximum position is searched and propagated to the next time step. In addition, the constructed map is built with respect to the maxima. Hence, all uncertainties related to the vehicle pose and map states are simply

omitted from time to time. This is where a solution with evidential theory background comes in.

The evidential theory or more commonly the Transferable Belief Model Framework is proposed in (Smets and Kennes 1994; Shafer 1976). The theory provides a way to reasoning with evidences by using two levels of knowledge interpretation: (1) a *credal* level where beliefs are entertained and quantified by belief functions, (2) a *pignistic* level where beliefs can be used to make decisions and are quantified by probability functions. It allows reasoning on belief functions so that it handles better the case where an even cannot be completely described by a finite set of hypotheses.

Most of the probabilistic SLAM approaches assume a static world at a given moment then start to relax the condition later to track mobile objects. This assumption introduces uncertainties into the probability evaluation. By using the evidential theory, mobile objects are then better described in a grid-based map. As a consequence, a potential improvement for the SLAM performance in crowded situations is presented.

Using this core idea, an Evidential-SLAM algorithm is proposed and illustrated as in Figure 5.9. In this algorithm, a polar grid is used to represent a laser scan. Such illustration is well adapted to the characteristic of a LiDAR sensor as the scan the environment by firing consecutives laser beam to the surrounding. For each cell, instead of just two possible values occupied or free as in probabilistic approach, the evidential cell has four possibilities: Occupied, Free, Uncertain and Not-know. While cells with multiple contradicting sources of information is marked as uncertain, area without range of the laser sensor (or not explored) is labelled as not-known.

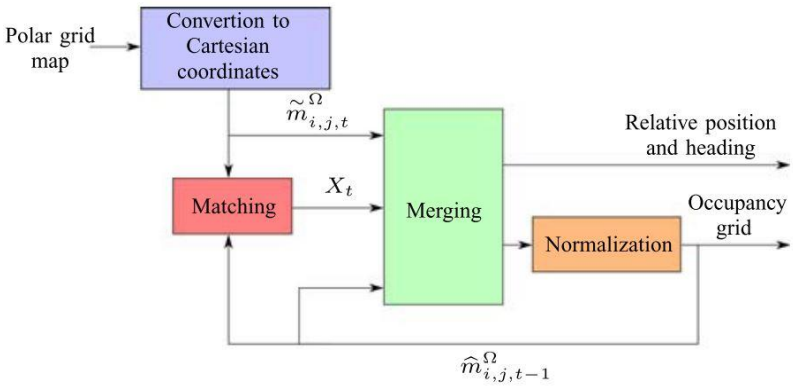

Figure 5.9 General architecture for Evidential SLAM (Trehard et al. 2014)

Each cell in the map is evaluated using Evidence Theory will have a basic belief assignment of following set:

$$2^{\Omega} = \{Free, Occupied, \Omega, \emptyset\} \qquad 5.34$$

Where

$$\sum_{x \in 2^{\Omega}} m^{\Omega}(x) = 1 \qquad 5.35$$

With *m* is defined as a mass (or a weight) of a hypothesis and *x* is all four possible cases.

A map is then estimated by comparing the information with the previous known map through the map matching process. Information will be merged (newly obtained map and old map) and the relative position of the vehicle is calculated.

Evaluation on the KITTI database shows a 1.3% of translation error and 6.2 degree of rotational error after a 2.2km test drive. Test drive and the localization result is shown in Figure 5.10.

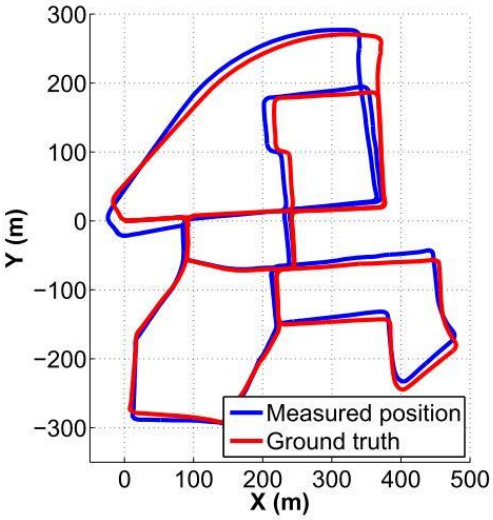

Figure 5.10 Evidential SLAM test drive in KITTI database (Trehard et al. 2014)

5.5.2 PML-SLAM

The PML-SLAM (stands for Probabilistic Maximum Likelihood SLAM) is a version of SLAM that belongs to the classical probabilistic background category. In contrast to the Evidential SLAM presented in section 5.5.1, the study in (Alsayed et al. 2015) proposes a complete solution with large scale map management, maximum likelihood scoring function and an adaptive parameter matching algorithm. The general architecture is presented in Figure 5.11.

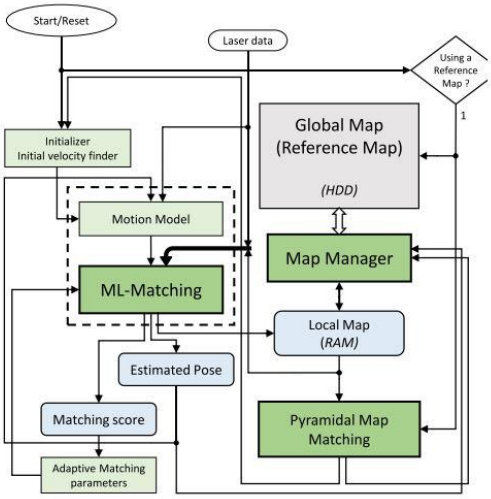

Figure 5.11 General flowchart of the PML-SLAM algorithm (Alsayed et al. 2015)

Although the maximum likelihood matching and grid map of this solution are generally similar to other probabilistic based SLAM approaches, the solution does propose a large scale environment map management which is crucial for a real life application. The solution is then validated on the KITTI database (Figure 5.12) with promising results of 5cm of displacement error and 0.3 degree of heading error. After more than 2.2km of traveling, the accumulated error in localization is about 6m with 0.1 degree of heading error. The deviation in distance and heading are shown in Figure 5.13.

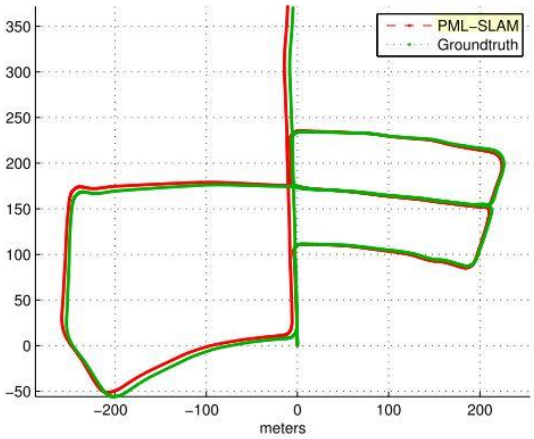

Figure 5.12 Test drive on KITTI database with PML-SLAM (Alsayed et al. 2015)

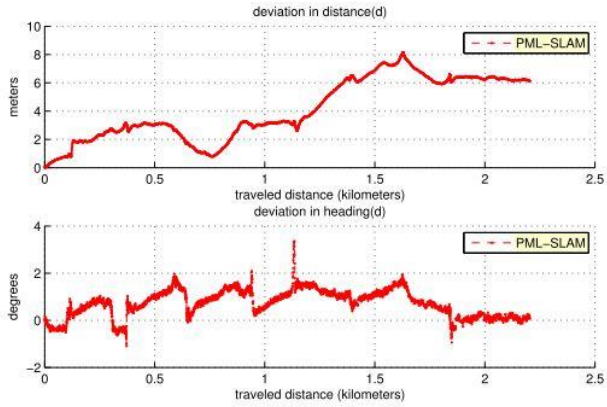

Figure 5.13 Deviation of distance and heading for PML SLAM (Alsayed et al. 2015)

Compare to the Evidential-based SLAM, the PML SLAM is a classical approach for the problem using the probability framework. While the evidential-based SLAM version has no map control algorithm (hence limitation in large scale positioning), the PML SLAM appears to be ready for a large scale environment localization and mapping.

5.5.3 SLAM in Global Coordinate Frame

Usually, the SLAM technique does not provide any link with global reference. It is an accurate relative localization system but does not provide result in any global coordinate frame. Still, as discussed earlier, there are number of advantages of fusing SLAM system with a global localization one. Those advantages are: (1) Enable drift correction, (2) Allow loop-closure in SLAM and (3) Provide rich semantic information of the surrounding environment. Given those advantages, it is tempting to translate the SLAM local coordinate frame into a global one and therefore giving a chance for possible fusion.

Without a pre-built map, the only way to translate the SLAM local coordinate frame into a global coordinate frame is to estimate the corresponding global coordinates to a SLAM local coordinates. The transformation matrix is then built upon this link. In theory, this task is feasible since it does not require any complex calculation. However, in practice, any error in measurement of the coordinate pairs could not be estimated easily. And this error, no matter how small, could lead to a potential huge drift.

In this thesis, an attempt to translate the local coordinate frame of SLAM into a global one is made. A transformation matrix can be calculated by having two arbitrary positions in SLAM local coordinates with its corresponding position in global coordinates using a highly accurate

RTK-GPS. This transformation matrix provides a possibility of fusing the Wi-Fi fingerprinting localization result into laser-SLAM.

In the original SLAM matching operator, a search for the maximum pose in a set of candidates at a given time are performed using the sensors readingz_t, control inputs u_t and a possible inclusion of the previous map s. The process is formularized in Eq.5.36 for the probabilistic maximum likelihood based SLAM (Alsayed et al. 2015).

$$x^* = argmax(P(z_t|x_{t|t-1}, s_{t-1}) \times P(x_{t|t-1}|x_{t-1}, u_t)) \qquad 5.36$$

In case of the evidential SLAM, a belief operator (conjunctive, disjunctive, or disjunctive orthogonal operator) is applied. The choice of the matching operator is vary but a conjunctive approach is chosen in (Trehard 2015) and is shown in Eq5.37.

$$x^* = argmax(\mathcal{O}_{\oplus}(x_t|z_t, u_{1:t}, s)) \qquad 5.37$$

An additional observation o_t from the Wi-Fi fingerprinting localization is fed into the matching operator above. Originally, the observation from the Wi-Fi fingerprinting localization system is in global coordinate frame. However, with a transformation matrix between the local SLAM coordinate frame and the global coordinate frame, it is now possible to convert this observation into the local SLAM coordinate frame. The original candidates' scores for the SLAM matching operator are now confronting with the information from the Wi-Fi observation. The new pose is then selected as in Eq.5.38.

$$x^* = \begin{cases} argmax(\mathcal{N}(x_{1:t},\ o_t,\ \sigma_{wifi}) \times P\ ), & PML - SLAM \\ argmax(\mathcal{N}(x_{1:t},\ o_t,\ \sigma_{wifi}) \times \mathcal{O}_{\oplus}\ ), & Evidential\ SLAM \end{cases} \qquad 5.38$$

The candidate with the maximum score is then taken as the localization result and could be converted back to the global coordinate frame. This enables an absolute correction to be injected into the SLAM process and at the same time allows the SLAM to return results in the global coordinate frame.

Although in this thesis, the approach does not yield a stable localization result, it is worth to mention this as a better strategy to find the transformation matrix could potentially improve the method vastly. Also, there is a possibility of including the global semantic map into the SLAM map and therefore enhancing the mapping process of SLAM. The result of localization for this approaches will be presented in Section 5.6.

5.5.4 SLAM as Odometry Measurements

As explained in the previous section, another possible fusion scheme is to treat the laser-SLAM outputs as Odometry measurements. With the expectation for a highly accurate local step of laser-SLAM, the estimations for the vehicle current velocity and yaw rate are supposed to be much more accurate than a standard IMU outputs. In addition, there is no need of a transformation matrix in this fusion strategy since only the dynamics estimation of the vehicle are extracted from the laser-SLAM.

5.5.4.1 Prediction Step

With the sampling frequency of a laser sensor at least 10Hz, the time between two consecutive estimations is small enough to assume constant speed and constant yaw rate model as in Eq.5.39, Eq.5.40.

$$v^t = \frac{\Delta d}{\Delta t} \qquad 5.39$$

$$\omega^t = \frac{\Delta \theta}{\Delta t} \qquad 5.40$$

Note that, Δd and $\Delta \theta$ are respectively distance displacement and angular displacement thus there is no coordinate transformation required. In this way, the laser-SLAM can be fused with an absolute localization system in an unknown environment without a complex initialization step. The fusion strategy for laser-SLAM into the proposed system is shown in Figure 5.14.

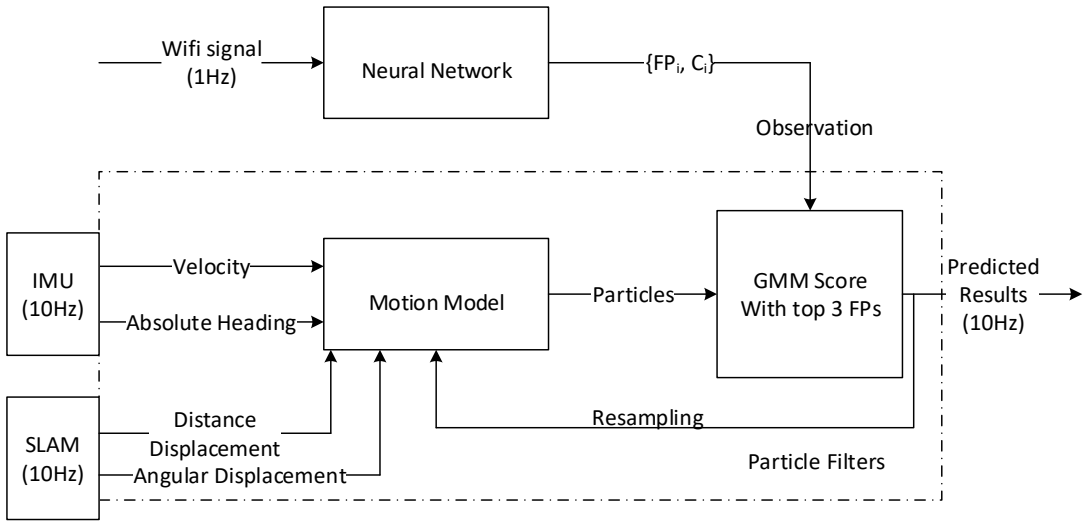

Figure 5.14 Fusion of laser-SLAM, Wi-Fi fingerprinting and IMU

Not only allowing laser-SLAM to be fused without initialization step, this solution also provides a necessary redundancy for the prediction step of the particle filter. In case one of the two sources (IMU and SLAM) fails to function properly, the other can provide an alternative.

If both function correctly and independently, they should provide two distinct sets of particles evolution. These two sets of particles should, however, overlap for the majority of their areas since. This helps to identify outlier particles which are out of the overlapping area. Moreover, the overlapping area is not necessary to be computed precisely in any prediction step computation. Assuming all particles are equally weighted and the final prediction is calculated by Eq.5.9 then all outliers' impacts will be neglected due to the higher particles density of the overlapping area.

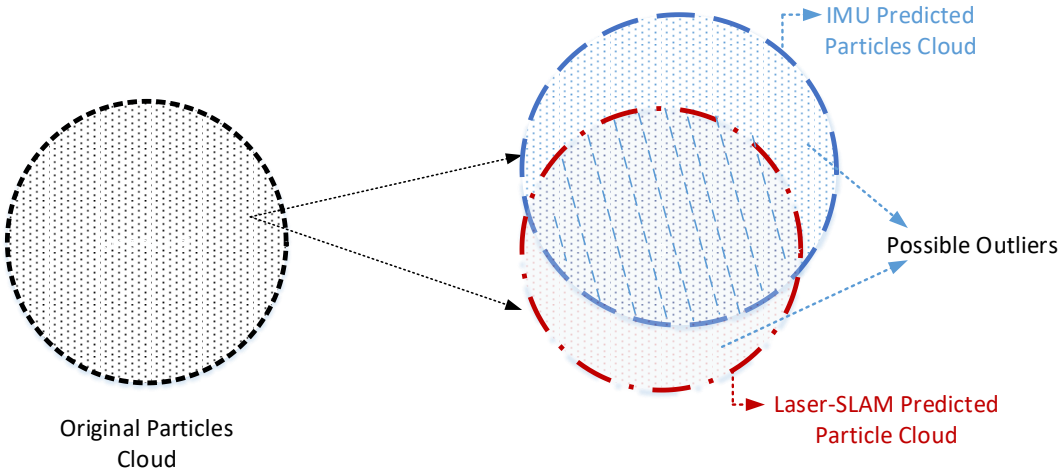

Figure 5.15 Laser-SLAM and IMU particles clouds

5.5.4.2 Selection & Resampling

Having this new cloud of particles, the final estimation for the vehicle position should be as follow:

$$\hat{\boldsymbol{x}}^t = \frac{1}{N+M}\left(N\sum_{i=1}^{N} x_i^t w_i^t + M\sum_{j=1}^{M} x_j^t w_j^t\right) \qquad 5.41$$

Where N and M are dimensions of IMU and SLAM particle filter respectively.

Also, the Effective Particles Size (EPS) also need to be rewritten as:

$$EPS = \frac{N}{1+CV_{IMU}} + \frac{M}{1+CV_{SLAM}} \qquad 5.42$$

Consequently, the condition for resampling to occur is:

$$EPS < \frac{1}{2}(N+M) \qquad 5.43$$

5.6 Experiments and Results

5.6.1 Wi-Fi Fingerprinting Localization and IMU Fusion

In this section, experiments for the fusion system with IMU are presented. The experiments setup are similar to the Wi-Fi fingerprinting localization experiments explained in Section 4.4. Test runs will be conducted in INRIA campus, at Rocquencourt using two vehicles: a cybercar and a Citroen C1 car.

Since the particle filter is a non-deterministic algorithm, several factors are examined such as: number of particles required, the stability of the particle filter outcomes, particle filter convergence given different starting conditions and results of the fusion solution under different datasets.

Experiments of the Wi-Fi Fingerprinting and IMU fusion system will be explained with the four steps of a particle filter: Initialization, Prediction, Correction and Selection & Resampling. In each step, studies for some significant parameters and their impact to the particle filter will be conducted and analysed in detail.

5.6.1.1 Initialization Step

The initialization phase has a significantly contribution to the convergence rate of the particle filter. As there is no other prior knowledge assumed, the particle filter in this thesis will be initialized with the first observation available from the Wi-Fi fingerprinting localization system. In other word, at the first moment of entering the car park, the car will briefly wait for at most one second for a positioning result from the Wi-Fi fingerprinting localization (since the sampling frequency of the Wi-Fi system is 1Hz). Having the first classification results, the top three fingerprints with highest confidence score will be selected. The weighted sum of these fingerprints and their normalized scores will be calculated and taken as the assumed true position as in Eq.5.44.

$$\boldsymbol{x}^{t=0} = \sum_{j=1}^{3} FP_j c_j \qquad 5.44$$

With this first position, particles will be generated around it with $\boldsymbol{x}^{t=0}$ as the expected mean and the Wi-Fi standard deviation taken from statistic in experiments of Chapter 4 σ_{wifi}. Assume the distribution of these particles follows Gaussian distribution, the ith generated particle is calculated as:

$$\boldsymbol{x}_i^0 = \mathcal{N}(\boldsymbol{x}^{t=0}, \sigma_{wifi}) \qquad 5.45$$

Where N(.) is a Gaussian Noise generator algorithm using Box-Muller transformation (Lee et al. 2006; Box and Muller 1958).

One of the main concerns in this step is the number of particles should be generated or the dimension of the particle filter. Theoretically, the higher the number of generated particles, the more computing power is required to achieve the real-time performance. At the same time, with more particles, the particle cloud should demonstrate a closer characteristic to the prior distribution. For a single dataset, following number of particles will be examined: 500, 800, 1000, 2000, 4000 particles. For each number of particles N, 100 runs of the algorithm on the same experiment dataset will be performed to estimate the localization error. This is because the particle filter is a non-deterministic algorithm thus a conclusion can only be made with a sufficient number of tests.

Another criteria need to be addressed is the true position of the vehicle in the initialization phase. Regarding to the scan range definition discussed in Section 4.3.1 and the mean distance between two consecutive fingerprints in the experiment is 6meters (Section 4.4.1 and 4.4.2) there are two possible areas for the true position of the vehicle during the initialization step. These two areas are illustrated in red (within a definition of a fingerprint) and blue (out of fingerprint area) respectively (Figure 5.16). When the vehicle starts within a fingerprint area, the Wi-Fi fingerprinting localization system should theoretically give a better estimation for the initialization step of the particle filter compares to the other case. Thus, the two cases will be studied to understand the stability of the algorithm.

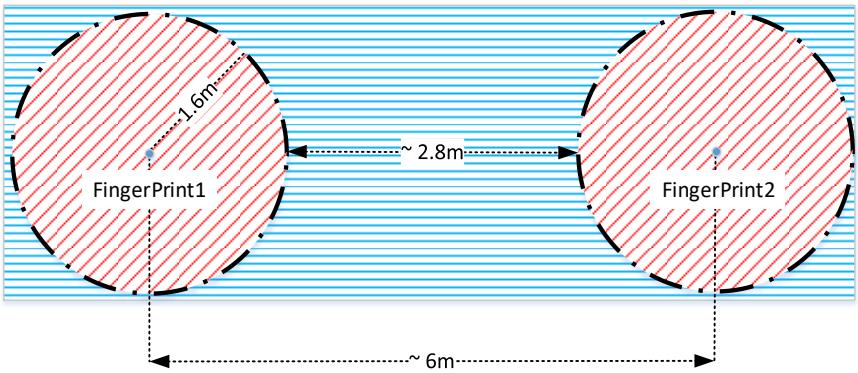

Figure 5.16 True position during the initialization step: within fingerprint area (red) and outside fingerprint area (blue)

5.6.1.2 Prediction Step

The constant acceleration motion model will be applied on IMU-based prediction to evolve particles in this step. From the IMU inputs, the vehicle velocity and absolute heading angle is directly fed into the particle filter with a given standard deviation for measurement error. Both the cybercar and Citroen C1 are equipped with the same IMU sensor thus the performance of the fusion on these two vehicles is expected to be identical. Experiments are carried out on both vehicles with average speed from 2.5-3.5 m/s.

5.6.1.3 Correction Step

The number of considered fingerprints for the Gaussian mixture model is chosen to be $k = 3$. This number is justified from the statistic in Section 4.4.2 where top 3 highest score fingerprints will cover the optimal selection for over 82% of the cases. The higher k is not only affecting the real-time performance of the algorithm but also is not expected to improve the result. In addition, the Wi-Fi fingerprinting localization result standard deviation is estimated around $\sigma_{wifi} = 1.5$ from Wi-Fi localization experiments.

5.6.1.4 Selection and Resampling Step

Having a particles cloud together with their weight, the final estimation for localization result is calculated using weighted sum of all particles as in Eq.5.9. The estimated result will be compared directly to the corresponding RTK-GPS positioning result (with expected error under 10 centimetre with level 3 or above of the signal quality). The error of localization is defined as Euclidian distance between the estimated position and the RTK-GPS position.

For resampling step of particle filter, there are several algorithms for particle filter resampling strategy including: Multinomial Resampling, Residual Resampling, Stratified Resampling, Systematic Resampling (Douc, Cappé, and Moulines 2005). Each of these strategies has its advantages and disadvantages but there is no clear winner. In this thesis, the Multinomial resampling algorithm is applied for introducing new particles into the particle cloud.

5.6.1.5 Results and Discussion

Firstly, two types of the vehicle true initial position are tested: one within fingerprint defined area and one outside of any fingerprint defined area. One single test result of the first case is illustrated in Figure 5.17. The y-axis is the Euclidian distance localization error while each time step in the x-axis is equal to 1/10 of a second. With a good initialization position, the Gaussian mixture model particle filter shows a good performance in term of convergence and localization accuracy.

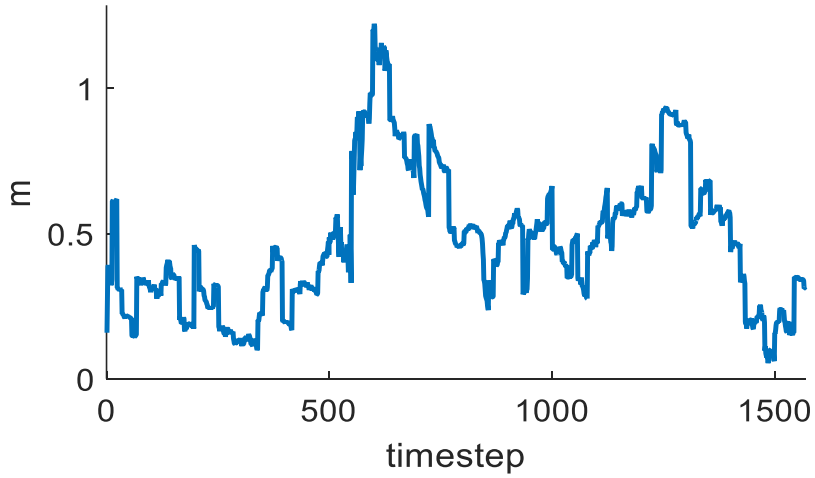

Figure 5.17 Initial position within the defined fingerprint area case

The moving path can be seen in Figure 5.18 below:

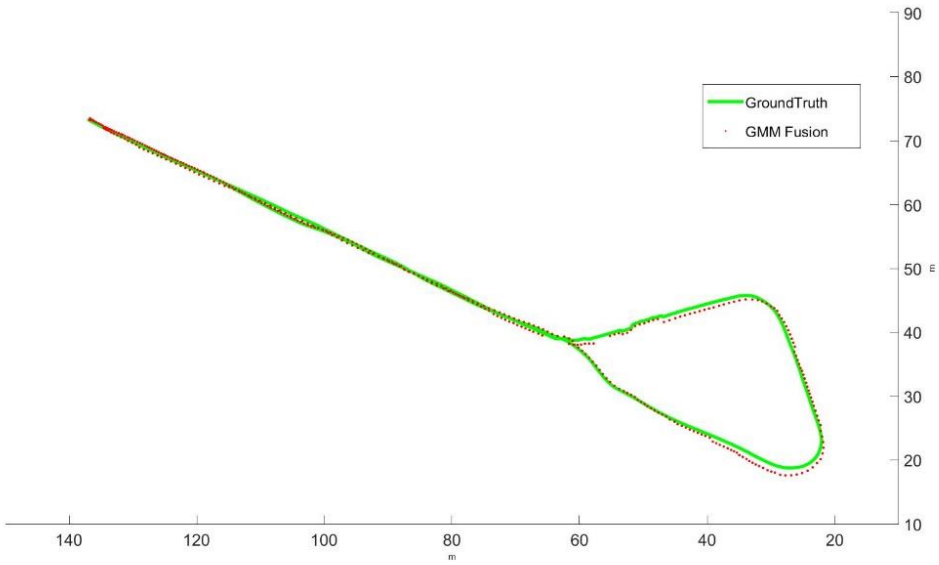

Figure 5.18 Experiment test run

Despite good overall localization error shown in Figure 5.17 and Figure 5.18, there are still some peak in Figure 5.17 error plot where the localization accuracy is around 1 meter. This can be partially explained with the ground truth RTK GPS. Due to its high sensitivity, the RTK-GPS is not guaranteed to always function at centimetre of localization error. In fact, there are cases where the quality of the RTK GPS ground truth drops significantly (up to few decimetres or even 1 meter of error).

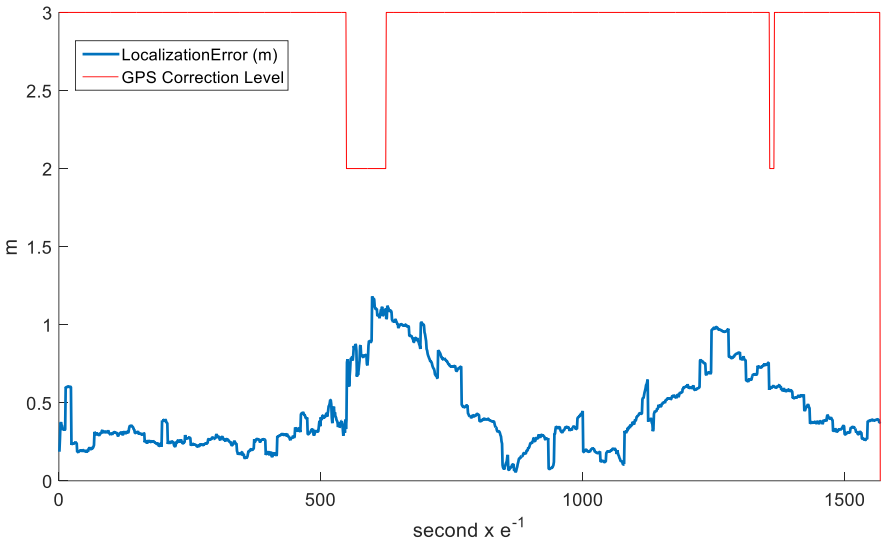

Figure 5.19 Localization error with corresponding ground truth quality

In Figure 5.19, the RTK GPS quality is measured as the correction level shown in red line. At level 3, the expected positioning error is centimetres. However, when the correction level drops to level 2, the expected positioning error is from few decimetres to 1 metres. Naturally, the localization error tends to increases with a low quality ground truth. Unfortunately, this is inevitable due to the obstruction from buildings around. The corresponding areas for the drop in RTK-GPS quality is shown in Figure 5.20 in blue as the GPS failure area.

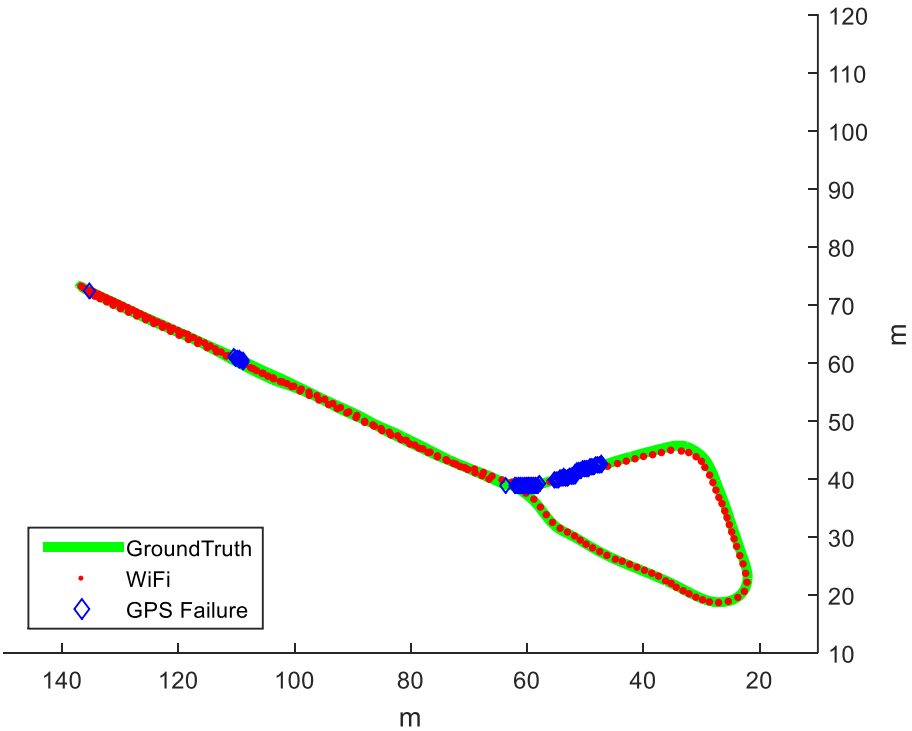

Figure 5.20 Travel path with RTK GPS quality

One more possible cause for the increase of localization error is the lack of good classification from the ensemble neural network for Wi-Fi fingerprinting localization. As the top three highest confidence fingerprints only cover 82% of the good classification cases (see Section 4.4.2), it is possible that the particle filter does not receive any good classification for a short duration. In this case, the system only function as a dead-reckoning localization algorithm and hence introduces high accumulated error. Still, in either case, the particle filter shows a good recovery to converge to a highly accurate localization error.

Another case for which the vehicle starts from outside of any fingerprint defined area is examined. The localization error is shown in Figure 5.21. In this case, due to the initial position is outside of the fingerprinting area, the best observation obtained from the Wi-Fi fingerprinting localization has an error of 3.2m. From this position, the particle filter takes around 30-40 timesteps (3-4 seconds) to reduce the error around 40% then slowly converge to below 1meter of localization error after 30 seconds. This happens due to after few first second, the vehicle slowly move to the area of the fingerprint which results in better observations from Wi-Fi fingerprinting localization. Together with a high number of particles count, the particle filter is able to recover from the high error start.

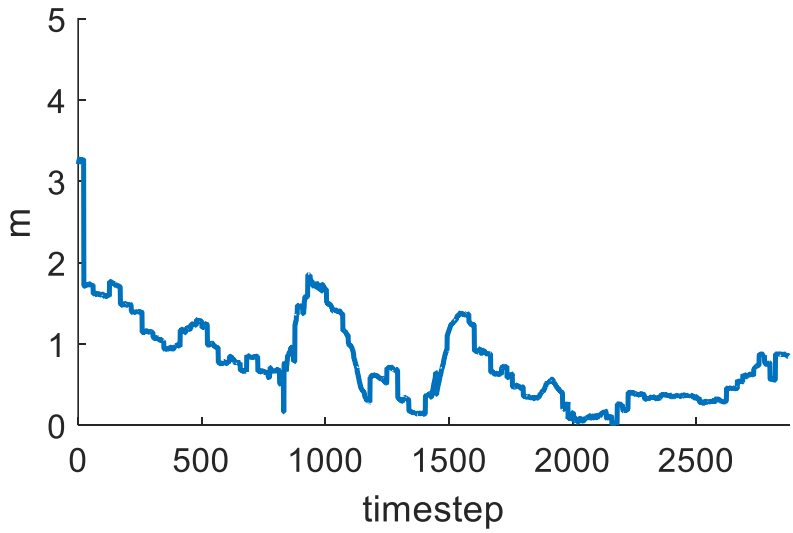

Figure 5.21 Initial position outside the defined fingerprint area case

This test run is illustrated below:

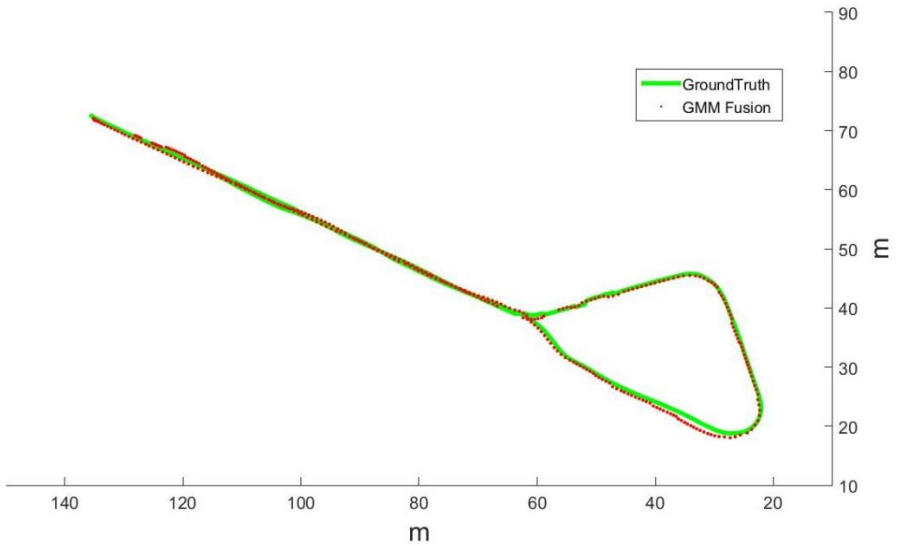

Figure 5.22 Experiment test run

Secondly, to evaluate the number of particles required, one experiment data is run repeatedly for 100 iterations (each iteration is independent from others). Both two cases: the initial true position is within the Fingerprint (FP) area and outside the Fingerprint area are studied. The mean localization errors and standard deviation after 100 iterations with different number of particles count in the particles filter is shown in Table 11. For the initial position outside of the Fingerprint area case, a statistic excluding first 4 seconds where the localization errors are stabilized.

Table 11 Particles count and the localization error statistic

Particles Count	*Within FP area*	*Outside FP area*	
	Localization Error Mean & Std	Localization Error Mean & Std	Excluding first 4 seconds
500	0.6121 ± 0.1283	1.0545 ± 0.3246	0.9457 ± 0.2827
800	0.5981 ± 0.1266	1.0123 ± 0.3060	0.9240 ± 0.2605
1000	0.5819 ± 0.1262	0.9819 ± 0.2557	0.9184 ± 0.2448
2000	$0.5773 \pm \mathbf{0.1216}$	0.9403 ± 0.2557	0.8977 ± 0.2167
4000	$\mathbf{0.5719} \pm 0.1308$	$\mathbf{0.8579} \pm 0.2270$	0.8261 ± 0.1856
5000	0.5720 ± 0.1289	0.8681 ± 0.2302	0.8377 ± 0.1904

For experiment with the initial position of the vehicle within a fingerprint area, the mean localization error as well as the standard deviation of errors reduce significantly as the number of particles increases from 500 to 1000 particles. However, for more than 1000 particles, as shown in Figure 5.23, there is no significant improvement. This indicates that the particle filter in this case should perform well with only 1000 particles generated.

For experiments with the initial position lies outside of any fingerprint area, in Figure 5.24, there is a notable improvement in term of mean localization error when the number of particles filter is high (2000 – 4000 particles). This is because with higher number of particles, the particle filter is likely to find the global optimal and converge faster. Unlike in the previous case where the initial assumption of the particle filter is fairly accurate, with a bad starting position, the higher particles count should improve the filter's convergence rate (thus improving the mean localization error).

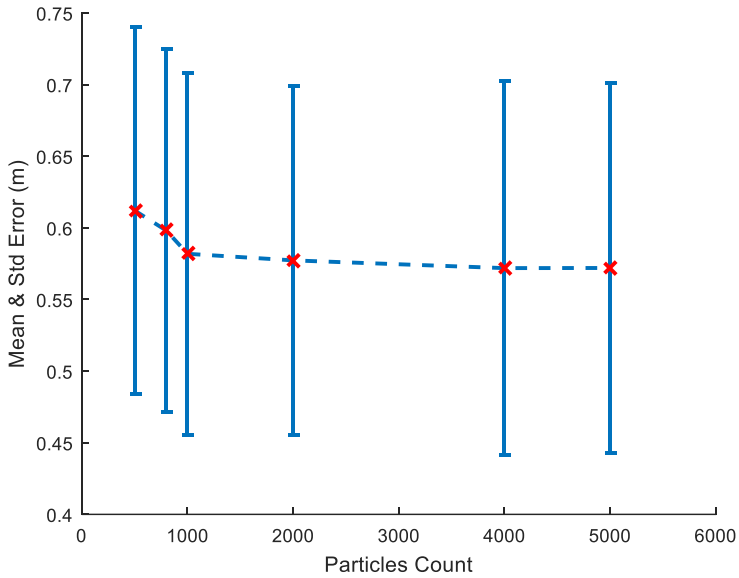

Figure 5.23 Initial position within a fingerprint area

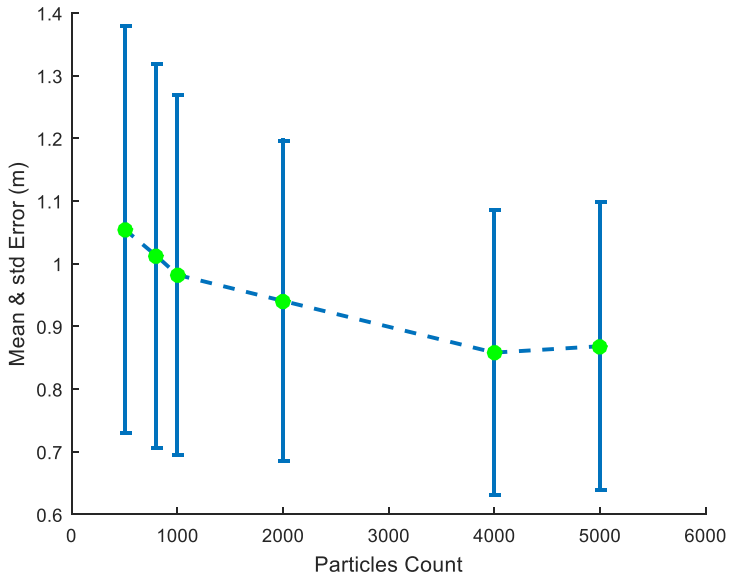

Figure 5.24 Initial position outside a fingerprint area

These results suggest that the solution should perform reasonably well with a low number of particles count (around 2000 – 4000 particles). The low number of particles count also allows the algorithm to process the input data in real-time.

Finally, in total 64 experiments were conducted with a random starting position during nearly a year. The results of all experiments are shown in Figure 5.25 and Figure 5.26. In these experiments, the particle filter has 4000 particles. The mean error is estimated at 0.859m and standard deviation is 0.2320. The cumulative sum of errors shows that around 90.27% of the errors is under 1.5m which is one sigma ($\sigma_{wifi} = 1.5$).

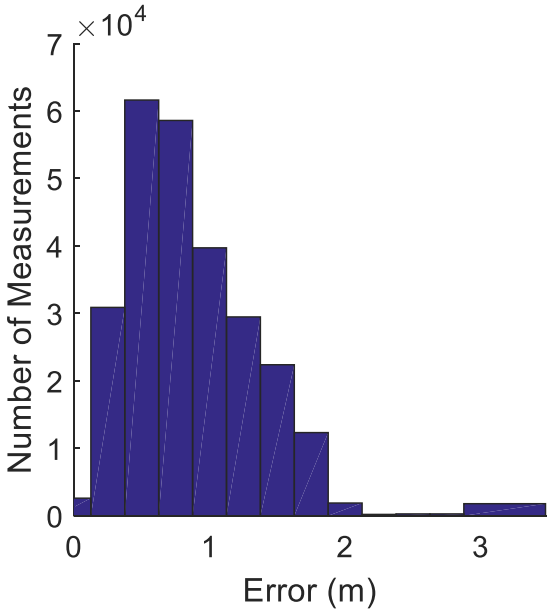

Figure 5.25 Localization error histogram of all experiments

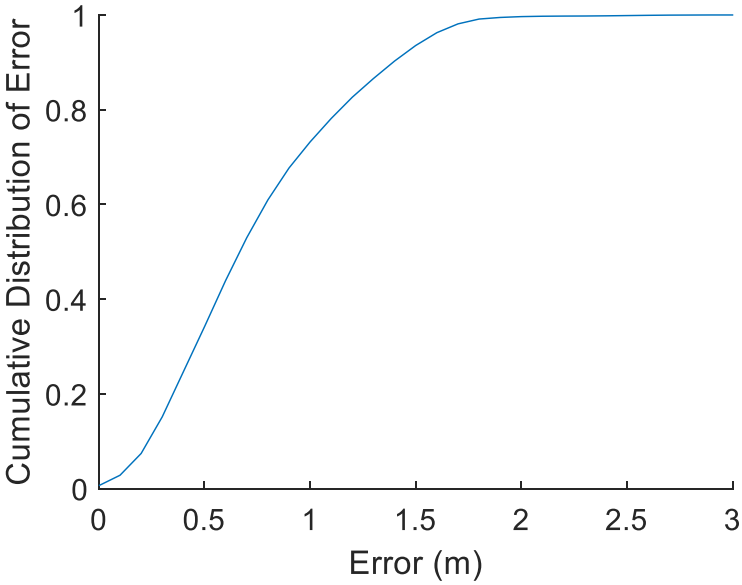

Figure 5.26 Cumulative sum of errors for all experiments

If we assume a good starting position is provided (which is realistic since the initial position of a vehicle entering a car park can be approximately predicted) then a much better result will be obtained. With only 2000 particles, the mean error is around 0.5885m and the standard deviation is 0.1270. Also, in this case, 98.81% of the errors are under one sigma ($\sigma_{wifi} = 1.5$) (Figure 5.27, Figure 5.28).

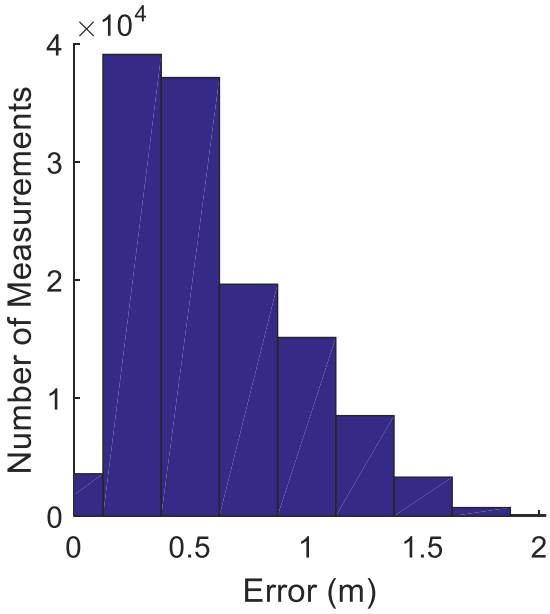

Figure 5.27 Localization error histogram (good initial position)

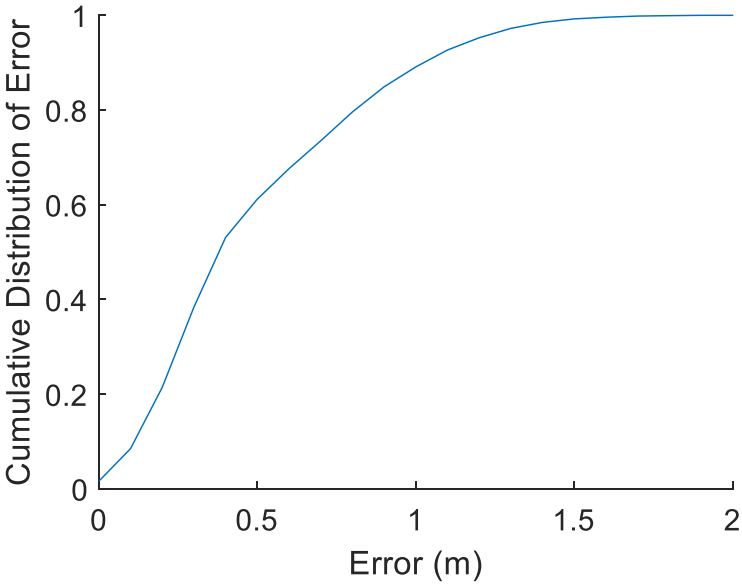

Figure 5.28 Cumulative sum of localization error (good initial position)

5.6.2 Wi-Fi Fingerprinting Localization, IMU and Laser-SLAM fusion

5.6.2.1 Laser-SLAM in Global Coordinate Frame

In this solution, the transformation matrix needs first to be found using the RTK-GPS. However, any small error in the estimation for the transformation matrix will be accumulated as the vehicle moves further. In practice, even with the RTK-GPS, the resulted transformation matrix would still suffer from noise. Figure 5.29 illustrates a test case for the conversion of the SLAM local coordinate frame into the global coordinate frame. Even though the first 10 meters of the moving path, the laser-SLAM result in global coordinates seem to be accurate, a rapid growth in localization error could be seen afterward. There are two possible causes for this problem: (1) an incorrect transformation matrix and (2) the accumulated error of the laser-SLAM itself (or the drifting issue).

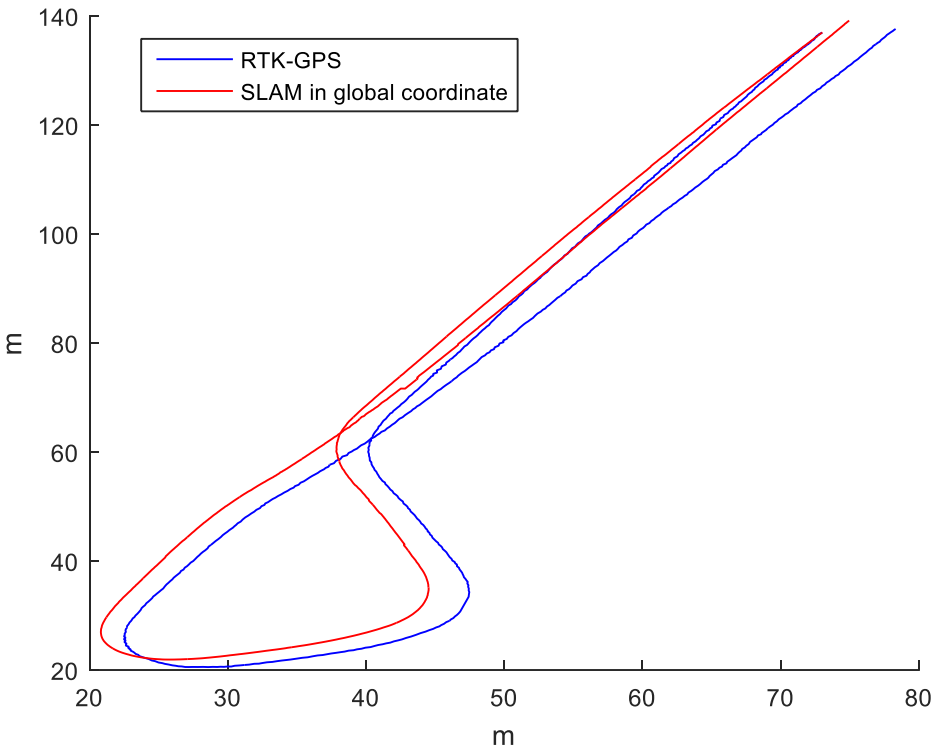

Figure 5.29 laser-SLAM in Global Coordinate

While it is possible that both sources of error above are true the accumulated error issue could be fix with the injection of the Wi-Fi observation. Still, it is extremely difficult to deal with the calculation of a transformation matrix issue in practice.

An attempt to fuse the Wi-Fi fingerprinting system into the SLAM (both Evidential SLAM and PML SLAM) is made. The result of localization can be seen in Figure 5.30. Clearly, with the

injection of an absolute correction such as the Wi-Fi fingerprinting localization system, the fusion system is able to track the vehicle around its ground truth. Still, with a maximum error of 2.7m, this solution is inadequate.

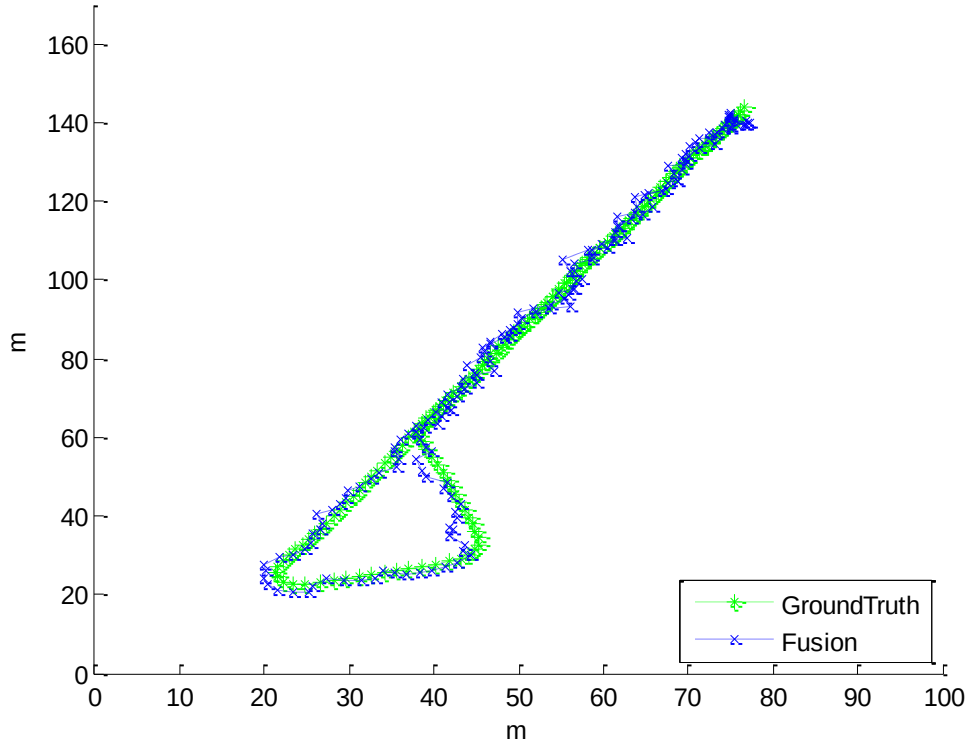

Figure 5.30 Fusion System (Wi-Fi and laser-SLAM) in the Global Coordinate Frame

5.6.2.2 Laser-SLAM as Odometry measurements

The fusion of Laser-SLAM is also tested to verify the proposed fusion strategy. A version of PML laser-SLAM (Alsayed et al. 2015) is adopted for the Citroen C1 with two Ibeolux LiDAR sensors at the front. This SLAM version has no loop closure algorithm implemented thus without additional static references, drifting is expected in the first run of this SLAM on a new environment.

Due to some technical difficulties (with the LiDAR as well as the RTK-GPS) and constraints in time, the number of SLAM fusion experiments is limited. With all four steps similar to the experiments of IMU fusion, only the localization results will be discussed here.

For this fusion, the total number of particles are chosen to be 2000 particles split equally for both IMU and SLAM based prediction phase. In a single run, the results of localization is shown below:

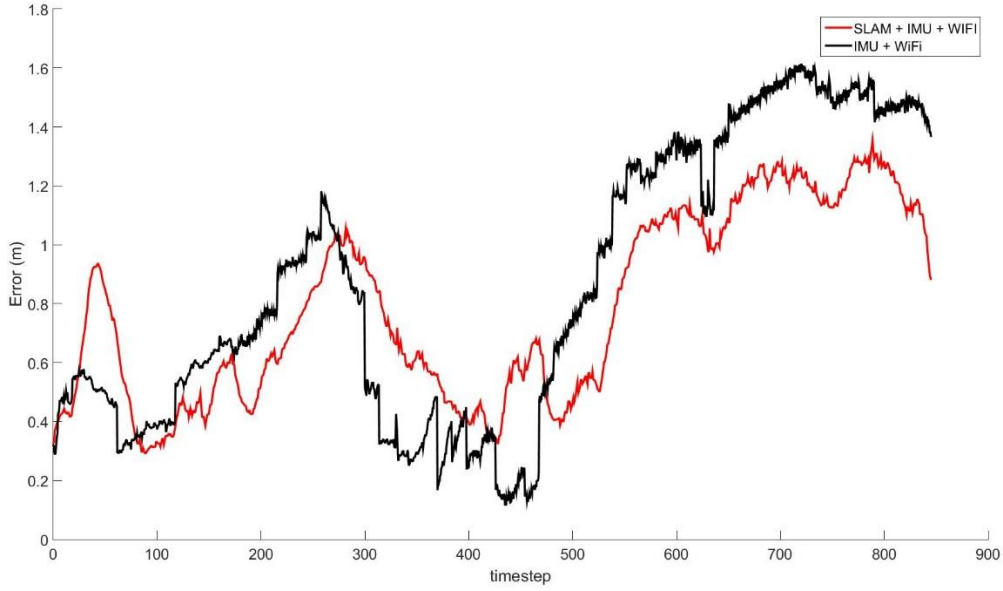

Figure 5.31 Localization error of fusion solution

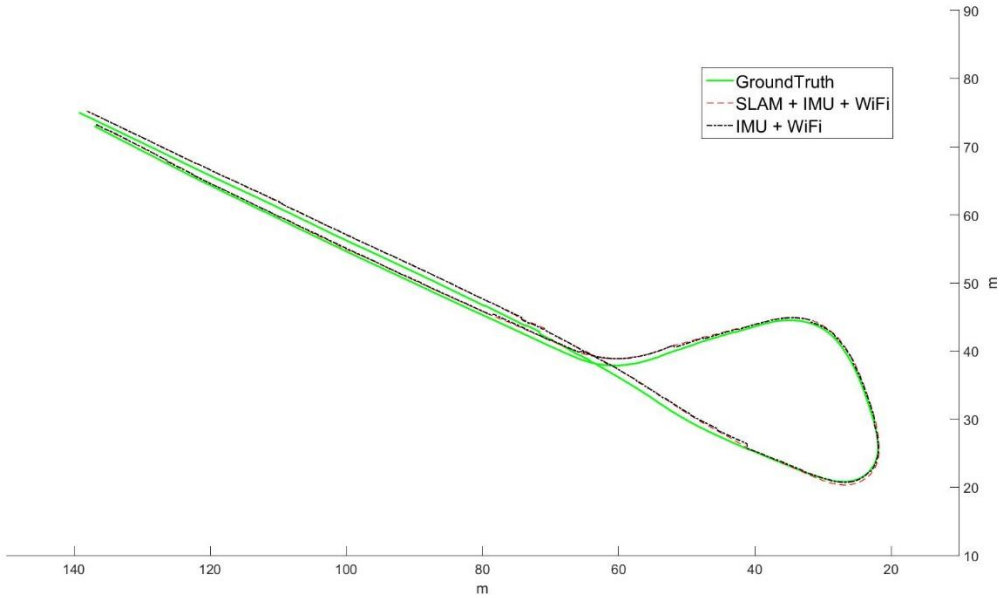

Figure 5.32 Experiment test run

The fusion results with laser-SLAM does seem to improve in general compare to the fusion of IMU and Wi-Fi alone. As for the IMU and Wi-Fi fusion, the mean localization error is estimated around 0.57m for a good start with 2000 particles. In this fusion, the mean error is only 0.49m with the same number of particles. The improvement can be seen in Figure 5.31 when the IMU based prediction seems to make a lot of error, the laser-SLAM can still provide some recovery. This is because in a local frame, the estimation of velocity and delta heading angle of the laser-

SLAM are expected to be more accurate than the IMU outputs. In case that there is no correction from the Wi-Fi fingerprinting, the fusion system is degraded to a dead-reckoning system. Naturally, the laser-based evolution should provide a much better estimation as well as lower accumulated error than the IMU (Scrapper, Madhavan, and Balakirsky 2018).

There are still cases where the fusion with laser-SLAM results in higher localization errors compared to the Wi-Fi and IMU only. One possible cause for this is the noisy reading of laser-SLAM leads to inaccurate velocity and yaw rate estimation. In Figure 5.33, the left side of the vehicle (circled) has noisy reading while there is no clear feature on the right side. This is a potential erroneous laser-SLAM estimation scenario.

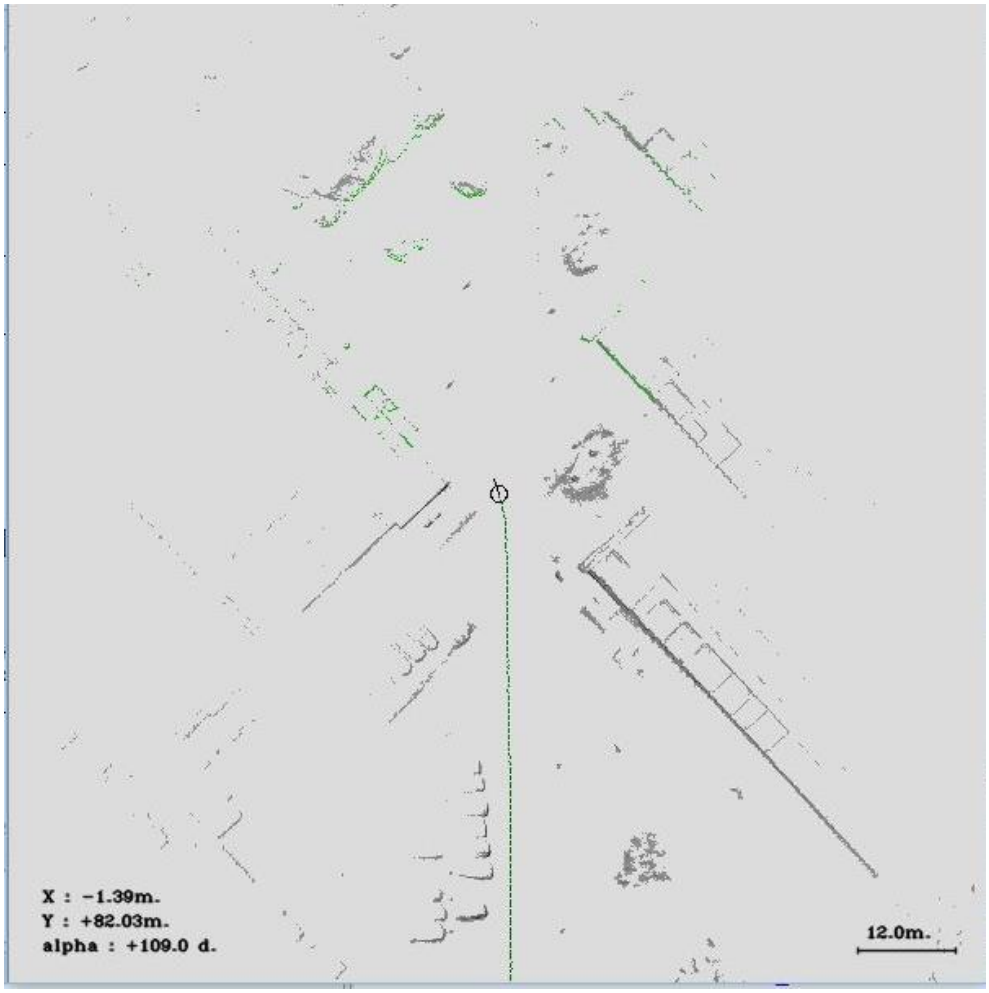

Figure 5.33 PML-SLAM online map

Similarly, in case of evidential SLAM, there are cases where the algorithm failed to identify a clear feature. In Figure 5.34, green area illustrates the free space, red dots are obstacles, blue are the area without information and conflicted cells are shown in small black dots. The current vehicle estimated position is the pink circle. Notice that the left side of the map are significantly

softer compared to the right. This is because there are confirmed obstacles detected in the right side while the left side are filled with black dots for conflicted cells. These conflicted cells have a huge impact on the final estimation of the Evidential SLAM process.

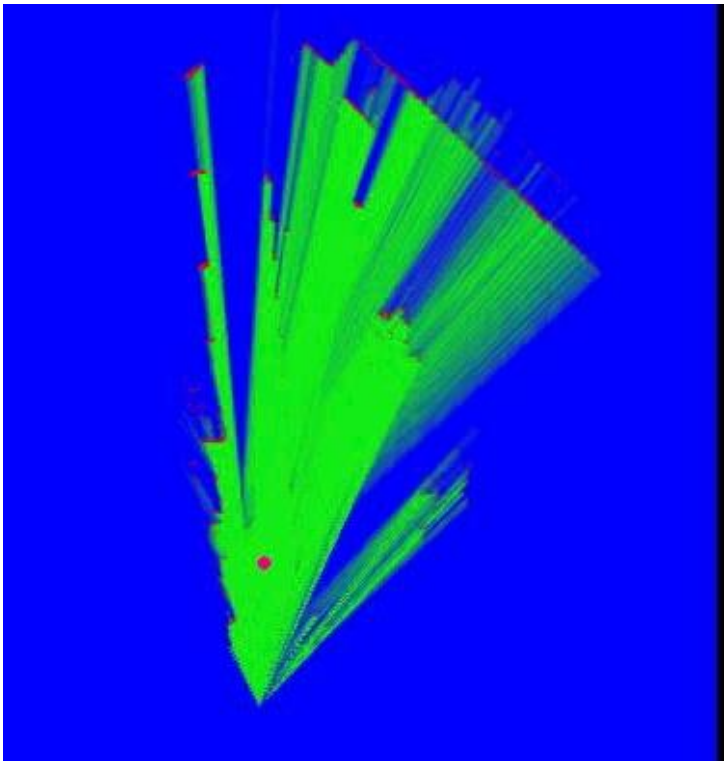

Figure 5.34 Evidential SLAM online map

5.7 Discussion

This chapter presents a fusion framework for the car park localization system using multiple sensors including: the Wi-Fi fingerprinting, the IMU and the laser-SLAM. To compliment the low sampling rate, absolute localization from Wi-Fi fingerprinting, a Gaussian mixture model particle filter is employed. With high frequency inputs from the IMU or laser-SLAM, particles in the particle filter are evolved in real time. Once observation from the Wi-Fi fingerprinting localization system available, correction using Gaussian mixture scoring function is made to eliminate the accumulated error.

A major contribution in this chapter is the Gaussian mixture scoring function that enables the particle filter to recover from both a bad initial position and bad observations during the movement. Firstly, as discussed in Section 5.6.1.1, a good initial guess of the starting position would significantly boost the convergence rate of the particle filter. Using the mixture of few top fingerprints as the initial position not only allows the particle to converge faster but also eliminate any condition required for the localization system to start (i.e. starting from a known

position). Moreover, even with a bad starting position, the Gaussian mixture scoring function helps the particle to quickly converge. This is shown in experiment results of test cases where the initial position is out of the fingerprint area. The localization error is quickly reduced once the vehicle moves closer to a fingerprint. Secondly, observations from the Wi-Fi fingerprinting localization system is not always giving good estimation of the true position. Instead, a real test case shown in Section 5.3.2 where the highest confidence classification result of the Wi-Fi fingerprinting localization is not a *good classification* result. However, the Gaussian mixture model scoring function gives the particle filter a chance to overcome such situation by taking into account other top classification results which should theoretically bring the estimation closer to the true position.

Another notable proposal in this chapter is the strategy to the fuse laser-SLAM into a global coordinate system without the need of an initialization process or a predefined laser map. Unlike other solutions mentioned in Chapter 2, this fusion framework does not require a carefully calibrated initial position for laser-SLAM nor a prebuilt map to formulize a transformation matrix between the SLAM coordinate and the global coordinate. Instead, taking advantage of the SLAM high precision in the local step estimation, the fusion framework incorporate the laser-SLAM as an IMU which reduces the need for a transformation matrix.

During a year of experiments, the fusion of IMU and Wi-Fi fingerprinting localization is tested with different criteria such as: stability of the particle filter, number particles and the behaviour of the system with different initial starting positions.

To understand the designed particle filter stability, the fusion system is tested in two perspectives: multiple runs on the same dataset and different datasets. In the first perspective, a single dataset is independently fed into the algorithm for a 100 iterations. The mean localization error and its standard deviation is calculated on top of all 100 iterations. A low mean error (around 0.8m for all cases, and 0.5m for a good starting position) as well as low standard deviation (~ 0.22) indicate that the particle filter is stable. For the second perspective, a total of 84 independent experiments were conducted. The final results yield a similar outcome with mean error and standard deviation is 0.859m and 0.232 for all cases and 0.588m and 0.127 for a good initial position. Thus, the designed particle filter is proven to be stable.

The number of particles in a particle filter (or its dimension) is also an important parameter. This decides the resources needed for the algorithm to run in real time. To learn this parameter,

different number of particles are tested in the same dataset. Finally, with only 2000 particles, the fusion solution is able to achieve the optimal result.

Different initial positions for test runs are also studied to understand the generalization of the algorithm. There are two possibilities for place for the initial position: either within or outside a fingerprint area. If the initial position is within a fingerprint area, a good initial guess can be expected. This results in a low mean localization error of 0.588m. Otherwise, since the particle filter needs time to converge to the true position, the mean localization error in this case is around 0.859m. This high mean error is mostly due to the initial large positioning error. In addition, it is reasonable to expect the initial position of a vehicle entering a car park is relatively known. Hence, a good accuracy can be expected from the fusion system in general.

Although, the average movement speed in all experiments is around 3.3m/s, there is a possibility of extending the thesis result to a higher movement speed. In order to accomplish this, a solution to enhance Wi-Fi fingerprinting localization sampling frequency must be found. One potential way is to use multiple Wi-Fi antenna with different processors, each has a small delay to the other. In this way, the sampling frequency of Wi-Fi scan can be increased proportional to the number of antennas. Unfortunately, with limited time, the thesis could not be extended to cover the idea.

Finally, the proposed fusion framework allows not only the fusion of Wi-Fi fingerprinting with other sensors but it has the potential to combine different strategies such as the GPS with laser-SLAM, GPS with camera-based localization system, etc.. With that being said, this framework can be applied to multiple scenarios but not just GPS-denied environment or car park.

6. CONCLUSION

Résumé

Le chapitre conclut la thèse avec deux contributions majeures et une perspective pour les travaux futurs. Après avoir défini le problème au début, une solution basée sur le réseau de capteurs sans fil est proposée. Le chapitre 4 explique pourquoi un système de localisation d'empreintes digitales Wi-Fi peut répondre aux quatre critères. À condition que, un réseau de neurones d'ensemble pour l'empreinte Wi-Fi est proposé. La base de données hybride d'empreintes digitales et un réseau de neurones d'ensemble destinés à aider la localisation d'empreintes digitales Wi-Fi à s'adapter à la circulation d'un véhicule dans un parking sont deux contributions majeures. Des expériences sur des véhicules réels ont été menées pendant une année pour valider le système proposé. Avec deux véhicules différents, 64 expériences, le système fournit une erreur de localisation moyenne de 2,25 m. Cela prouve que le système de localisation d'empreintes digitales Wi-Fi proposé est capable de remplacer le GPS dans un environnement sans GPS.

Toutefois, comme indiqué dans le champ d'application, l'erreur de localisation souhaitée pour un véhicule intelligent est d'environ 0,2 m. De plus, le système devrait pouvoir localiser le véhicule à haute fréquence pour faire face aux mouvements à grande vitesse. Par conséquent, un cadre de fusion pour la localisation d'empreintes digitales Wi-Fi et un autre système tel que l'IMU ou le laser-SLAM est proposé. L'objectif de ces systèmes est d'améliorer progressivement la fréquence de localisation, la précision et la transition de l'environnement assisté par GPS à un environnement refusé par GPS. Afin d'accomplir cette tâche, le filtre de

particules d'amorçage, une méthode de filtrage non linéaire est choisie. Comparé à un autre algorithme de filtrage, le filtre à particules semble offrir de meilleures performances en matière d'estimation non linéaire. En général, l'étape de correction du filtre à particules prendra en compte les observations disponibles pour peser sur l'ensemble candidat de positionnement (ou les particules). Compte tenu des observations absolues de méthodes telles que la localisation GPS, par caméra ou Wi-Fi, la meilleure estimation est souvent prise en compte pour évaluer l'ensemble de positionnement candidat. Dans cette thèse, la correction est prise à partir du système de localisation d'empreintes digitales Wi-Fi. Avec une étude statistique du chapitre 4, il est justifié que les 3 premiers résultats de la classification donnent une bien meilleure estimation de la position réelle que seulement le score le plus élevé. Par conséquent, au lieu de considérer uniquement le score de confiance le plus élevé du résultat de la localisation Wi-Fi, le filtre prend en compte plusieurs scores possibles (3 en haut dans cette thèse) sous forme d'observations. Une fonction de notation utilisant un modèle de mélange gaussien de ces observations est définie. Les avantages de cette approche sont décrits à la section 5.3.

Parmi les différents capteurs, deux des capteurs les plus courants pour véhicules autonomes sont choisis pour la fusion dans cette thèse, à savoir l'unité de mesure inertielle (IMU) et le LiDAR. Bien qu'il s'agisse d'un couplage standard du GPS et du LiDAR (ou Velodyme) dans l'environnement assisté par GPS pour la localisation précise de véhicules intelligents, ce n'est pas le cas pour l'environnement assisté par GPS. Ainsi, une combinaison de la localisation Wi-Fi et du SLAM laser est proposée. À ce jour, le travail de thèse est également la première tentative de fusion de la localisation Wi-Fi et du laser-SLAM pour le positionnement de véhicules autonomes. Les détails de la stratégie de fusion sont expliqués au chapitre 5.

Enfin, avec de plus en plus d'études sur le même sujet chaque année, l'auteur estime que la solution de localisation de réseaux de capteurs sans fil deviendrait éventuellement une solution mature pour le positionnement de véhicules intelligents dans des environnements intérieurs.

6.1 Thesis motivation

In this thesis, the author has introduced the motivation to solve the localization problem of intelligent vehicles in the GPS-denied environment, especially a car park. The thesis pointed out that by having an autonomous navigation system for vehicles, an approximately 700 million euros loss can be avoided for France alone. Reports show that approximately 62% of carpark space will be saved if all vehicles are autonomously parked. In addition, car parks uses are

increasingly exceeding their original purpose. Features such as electric chargers for electric cars, online booking of parking spaces, dynamic guidance, etc. are growing demands. As France is committed to a digital Republic by October 2018, this thesis is expected to be a timely solution for environments such as car park.

However, a throughout study of literature for car park localization of intelligent vehicles does not seems to agree on a single architecture. It does, however, emphasize the need for an absolute correction system to couple with another dead-reckoning algorithm for the GPS-denied environment. Workarounds including laser or camera based SLAM, vision map matching or geo-referencing of environment landmarks are proposed with promising results. Still, these solutions do not comply with four criteria of a universal solution: availability, scalability, universal and accuracy. More specifically, most of the solutions violate the scalability and universal criteria as a costly mapping (and maintaining) process is required, or dedicated sensors calibration needed. On a large-scale, dynamic environments where changes happen every day, these costly procedures are soon to be a huge burden on the entire system.

In addition, with the growth of the wireless sensors networks infrastructure, it is interesting to investigate a possible solution using these readily available sensors to locate intelligent vehicles. Furthermore, from the beginning of 2017, the research community for indoor localization system using wireless sensors networks starts to address the autonomous driving problem for indoor environments. Notable conferences such as IPIN (Indoor Positioning and Indoor Navigation), the Microsoft indoor localization competition IPSN are embracing the idea of preparing and developing a navigation system for vehicles in indoor environments. Still, works on this topic are far from reaching the system requirements as pointed out in Section 4.2.

6.2 Thesis contributions

Having defined the problem and its requirements, a solution based on Wireless Sensors Network is proposed. Chapter 4 gives a discussion on why a Wi-Fi fingerprinting localization system could satisfy all four criteria. Provided that, an ensemble neural network for Wi-Fi fingerprinting is proposed. Two major contributions are the hybrid database of fingerprints as well as an ensemble neural network to help the Wi-Fi fingerprinting localization adapt to a vehicle movement inside a car park. Experiments on real vehicles were conducted for a duration of one year to validate the proposed system. With two different vehicles, 64 experiments, the system provides a 2.25m of average localization error. This proves that the proposed Wi-Fi

fingerprinting localization system is capable of replacing the GPS in a GPS-denied environment.

Still, as stated in the scope, the desired localization error for an intelligent vehicle is around 0.2m. In addition, the system should be able to locate the vehicle in high frequency to cope with high-speed movement. Therefore, a fusion framework for the Wi-Fi fingerprinting localization and another system such as the IMU or laser-SLAM is proposed. The goal of such systems is to smoothly improve localization frequency, accuracy as well as the transition from the GPS-aided environment to GPS-denied environment. In order to accomplish the task, the bootstrap particle filter, a non-linear filtering method is chosen. Compare to other filtering algorithm, the particle filter appears to have better performance when it comes to non-linear estimation. In general, the correction step of the particle filter will take into account available observations to put weight on the positioning candidate set (or the particles). Given absolute observations from methods such as GPS, camera or Wi-Fi localization, often, the best estimation is taken into account evaluate the positioning candidate set. In this thesis, the correction is taken from the Wi-Fi fingerprinting localization system. Having a statistic study from Chapter 4, it is justified that the top 3 classification results give a much better estimation of the true position than only the highest score one. Hence, instead of considering just the highest confidence score from the Wi-Fi localization result, the filter takes into account multiple possible ones (3-top in this thesis) as observations. A scoring function using Gaussian mixture model of those observations is defined. The benefit of this approach is described in Section 5.3.

Among different sensors, two of the most common ones for autonomous vehicles are chosen for fusion in this thesis namely the Inertial Measurement Unit (IMU) and LiDAR. While it is a standard coupling of the GPS and LiDAR (or Velodyme) in the GPS-aided environment for the precise localization of intelligent vehicles, it is not the case for the GPS-aided environment. Thus, a combination of the Wi-Fi localization and the laser-based SLAM is proposed. To this date, the thesis work is also the first attempt to fuse the Wi-Fi localization and the laser-SLAM for autonomous vehicles positioning. Details of the fusion strategy is explained in Chapter 5.

Since the particle filter is non-deterministic process, it is important to study the stability as well as the accuracy of the framework. There are two ways to analyze: to iterate the algorithm on the same dataset multiple times and to test the algorithm on different datasets. The first way is to understand the behaviour of the particle filter on the same dataset in different run. If the results of multiple runs agree on the same accuracy, it is likely that the particle filter is stable. The second way is to explore the particle filter reaction to different datasets. Given different

conditions and testing data, the particle filter should also deliver a stable result. In total, there are 64 different datasets for the fusion of Wi-Fi, IMU and laser-SLAM. Each of these datasets is repeatedly fed into the fusion framework for 100 times. Finally, given a good starting condition (which is expected for a vehicle when entering a car park, its first initial position is predicted), the system accuracy is around 0.58m with a low standard deviation of 0.12. Although such accuracy is still far from the desired one, it is important to note that this accuracy is calculated on the global coordinate system. Hence, further fine-tuning can be expected within local localization level (such as laser, camera, etc.).

6.3 Future work

Until now, most of commercial systems for carpark navigation from companies like BMW, Volvo, etc. are demonstrating at a low speed (around 3m/s). The survey from (Belloche 2015) also confirmed that the average speed for vehicles inside carparks is around 3-4m/s. However, the demand for a higher speed of navigation is expected in the future when the infrastructure and the transportation agents (vehicles, drivers, etc.) are ready. The benefit of such high speed navigation is obvious as it will increase the transportation flows vastly. Even though the study in the thesis focuses on a car park with an average speed of 3.3m/s, a potential solution for higher speed movement is also discussed in Section 5.7. With multiple Wi-Fi antennas to enhance the Wi-Fi sampling rate, it is possible that the fusion solution can localize vehicles at a higher speed. The future work of this thesis will study the possibility of pushing the navigation speed to a new limit.

Also, it is highly likely that an HD (high definition) map of the environment captured by sensors such as LIDAR or camera is eventually needed for centimetre level of positioning accuracy. Should the map is ready, the work in this thesis is believed to maintain a major impact. There are three reasons for this. First, with only an IMU and the Wi-Fi system, this thesis can provide an excellent loop-closure detection mechanism for the SLAM process in its initial map recording. More often, the SLAM tends to drift in its first run. This drift leads to a potential failure to close the loop on the map when the vehicle returns to the starting point. In this case, an absolute correction is required to help to reduce the accumulated error and to detect the previously visited area. Second, the fusion framework in this thesis can be extended to multiple sensors and localization systems such as camera, magnetic, ultra-wideband, etc. The concept of Gaussian mixture model allows the framework to incorporate information from different sources for a better estimation. Finally, having redundancy for a critical system such as

positioning for intelligent vehicles is extremely important. In unexpected situations, even the pre-recorded HD map approach could fail to locate the vehicle (or worse, return a huge positioning error). The IMU and Wi-Fi fusion could then be used as an anomaly detection in those situations and provide relatively accurate positioning information for the vehicle.

In the near future, a more comprehensive study of the proposed system is expected. Ideas such as multiple antennas, anomaly detection for map-based methods or the fusion with laser/camera based SLAM are among possible research directions. Special techniques such as Channel State Information (CSI) for reading the Wi-Fi information to replace the unstable RSSIs could also be exploited as hardware becomes more and more available. The combination of those ideas could lead to a considerable improvement in the Wi-Fi, IMU and SLAM fusion system accuracy.

Regarding the carpark situation, the absolute localization approach in this thesis brings an opportunity for location-based context aware services such as mobile payment, parking slot reservation, car-finding and charging station for electric vehicles. Moreover, the author also hopes to apply the proposed framework for other scenarios such as indoor robots navigation, vehicle navigation in industrial warehouses, or university campus buses. Each of these scenarios, however, will have different requirements (i.e. average movement speed, localization accuracy requirement, power consumption level or deployment cost, etc.). The author believes that the proposed system could be deployed effortlessly for those scenarios given the flexibility of the fusion framework.

Not only that more Wi-Fi access points are naturally added to the environment, the quality of these off the shelf, but consumer-grade hardware are also becoming better and better. While technologies such as Bluetooth Low Energy (BLE), ultra-wideband or 5G were not even mentioned ten years ago, they now can all be integrated in the indoor localization system. This shows that a potential of replacing the GPS with wireless sensor networks for indoor or even urban area is high. Besides, with more and more studies are being found in the same topic each year, the author believes that the wireless sensor networks localization solution would eventually be a mature solution for intelligent vehicles positioning in the indoor environments.

6.4 Conclusion

In conclusion, the thesis proposes a fusion system for localizing intelligent vehicles in the GPS-denied environment, more specifically the carpark situation. The practical necessity of the problem is explained in Chapter 1. It is reported that by accomplishing the task of autonomous

navigation for vehicles in carpark, there will be a huge benefit economically. While the existing solutions are not fully address the problem (or not cost-effective), the literature review in Chapter 2 does not yield a complete solution as well. By identifying four major criteria for the system, a fusion framework of Wi-Fi fingerprinting localization, IMU and laser-SLAM are designed. Experiments show promising results with room for improvement in the future.

7. REFERENCES

Abdallah, Ali A., Samer S. Saab, and Zaher M. Kassas. 2018. "A Machine Learning Approach for Localization in Cellular Environments." In *2018 IEEE/ION Position, Location and Navigation Symposium (PLANS)*, 1223–27. IEEE. doi:10.1109/PLANS.2018.8373508.

Agamennoni, Gabriel, Simone Fontana, Roland Y Siegwart, and Domenico G Sorrenti. 2016. "Point Clouds Registration with Probabilistic Data Association." *Proceedings of the IEEE/RSJ International Conference on Intelligent Robots and Systems (IROS)*, 4092–98. doi:10.1109/IROS.2016.7759602.

Agashe, Anil a., Amrita a. Agashe, and R.S. Patil. 2012. "Evaluation of DV Hop Localization Algorithm in Wireless Sensor Networks." *2012 International Conference on Advances in Mobile Network, Communication and Its Applications*, 79–82. doi:10.1109/MNCApps.2012.21.

Akai, Naoki, Luis Yoichi Morales, Takuma Yamaguchi, Eijiro Takeuchi, Yuki Yoshihara, Hiroyuki Okuda, Tatsuya Suzuki, and Yoshiki Ninomiya. 2017. "Autonomous Driving Based on Accurate Localization Using Multilayer LiDAR and Dead Reckoning." In *2017 IEEE 20th International Conference on Intelligent Transportation Systems (ITSC)*, 1–6. IEEE. doi:10.1109/ITSC.2017.8317797.

Alarifi, Abdulrahman, AbdulMalik Al-Salman, Mansour Alsaleh, Ahmad Alnafessah, Suheer Al-Hadhrami, Mai A Al-Ammar, and Hend S Al-Khalifa. 2016. "Ultra Wideband Indoor Positioning Technologies: Analysis and Recent Advances." *Sensors (Basel, Switzerland)* 16 (5). Multidisciplinary Digital Publishing Institute (MDPI). doi:10.3390/s16050707.

Alsayed, Zayed, Guillaume Bresson, Fawzi Nashashibi, and Anne Verroust-blondet. 2015. "PML-SLAM : A Solution for Localization in Large-Scale Urban Environments." *IROS PPNIV the 7th Workshop on Planning, Perception and Navigation for Intelligent Vehicles*.

Amini, Arghavan, Reza Monir Vaghefi, Jesus M De Garza, and R Michael Buehrer. 2014. "Improving GPS-Based Vehicle Positioning for Intelligent Transportation Systems," no. Iv: 1023–29.

Anderson, Frank C., and Marcus G. Pandy. 2001. "Dynamic Optimization of Human Walking." *Journal of Biomechanical Engineering* 123 (5): 381. doi:10.1115/1.1392310.

Ang, Chee-wei. 2018. “Vehicle Positioning Using WIFI Fingerprinting in Urban Environment.” In *2018 IEEE 4th World Forum on Internet of Things (WF-IoT)*, 4th:652–57. doi:10.1109/WF-IoT.2018.8355136.

Arulampalam, M. Sanjeev, Simon Maskell, Neil Gordon, and Tim Clapp. 2007. “A Tutorial on Particle Filters for Online Nonlinear/Nongaussian Bayesian Tracking.” *Bayesian Bounds for Parameter Estimation and Nonlinear Filtering/Tracking* 50 (2): 723–37. doi:10.1109/9780470544198.ch73.

Bar-Shalom, Yaakov, X.-Rong Li, and Thiagalingam Kirubarajan. 2001. *Estimation with Applications to Tracking and Navigation*. New York, USA: John Wiley & Sons, Inc. doi:10.1002/0471221279.

Belagiannis, Vasileios, Christian Rupprecht, Gustavo Carneiro, and Nassir Navab. 2015. “Robust Optimization for Deep Regression.” *Proceedings of the IEEE International Conference on Computer Vision* 2015 Inter: 2830–38. doi:10.1109/ICCV.2015.324.

Belloche, Sylvain. 2015. “On-Street Parking Search Time Modelling and Validation with Survey-Based Data.” *Transportation Research Procedia* 6 (June 2014). Elsevier B.V.: 313–24. doi:10.1016/j.trpro.2015.03.024.

Besl, P.J., and Neil D. McKay. 1992. “A Method for Registration of 3-D Shapes.” *IEEE Transactions on Pattern Analysis and Machine Intelligence* 14 (2): 239–56. doi:10.1109/34.121791.

Bhatt, Deepak, Swarna Ravindra Babu, and Haresh S. Chudgar. 2017. “A Novel Approach towards Utilizing Dempster Shafer Fusion Theory to Enhance WiFi Positioning System Accuracy.” *Pervasive and Mobile Computing* 37. Elsevier B.V.: 115–23. doi:10.1016/j.pmcj.2016.06.014.

Blumenthal, Jan, Ralf Grossmann, Frank Golatowski, and Dirk Timmermann. 2007. “Weighted Centroid Localization in Zigbee-Based Sensor Networks.” In *2007 IEEE International Symposium on Intelligent Signal Processing*, 1–6. IEEE. doi:10.1109/WISP.2007.4447528.

Bojja, J., M. Kirkko-Jaakkola, J. Collin, and J. Takala. 2013. “Indoor Localization Methods Using Dead Reckoning and 3D Map Matching.” *Journal of Signal Processing Systems*, 1–12. doi:10.1007/s11265-013-0865-9.

Borenstein, Johann. 1995. “Internal Correction of Dead-Reckoning Errors With a Dual-Drive

Compliant Linkage Mobile Robot." *Reprint from Journal of Robotic Systems* 12 (4): 257–73. http://www-personal.umich.edu/~johannb/Papers/paper48.pdf.

Borges, Paulo, Robert Zlot, Michael Bosse, Stephen Nuske, and Ashley Tews. 2010. "Vision-Based Localization Using an Edge Map Extracted from 3D Laser Range Data." *2010 IEEE International Conference on Robotics and Automation*, 4902–9. doi:10.1109/ROBOT.2010.5509517.

Boucher, Maxime, Fakhr-Eddine Ababsa, and Malik Mallem. 2013. "Reducing the SLAM Drift Error Propagation Using Sparse but Accurate 3D Models for Augmented Reality Applications." In *Proceedings of the Virtual Reality International Conference on Laval Virtual - VRIC '13*, 1. New York, New York, USA: ACM Press. doi:10.1145/2466816.2466828.

Boushaba, Mustapha, Abdelhakim Hafid, and Abderrahim Benslimane. 2009. "High Accuracy Localization Method Using AoA in Sensor Networks." *Computer Networks* 53 (18). Elsevier B.V.: 3076–88. doi:10.1016/j.comnet.2009.07.015.

Box, G. E. P., and Mervin E. Muller. 1958. "A Note on the Generation of Random Normal Deviates." *The Annals of Mathematical Statistics* 29 (2). Institute of Mathematical Statistics: 610–11. doi:10.1214/aoms/1177706645.

Breiman, Leo. 1996. "Bagging Predictors." *Machine Learning* 24: 123–40. doi:10.1007/BF00058655.

Bresson, Guillaume, Zayed Alsayed, Li Yu, and Sebastien Glaser. 2017. "Simultaneous Localization And Mapping: A Survey of Current Trends in Autonomous Driving." *IEEE Transactions on Intelligent Vehicles*, 1–1. doi:10.1109/TIV.2017.2749181.

Bresson, Guillaume, Romuald Aufr, Roland Chapuis, Guillaume Bresson, Romuald Aufr, Guillaume Bresson, and Romuald Aufr. 2016. "Improving SLAM with Drift Integration To Cite This Version :"

Caffery, J.J. 2000. "A New Approach to the Geometry of TOA Location." *Vehicular Technology Conference Fall 2000. IEEE VTS Fall VTC2000. 52nd Vehicular Technology Conference (Cat. No.00CH37152)* 4: 1943–49. doi:10.1109/VETECF.2000.886153.

Calvet, Laurent E., Veronika Czellar, and Elvezio Ronchetti. 2015. "Robust Filtering." *Journal of the American Statistical Association* 110 (512): 1591–1606. doi:10.1080/01621459.2014.983520.

Carlson, Justin, Charles Thorpe, and Brett Browning. 2010. “Mapping Large , Urban Environments with GPS-Aided SLAM.”

Chen, Hongyang, Pei Huang, Marcelo Martins, Hing Cheung So, and Kaoru Sezaki. 2008. “Novel Centroid Localization Algorithm for Three-Dimensional Wireless Sensor Networks.” In *2008 4th International Conference on Wireless Communications, Networking and Mobile Computing*, 1–4. IEEE. doi:10.1109/WiCom.2008.841.

Chen, Huijie, Fan Li, and Yu Wang. 2018. “SoundMark: Accurate Indoor Localization via Peer-Assisted Dead Reckoning.” *IEEE Internet of Things Journal*, 1–1. doi:10.1109/JIOT.2018.2821364.

Chen, Shaojian, Zihao Li, and Yunliang Long. 2017. “An Adaptive Hybrid Indoor WiFi Fingerprinting and Propagation Parameter Estimation Using RANSAC LASSO Regression.” In *2017 IEEE 5th International Symposium on Electromagnetic Compatibility (EMC-Beijing)*, 1–6. IEEE. doi:10.1109/EMC-B.2017.8260398.

Dao, Trung Kien, Hung Long Nguyen, Thanh Thuy Pham, Eric Castelli, Viet Tung Nguyen, and Dinh Van Nguyen. 2014. “User Localization in Complex Environments by Multimodal Combination of GPS, WiFi, RFID, and Pedometer Technologies.” *The Scientific World Journal* 2014. ScientificWorld Ltd. doi:10.1155/2014/814538.

Daum, Fred. 2005. “Nonlinear Filters: Beyond the Kalman Filter.” *IEEE Aerospace and Electronic Systems Magazine* 20 (8 II): 57–68. doi:10.1109/MAES.2005.1499276.

Daum, Fred, Jim Huang, and A Noushin. 2011. “Particle Flow for Nonlinear Filters.” *Proceedings of SPIE*, 5920–23. http://link.aip.org/link/?PSISDG/7697/769704/1%5Cnhttp://ieeexplore.ieee.org/xpls/abs_all.jsp?arnumber=5947709.

De Ponte Müller, Fabian, Estefanía Munoz Diaz, and Ibrahim Rashdan. 2017. “Cooperative Infrastructure-Based Vehicle Positioning.” *IEEE Vehicular Technology Conference*. doi:10.1109/VTCFall.2016.7880941.

Dellaert, F., D. Fox, W. Burgard, and S. Thrun. 2018. “Monte Carlo Localization for Mobile Robots.” In *Proceedings 1999 IEEE International Conference on Robotics and Automation (Cat. No.99CH36288C)*, 2:1322–28. IEEE. Accessed May 29. doi:10.1109/ROBOT.1999.772544.

Department Of Defense, U.S.a. 2008. “Global Positioning System Standard Positioning

Service." *Www.Gps.Gov*, no. September: 1–160. http://www.gps.gov/technical/ps/2008-SPS-performance-standard.pdf.

Dietterich, Thomas G. 2000. "Ensemble Methods in Machine Learning." *Multiple Classifier Systems* 1857: 1–15. doi:10.1007/3-540-45014-9.

"Differential GNSS - Navipedia." 2018. Accessed May 27. http://www.navipedia.net/index.php/Differential_GNSS.

Dongliang Huang, and H. Leung. 2004. "EM-IMM Based Land-Vehicle Navigation with GPS/INS." *Proceedings. The 7th International IEEE Conference on Intelligent Transportation Systems (IEEE Cat. No.04TH8749)*, no. Cv: 624–29. doi:10.1109/ITSC.2004.1398973.

Douc, Randal, Olivier Cappé, and Eric Moulines. 2005. "Comparison of Resampling Schemes for Particle Filtering," 1–10. doi:10.1109/ISPA.2005.195385.

Doucet, Arnaud, and Adam M. Johansen. 2011. "A Tutorial on Particle Filtering and Smoothing: Fiteen Years Later." *The Oxford Handbook of Nonlinear Filtering*, no. December 2008: 656–705. doi:10.1.1.157.772.

Drawil, Nabil Mohamed, and Otman Basir. 2010. "Intervehicle-Communication-Assisted Localization" 11 (3): 678–91.

Drew Bagnell. 2018. "Particle Filter: The Good, The Bad, The Ugly." Accessed August 5. http://en.wikipedia.org/w/index.php?title=Stochastic_universal_sampling&oldid=356360569.

Durrant-Whyte, H, and T Bailey. 2006. "Simultaneous Localization and Mapping (SLAM)." *IEEE Robotics & Automation Magazine* 13 (2): 99–116. doi:10.1109/MRA.2006.1638022.

Efron, Bradley., and Robert. Tibshirani. 1994. *An Introduction to the Bootstrap*. New York N.Y. ;;London: Chapman & Hall. http://www.worldcat.org/title/introduction-to-the-bootstrap/oclc/797437299.

El Faouzi, N.-E. 1997. "Heterogeneous Data Source Fusion for Impedance Indicators." *IFAC Proceedings Volumes* 30 (8). Elsevier: 1307–12. doi:10.1016/S1474-6670(17)44002-X.

Elfes, A. 2013. "Occupancy Grids: A Stochastic Spatial Representation for Active Robot Perception," March. http://arxiv.org/abs/1304.1098.

Eskandarian, Azim. 2012. *Handbook of Intelligent Vehicles*. Springer.

F.~Gustafsson. 2010. "Particle Filter Theory and Practice with Positioning Applications." *IEEE Transactions on Aerospace and Electronics Systems Magazine Part II: Tutorials* 25 (7): 53–82.

Faouzi, Nour Eddin El, Henry Leung, and Ajeesh Kurian. 2011. "Data Fusion in Intelligent Transportation Systems: Progress and Challenges - A Survey." *Information Fusion* 12 (1). Elsevier B.V.: 4–10. doi:10.1016/j.inffus.2010.06.001.

Fernández-Hernández, I, J Simón, R Blasi, C Payne, T Miquel, and J P Boyero. 2018. "The Galileo Commercial Service: Current Status and Prospects." Accessed August 16. https://www.researchgate.net/profile/Ignacio_Fernandez-Hernandez/publication/264762639_The_Galileo_Commercial_Service_Current_Status_and_Prospects/links/53ee3a1b0cf2981ada175ca3/The-Galileo-Commercial-Service-Current-Status-and-Prospects.pdf.

Fouque, Clément, Philippe Bonnifait, David Bétaille, and A Working. 2008. "Enhancement of Global Vehicle Localization Using Navigable Road Maps and Dead-Reckoning," 1286–91.

Fujii, Keisuke. 2018. "Extended Kalman Filter." Accessed June 10. http://www-jlc.kek.jp/2003oct/subg/offl/kaltest/doc/ReferenceManual.pdf.

"Galileo General Introduction - Navipedia." 2018. Accessed August 16. https://gssc.esa.int/navipedia/index.php/Galileo.

Gantelet, Eric, and Amélie Lefauconnier. 2006. "The Time Looking for a Parking Space: Strategies, Associated Nuisances and Stakes of Parking Management in France," 1–7.

Garip, Mevlut Turker, Paul Hyungmin Kim, Peter Reiher, and Mario Gerla. 2017. "INTERLOC: An Interference-Aware RSSI-Based Localization and Sybil Attack Detection Mechanism for Vehicular Ad Hoc Networks." *2017 14th IEEE Annual Consumer Communications & Networking Conference (CCNC)*, 1–6. doi:10.1109/CCNC.2017.8013424.

Giger, Adolf J, Senior Member, and William T Barnett. 1981. "Effects of Multipath Propagation on Digital Radio" C (9): 1345–52.

Gikas, Vassilis, Constantinos Antoniou, Guenther Retscher, Athanasios Panagopoulos, Allison Kealy, Harris Perakis, and Thanassis Mpimis. 2016. "A Low-Cost Wireless Sensors

Positioning Solution for Indoor Parking Facilities Management." *Journal of Location Based Services* 10 (4). Taylor & Francis: 241–61. doi:10.1080/17489725.2016.1231351.

"GLONASS Performances - Navipedia." 2018. Accessed August 16. https://gssc.esa.int/navipedia/index.php/GLONASS_Performances.

GPS Directorate. 2007. "Global Positioning System Precise Positioning Service (PPS) Performace Standard," no. February: 35. http://www.gps.gov/technical/ps/#spsps.

"GPS Performances - Navipedia." 2018. Accessed May 27. http://www.navipedia.net/index.php/GPS_Performances#cite_note-SPS-Standard-1.

Groh, Benjamin H, Martin Friedl, Andre G Linarth, and Elli Angelopoulou. 2014. "Advanced Real-Time Indoor Parking Localization Based on Semi-Static Objects." *Information Fusion (FUSION), 2014*, 1–7.

Guan, Yu, and Thomas Ploetz. 2017. "Ensembles of Deep LSTM Learners for Activity Recognition Using Wearables" 1 (2). doi:10.1145/3090076.

Guo, Xiansheng, Nirwan Ansari, Lin Li, and Huiyong Li. 2018. "Indoor Localization by Fusing a Group of Fingerprints Based on Random Forests." *IEEE Internet of Things Journal* XX (XX): 1–13. doi:10.1109/JIOT.2018.2810601.

Hahnel, D., W. Burgard, D. Fox, and S. Thrun. 2018. "An Efficient Fastslam Algorithm for Generating Maps of Large-Scale Cyclic Environments from Raw Laser Range Measurements." In *Proceedings 2003 IEEE/RSJ International Conference on Intelligent Robots and Systems (IROS 2003) (Cat. No.03CH37453)*, 1:206–11. IEEE. Accessed May 29. doi:10.1109/IROS.2003.1250629.

Han, Jiawei, Micheline Kamber, and Jian Pei. 2012. *Data Mining: Concepts and Techniques*. *San Francisco, CA, Itd: Morgan Kaufmann*. doi:10.1016/B978-0-12-381479-1.00001-0.

Hansen, Lars Kai, and Peter Salamon. 1990. "Neural Network Ensembles." *IEEE Transactions on Pattern Analysis and Machine Intelligence* 12 (10): 993–1001. doi:10.1109/34.58871.

Harkema, Susan, Andrea Behrman, and Hugues Barbeau. 2012. "Evidence-Based Therapy for Recovery of Function after Spinal Cord Injury." *Handbook of Clinical Neurology* 109 (January). Elsevier: 259–74. doi:10.1016/B978-0-444-52137-8.00016-4.

He, Suining, S.-H.G. Chan, Lei Yu, and Ning Liu. 2015. "Fusing Noisy Fingerprints with Distance Bounds for Indoor Localization." *Proc. IEEE INFOCOM*, no. 610713: 2506–14.

doi:10.1109/INFOCOM.2015.7218640.

He, Ying, Bin Liang, Jun Yang, Shunzhi Li, and Jin He. 2017. "An Iterative Closest Points Algorithm for Registration of 3D Laser Scanner Point Clouds with Geometric Features." *Sensors* 17 (8): 1862. doi:10.3390/s17081862.

Heaton, Jeff. 2008. *Introduction to Neural Networks with Java*. Heaton Research. https://books.google.it/books?id=Swlcw7M4uD8C&pg=PA158&lpg=PA158&dq=Introduction to Neural Networks for Java, Second Edition The Number of Hidden Layers&source=bl&ots=TJx9QaeWw6&sig=gZqg9e73K1oCqWBxmcBWAf2pbrE&hl=it&sa=X&ved=0CCUQ6AEwAGoVChMIudnOsJr1yAIVwjkaCh3AAgnU#v=onepage&q=Introduction to Neural Networks for Java%2C Second Edition The Number of Hidden Layers&f=false.

Hernández, Noelia, Jose M. Alonso, and Manuel Ocaña. 2017. "Fuzzy Classifier Ensembles for Hierarchical WiFi-Based Semantic Indoor Localization." *Expert Systems with Applications* 90: 394–404. doi:10.1016/j.eswa.2017.08.007.

Hernandez, Noelia, Ahmed Hussein, Daniel Cruzado, Ignacio Parra, and Jose Maria Armingol. 2017. "Applying Low Cost WiFi-Based Localization to in-Campus Autonomous Vehicles." In *2017 IEEE 20th International Conference on Intelligent Transportation Systems (ITSC)*, 1–6. IEEE. doi:10.1109/ITSC.2017.8317780.

Hofmann-Wellenhof, B., Herbert Lichtenegger, and Elmar. Wasle. 2018. *GNSS--Global Navigation Satellite Systems : GPS, GLONASS, Galileo, and More*. Accessed May 25. https://books.google.fr/books?hl=vi&lr=&id=Np7y43HU_m8C&oi=fnd&pg=PR20&dq=GNSS&ots=FfpF91OM94&sig=o89SQ2Fx3QR-Q-S_8POdu0L0EFY&redir_esc=y#v=onepage&q=GNSS&f=false.

Houben, S, M Komar, A Hohm, S Luke, M Neuhausen, and M Schlipsing. 2013. "On-Vehicle Video-Based Parking Lot Recognition with Fisheye Optics." *2013 16th International Ieee Conference on Intelligent Transportation Systems - (Itsc)*, no. Itsc: 7–12.

Ibisch, Andre, Stefan Stumper, Harald Altinger, Marcel Neuhausen, Marc Tschentscher, Marc Schlipsing, Jan Salinen, and Alois Knoll. 2013. "Towards Autonomous Driving in a Parking Garage: Vehicle Localization and Tracking Using Environment-Embedded LIDAR Sensors." *IEEE Intelligent Vehicles Symposium, Proceedings*, no. Iv: 829–34. doi:10.1109/IVS.2013.6629569.

"IEEE 802.11: Wireless LAN Medium Access Control (MAC) and Physical Layer (PHY) Specifications." 2016, December. doi:10.1109/IEEESTD.2016.7786995.

Ignacio, Fernandez Hernandez, Rodriguez Irma, and Tobias Guillermo. 2015. "Galileo's Commercial Service Testing GNSS High Accuracy and Authentication." http://spcomnav.uab.es/docs/journals/janfeb15-FERNANDEZ.pdf.

"Infsoft Ultra-Wideband Technology for Indoor Positioning." 2018. Accessed June 2. https://www.infsoft.com/technology/sensors/ultra-wideband.

Iter, Dan, Jonathan Kuck, and Philip Zhuang. 2016. "Target Tracking with Kalman Filtering, KNN and LSTMs."

James Eddy. 2017. "Introduction to LiDAR and Its Applications | Col-East | Aerial Photo, LiDAR, Topo Mapping and GIS Data." https://www.col-east.net/single-post/2017/11/17/Introduction-to-LiDAR-and-its-Applications.

Julier, S. J., and J. K. Uhlmann. 2001. "A Counter Example to the Theory of Simultaneous Localization and Map Building." *Proceedings - IEEE International Conference on Robotics and Automation* 4 (Ic): 4238–43. doi:10.1109/ROBOT.2001.933280.

Kalman, R. E. 1960. "A New Approach to Linear Filtering and Prediction Problems." *Journal of Basic Engineering*. doi:10.1115/1.3662552.

Kaune, R. 2012. "Accuracy Studies for TDOA and TOA Localization." *2012 15th International Conference on Information Fusion (FUSION)*, 408–15.

Kim, Jonghyuk. 2004. "SLAM Aided GPS / INS Navigation in GPS Denied and Unknown Environments," no. December.

Kos, T., I. Markezic, and J. Pokrajcic. 2010. "Effects of Multipath Reception on GPS Positioning Performance." *Elmar, 2010 Proceedings*, no. September: 15–17.

Kotaru, Manikanta, Kiran Joshi, Dinesh Bharadia, and Sachin Katti. n.d. "SpotOn: Indoor Localization Using Commercial off-the-Shelf WiFi NICs."

———. 2015. "SpotFi : Decimeter Level Localization Using WiFi." *Sigcomm 2015*, 269–82. doi:10.1145/2785956.2787487.

Krogh, Anders Jesper, Vedelsby. 1995. "Neural Network Ensembles , Cross Validation , and Active Learning." *Advances in Neural Information Processing Systems 7*, 231–38.

Kunz, Felix, Dominik Nuss, Jurgen Wiest, Hendrik Deusch, Stephan Reuter, Franz

Gritschneder, Alexander Scheel, et al. 2015. “Autonomous Driving at Ulm University: A Modular, Robust, and Sensor-Independent Fusion Approach.” *IEEE Intelligent Vehicles Symposium, Proceedings* 2015–Augus (Iv): 666–73. doi:10.1109/IVS.2015.7225761.

Kuter, Nazan, and Semih Kuter. 2010. “Accuracy Comparison between GPS and DGPS: A Field Study at METU Campus.” *Italian Journal of Remote Sensing*, October, 3–14. doi:10.5721/ItJRS20104231.

Lee, Dong-u, John D Villasenor, Senior Member, Wayne Luk, and Philip H W Leong. 2006. “The Box-Muller Method and Its Error Analysis.” *October* 55 (6): 659–71.

Levinson, Jesse, Michael Montemerlo, and Sebastian Thrun. 2008. “Map-Based Precision Vehicle Localization in Urban Environments.” *Robotics: Science and Systems III*, 121–28. http://citeseerx.ist.psu.edu/viewdoc/download?doi=10.1.1.117.222&rep=rep1&type=pdf.

Liu, Feng, and Hongbin Tan. 2012. “Research and Implementation of APIT Positioning Algorithm in WSN.” *Proceedings - 2012 9th International Conference on Fuzzy Systems and Knowledge Discovery, FSKD 2012*, no. Fskd: 2212–15. doi:10.1109/FSKD.2012.6234209.

Liu, Jingbin, Ruizhi Chen, Yuwei Chen, Ling Pei, and Liang Chen. 2012. “IParking: An Intelligent Indoor Location-Based Smartphone Parking Service,” 14612–29. doi:10.3390/s121114612.

Liu, Minjie, Shoudong Huang, Gamini Dissanayake, and Heng Wang. 2012. “A Convex Optimization Based Approach for Pose SLAM Problems.” In *2012 IEEE/RSJ International Conference on Intelligent Robots and Systems*, 1898–1903. IEEE. doi:10.1109/IROS.2012.6385742.

Liu, Zhenguang, Luming Zhang, Qi Liu, Yifang Yin, Li Cheng, and Roger Zimmermann. 2017. “Fusion of Magnetic and Visual Sensors for Indoor Localization: Infrastructure-Free and More Effective.” *IEEE Transactions on Multimedia* 19 (4): 874–88. doi:10.1109/TMM.2016.2636750.

“Loi Du 7 Octobre 2016 Pour Une République Numérique.” 2016. vie-publique.fr - Direction de l’information légale et administrative. http://www.vie-publique.fr/actualite/panorama/texte-discussion/projet-loi-pour-republique-numerique.html.

Magdon-Ismail, Malik, and Amir F. Atiya. 2000. “The Early Restart Algorithm.” *Neural Computation* 12 (6): 1303–12. doi:10.1162/089976600300015376.

Malys, Stephen, John H. Seago, Nikolaos K. Pavlis, P. Kenneth Seidelmann, and George H. Kaplan. 2015. “Why the Greenwich Meridian Moved.” *Journal of Geodesy* 89 (12): 1263–72. doi:10.1007/s00190-015-0844-y.

Mauro, M Di, G Della Corte, A L Robustelli, P Addesso, M Longo, and G.D.a Robustelli A.L.a Addesso P.b Longo M.b Mauro M.D.a Corte. 2009. “A WLAN-Based Location System for Indoor Parking Areas.” *SoftCOM 2009 - 17th International Conference on Software, Telecommunications and Computer Networks*, 186–90. http://www.scopus.com/inward/record.url?eid=2-s2.0-70649096311&partnerID=40&md5=4d0434d2434c1d242d8b91b438292a11.

Mohan, Mahesh, and K MadhavaKrishna. 2010. “Mapping Large Scale Environments by Combining Particle Filter and Information Filter.” In *2010 11th International Conference on Control Automation Robotics & Vision*, 1000–1005. IEEE. doi:10.1109/ICARCV.2010.5707412.

Montemerlo, Michael, Sebastian Thrun, Daphne Koller, and Ben Wegbreit. 2018. “FastSLAM: A Factored Solution to the Simultaneous Localization and Mapping Problem.” Accessed May 29. http://robots.stanford.edu/papers/montemerlo.fastslam-tr.pdf.

Moreira, Daniel, Sandra Avila, Mauricio Perez, Daniel Moraes, Vanessa Testoni, Eduardo Valle, Siome Goldenstein, and Anderson Rocha. 2019. “Multimodal Data Fusion for Sensitive Scene Localization.” *Information Fusion* 45 (January). Elsevier: 307–23. doi:10.1016/J.INFFUS.2018.03.001.

Moussawi, HN Al. 2012. “Some Signal Processing Techniques for Wireless Cooperative Localization and Tracking.” http://tel.archives-ouvertes.fr/tel-00787543/.

Nguyen, Dinh-Van, Eric Castelli, Trung-Kien Dao, Duc-Tho Le, Lan-Huong Nguyen, and Salim Attig. 2014. “Application of Environment Constraints in Improving Localization Accuracy.” In , 441–47. Springer, Berlin, Heidelberg. doi:10.1007/978-3-642-41671-2_56.

Niculescu, D., and Badri Nath. 2001. “Ad Hoc Positioning System (APS) Using AOA.” *IEEE INFOCOM 2003. Twenty-Second Annual Joint Conference of the IEEE Computer and Communications Societies (IEEE Cat. No.03CH37428)* 3: 1734–43.

doi:10.1109/INFCOM.2003.1209196.

"Norme Francaise, Parcs de Stationnement a Usage Privatif." 1996. https://www.leperreux94.fr/ckfinder/userfiles/files/6_17 Nome NF P 91-120 parcs de stationnement privatif.pdf.

Nourinejad, Mehdi, Sina Bahrami, and Matthew J Roorda. 2018. "Designing Parking Facilities for Autonomous Vehicles." Accessed September 19. http://uttri.utoronto.ca/files/2017/09/Designing-Parking-geometricDesign.pdf.

"Parking at the Service of Connected Urban Mobility and a Sustainable City - The Urban Mobility Blog." 2018. Accessed August 17. https://urbanmobilitydaily.com/le-parking-au-service-de-la-mobilite-urbaine-connectee-et-dune-ville-durable-2/?utm_source=AUTONOMY+-+whole+audience+list&utm_campaign=20569f61b6-EMAIL_CAMPAIGN_2018_07_17_02_44&utm_medium=email&utm_term=0_83c64bc903-20569f6.

"Parking Solutions - Solutions - OneSITU." 2018. Accessed May 20. https://www.onesitu.com/solutions/onesitu-parking/?lang=en.

"Parkmatic - Multi Parking." 2018. Accessed May 20. http://www.parkmatic.com/multi-parking.

Pierzchała, Marek, Philippe Giguère, and Rasmus Astrup. 2018. "Mapping Forests Using an Unmanned Ground Vehicle with 3D LiDAR and Graph-SLAM." *Computers and Electronics in Agriculture* 145 (February). Elsevier: 217–25. doi:10.1016/J.COMPAG.2017.12.034.

Pitt, Michael K., and Neil Shephard. 1999. "Filtering via Simulation: Auxiliary Particle Filters." *Journal of the American Statistical Association* 94 (446): 590–99. doi:10.1080/01621459.1999.10474153.

Pivato, Paolo, Luigi Palopoli, and Dario Petri. 2011. "Accuracy of RSS-Based Centroid Localization Algorithms in an Indoor Environment." *IEEE Transactions on Instrumentation and Measurement* 60 (10): 3451–60. doi:10.1109/TIM.2011.2134890.

Prechelt, Lutz. 2012. "Early Stopping - But When?" *Lecture Notes in Computer Science (Including Subseries Lecture Notes in Artificial Intelligence and Lecture Notes in Bioinformatics)* 7700 LECTU: 53–67. doi:10.1007/978-3-642-35289-8-5.

"Real Time Kinematics - Navipedia." 2018. Accessed May 27.

http://www.navipedia.net/index.php/Real_Time_Kinematics.

Reineking, T, and J Clemens. 2013. “Evidential FastSLAM for Grid Mapping.” *International Conference on Information Fusion (FUSION)*, no. i: 789–96.

Schleicher, David, Luis M. Bergasa, Manuel Ocaña, Rafael Barea, and María Elena López. 2009. “Real-Time Hierarchical Outdoor Slam Based on Stereovision and GPS Fusion.” *IEEE Transactions on Intelligent Transportation Systems* 10 (3): 440–52. doi:10.1109/TITS.2009.2026317.

Schwesinger, Ulrich, Mathias Burki, Julian Timpner, Stephan Rottmann, Lars Wolf, Lina Maria Paz, Hugo Grimmett, et al. 2016. “Automated Valet Parking and Charging for E-Mobility.” *IEEE Intelligent Vehicles Symposium, Proceedings* 2016–Augus (Iv): 157–64. doi:10.1109/IVS.2016.7535380.

Scrapper, C, R Madhavan, and S Balakirsky. 2018. “Stable Navigation Solutions for Robots in Complex Environments †.” Accessed August 16. https://ws680.nist.gov/publication/get_pdf.cfm?pub_id=824591.

Shafer, Glenn. 1976. *A Mathematical Theory of Evidence*. Princeton University Press. https://press.princeton.edu/titles/2439.html.

Shi, Yun, Shunping Ji, Zhongchao Shi, Yulin Duan, and Ryosuke Shibasaki. 2012. “GPS-Supported Visual SLAM with a Rigorous Sensor Model for a Panoramic Camera in Outdoor Environments.” *Sensors (Basel, Switzerland)* 13 (1): 119–36. doi:10.3390/s130100119.

Skyline Inc. 2018. “Innovative Automated Parking Solution | Skyline Parking | Skyline Parking.” Accessed May 20. https://skyline-parking.com/automated-parking-systems/.

Smets, Philippe, and Robert Kennes. 1994. “The Transferable Belief Model.” *Artificial Intelligence* 66 (2). Elsevier: 191–234. doi:10.1016/0004-3702(94)90026-4.

Smith, Randall C, and Peter Cheeseman. 2018. “On the Representation and Estimation Of.” Accessed May 29. https://www.frc.ri.cmu.edu/~hpm/project.archive/reference.file/Smith&Cheeseman.pdf.

Ta, Viet Cuong, Dominique Vaufreydaz, Trung-kien Dao, Eric Castelli, Viet Cuong Ta, Dominique Vaufreydaz, Trung-kien Dao, et al. 2016. “Smartphone-Based User Location Tracking in Indoor Environment To Cite This Version : HAL Id : Hal-01370252 Smartphone-Based User Location Tracking in Indoor Environment.”

Torres-Sospedra, Joaquin, German M. Mendoza-Silva, Raul Montoliu, Oscar Belmonte, Fernando Benitez, and Joaquin Huerta. 2016. "Ensembles of Indoor Positioning Systems Based on Fingerprinting: Simplifying Parameter Selection and Obtaining Robust Systems." In *2016 International Conference on Indoor Positioning and Indoor Navigation (IPIN)*, 1–8. IEEE. doi:10.1109/IPIN.2016.7743679.

Trehard, Guillaume. 2015. "Evidence Theory Applications for Localization and Mapping in an Urban Context." l'École nationale supérieure des mines de Paris.

Trehard, Guillaume, Zayed Alsayed, Evangeline Pollard, Benazouz Bradai, and Fawzi Nashashibi. 2014. "Credibilist Simultaneous Localization and Mapping with a LIDAR." *IEEE International Conference on Intelligent Robots and Systems*, 2699–2706. doi:10.1109/IROS.2014.6942931.

Venkatraman, Saipradeep, James Caffery, and Heung Ryeol You. 2004. "A Novel ToA Location Algorithm Using LoS Range Estimation for NLoS Environments." *IEEE Transactions on Vehicular Technology* 53 (5): 1515–24. doi:10.1109/TVT.2004.832384.

Vivacqua, Rafael Peixoto Derenzi, Massimo Bertozzi, Pietro Cerri, Felipe Nascimento Martins, and Raquel Frizera Vassallo. 2018. "Self-Localization Based on Visual Lane Marking Maps: An Accurate Low-Cost Approach for Autonomous Driving." *IEEE Transactions on Intelligent Transportation Systems* 19 (2): 582–97. doi:10.1109/TITS.2017.2752461.

Wahl, Steffen, Peter Schlumberger, Raul Rojas, and Martin Stampfle. 2015. "Localization inside a Populated Parking Garage by Using Particle Filters with a Map of the Static Environment." *IEEE Intelligent Vehicles Symposium, Proceedings* 2015–Augus (Iv): 95–100. doi:10.1109/IVS.2015.7225669.

Wang, Xuyu, Lingjun Gao, Shiwen Mao, and Santosh Pandey. 2017. "CSI-Based Fingerprinting for Indoor Localization: A Deep Learning Approach." *IEEE Transactions on Vehicular Technology* 66 (1): 763–76. doi:10.1109/TVT.2016.2545523.

Weiss, Thorsten, Bruno Schiele, and Klaus Dietmayer. 2007. "Robust Driving Path Detection in Urban and Highway Scenarios Using a Laser Scanner and Online Occupancy Grids." In *2007 IEEE Intelligent Vehicles Symposium*, 184–89. IEEE. doi:10.1109/IVS.2007.4290112.

Wietrzykowski, Jan, Michał Nowicki, and Piotr Skrzypczyński. 2017. "Adopting the FAB-MAP Algorithm for Indoor Localization with WiFi Fingerprints." In , 585–94. Springer,

Cham. doi:10.1007/978-3-319-54042-9_58.

Wilfinger, Roman, and Master S Thesis. 2015. “Absolute Positioning of Vehicles in Indoor Environments Using Wireless LAN and Bluetooth LE,” no. April.

“Wireless Sensors Networks.” 2018. *Wikipedia*. Accessed May 31. https://en.wikipedia.org/wiki/Wireless_sensor_network.

“World Geodetic System (WGS84) - GIS Geography.” 2018. Accessed May 22. https://gisgeography.com/wgs84-world-geodetic-system/.

Xie, Jianping, Fawzi Nashashibi, Michel Parent, Olivier Garcia-favrot, Jianping Xie, Fawzi Nashashibi, Michel Parent, et al. 2011. “A Real-Time Robust Global Localization for Autonomous Mobile Robots in Large Environments To Cite This Version : A Real-Time Robust Global Localization for Autonomous Mobile Robots in Large Environments.”

Xiong, J, and K Jamieson. 2013. “ArrayTrack: A Fine-Grained Indoor Location System.” *USENIX Symposium on Networked Systems Design and Implementation*, no. 279976: 71–84. http://discovery.ucl.ac.uk/1329002/.

Yin, Jihao, Qun Wan, Shiwen Yang, and K. C. Ho. 2016. “A Simple and Accurate TDOA-AOA Localization Method Using Two Stations.” *IEEE Signal Processing Letters* 23 (1): 144–48. doi:10.1109/LSP.2015.2505138.

Zhang, Wei, Kan Liu, Weidong Zhang, Youmei Zhang, and Jason Gu. 2016. “Deep Neural Networks for Wireless Localization in Indoor and Outdoor Environments.” *Neurocomputing* 194. Elsevier: 279–87. doi:10.1016/j.neucom.2016.02.055.

Zhou, Rui, Shuai Lu, Jiesong Chen, and Zhiqiang Li. 2017. “An Optimized Space Partitioning Technique to Support Two-Layer WiFi Fingerprinting.” In *2017 IEEE Wireless Communications and Networking Conference (WCNC)*, 1–6. IEEE. doi:10.1109/WCNC.2017.7925445.

Zhou, Rui, Xiang Lu, Pengbiao Zhao, and Jiesong Chen. 2017. “Device-Free Presence Detection and Localization with SVM and CSI Fingerprinting.” *IEEE Sensors Journal* 17 (23): 7990–99. doi:10.1109/JSEN.2017.2762428.

Ziegler, Julius, Philipp Bender, Markus Schreiber, Henning Lategahn, Tobias Strauss, Christoph Stiller, Thao Dang, et al. 2014. “Making Bertha Drive—An Autonomous Journey on a Historic Route.” *IEEE Intelligent Transportation Systems Magazine* 6 (2): 8–20. doi:10.1109/MITS.2014.2306552.

8. APPENDIX 1: RÉSUMÉ

Chapter 1

Le chapitre présente la motivation, la portée et le but de la thèse. Cette thèse débute avec la collaboration de deux unités de recherche, l'équipe RITS, l'INRIA France et l'institut MICA, et est financée par le programme de bourses d'études 911 du gouvernement vietnamien. comme autoroute, rues urbaines, etc. L'environnement sans GPS, qui est également un scénario important pour les applications de véhicules intelligents, n'a pas encore été totalement traité. Un environnement notable pour un tel scénario est un parking couvert. Cette thèse a pour objectif de trouver une nouvelle solution au problème de localisation dans un environnement sans GPS. Les solutions existantes pour ce scénario sont coûteuses à déployer ou ne permettent pas de résoudre complètement le problème. Par conséquent, la solution doit être une méthode de localisation globale qui permette une transition transparente entre la localisation d'environnement assistée par GPS et celle qui est refusée par le GPS et satisfasse à quatre critères: disponibilité, évolutivité, universalité et précision. Deux contributions principales sont proposées: un système de localisation d'empreintes digitales d'ensemble Wi-Fi capable de reproduire le comportement du GPS pour l'environnement sans GPS et un cadre de fusion de filtres à particules mélangées gaussien permettant la fusion de techniques de localisation multiples.

Chapter 2

Dans ce chapitre, quelques techniques générales pour la localisation de véhicules intelligents sont examinées. En outre, une étude des solutions existantes pour la localisation de véhicules intelligents dans des environnements sans GPS est présentée.

En général, les techniques de localisation IV peuvent être divisées en deux catégories: la localisation globale et la localisation locale. Souvent, la catégorie de localisation globale est une méthode de localisation basée sur GNSS. Ces méthodes utilisent les signaux satellites pour déterminer les informations de position 3D du récepteur dans une référence globale (telle que WGS84). Le terme GPS fait référence au système de positionnement global qui est régi par les États-Unis d'Amérique. Il existe d'autres systèmes mondiaux de navigation par satellite (GNSS) tels que GLONASS (Russie), Galileo (Europe) et Beidou (Chine). Pour simplifier le problème,

la thèse se concentrera sur les performances du GPS en tant que représentant d'autres GNSS. Le principe de calcul de la position du récepteur est basé sur la connaissance des positions des satellites, puis sur la déduction des «pseudo-distances» respectives entre ces satellites et le récepteur, comme illustré à la figure 2.2. Ici, le terme "pseudo-distance" se réfère à la distance calculée entre les satellites et le récepteur mobile. Étant donné que les satellites se déplacent constamment, cette distance n'est pas une valeur fixe. Pour calculer la position 3D d'un récepteur, il faut au moins quatre satellites. Vous trouverez un aperçu du système GPS dans (Hofmann-Wellenhof, Lichtenegger et Wasle 2018).

Il existe deux niveaux de services GPS, à savoir le service de positionnement standard (SPS) et le service de positionnement précis (PPS). Alors que SPS est accessible aux utilisateurs publics, les PPS de haute précision ne sont accessibles qu'aux utilisateurs autorisés (personnel militaire, agents de l'État). Le tableau 1 et le tableau 2 récapitulent les performances SPS et PPS. En général, SPS fournit une erreur de localisation maximale de 7,8 m dans 95% des cas, et le système PPS offre une meilleure précision avec une erreur de localisation maximale de 5,9 m dans 95% des heures. temps. En outre, la précision verticale devrait être inférieure à la précision horizontale dans toutes les mesures GPS. Dans le meilleur des cas, une solution DGPS de haute précision appelée GPS cinématique en temps réel (RTK GPS) peut offrir une précision de quelques centimètres. Cependant, le procédé nécessite des stations de base dédiées, des capteurs, des signaux GPS continus et un prix excessif pour le déploiement et la maintenance. Cela rend le RTK non adapté à la plupart des applications urbaines («Real Time Kinematics - Navipedia» 2018).

À l'instar des États-Unis, l'Union européenne a également mis au point un système de positionnement global appelé Galileo, destiné à fournir un système de positionnement global indépendant de haute précision aux pays européens. Le système est censé aider les pays de l'UE à ne pas compter sur le chinois BeiDou, le russe GLONASS ou, plus important encore, sur le GPS américain. Dans de bonnes conditions, telles que des satellites pleinement fonctionnels (jusqu'à 30 unités), une vision claire du récepteur aux satellites, etc., le libre accès libre pour la navigation du système Galileo à la frontière de l'UE devrait être d'environ 4 mètres de précision («Galileo Introduction générale - Navipedia "2018). Le GLONASS développé par la Russie dans les années 1980 est un autre système qui mérite d'être mentionné. En 2010, le GLONASS couvrait l'ensemble du territoire russe, puis après octobre 2011, la couverture mondiale est atteinte. L'évolution de la précision de positionnement du GLONASS est illustrée à la figure 2.5. Jusqu'à présent, sous un ciel statique, la précision du GLONASS pour l'accès public était

de 2,8 mètres. Vous trouverez une comparaison rapide des différents systèmes de localisation globale dans le tableau 3.

Une méthode de localisation locale notable est la localisation au laser. En utilisant une technique de télémètre basée sur les rayons laser, le capteur estime avec précision la distance aux autres objets de l'environnement. Le LiDAR (James Eddy 2017) (détection de la lumière et télémétrie) est une forme importante de capteur laser qui déclenche des faisceaux laser en continu dans l'environnement. Cela aide à estimer la distance aux obstacles environnants et permet de cartographier l'environnement à haute résolution. Lorsqu'il s'agit de capteur laser, la majorité de ses algorithmes de localisation impliquent la résolution totale ou partielle d'un problème de localisation et de cartographie simultanées (Smith et Cheeseman 2018), (Durrant-Whyte et Bailey 2006), (Dellaert et al. 2018) . L'objectif du SLAM est d'estimer la trajectoire du véhicule (ou de le poser en mode SLAM en ligne) et en même temps de cartographier l'environnement voisin à partir des entrées des capteurs du véhicule. Une représentation graphique du problème SLAM complet et du problème SLAM en ligne est présentée aux figures 2.6a et 2.6b, respectivement. Dans le problème du SLAM complet, l'algorithme est supposé estimer la trajectoire entière du véhicule, formulée par une liste de ses poses sur le pas de temps k: x_k avec des capteurs lisant z_k, une entrée de commande u_k et construisant en même temps la carte m environnement. Cette tâche exigeante devient de plus en plus complexe avec le temps et il est difficile d'être gérée en temps réel. L'idée du SLAM en ligne, censé être fait en temps réel, est ensuite introduite. Le SLAM en ligne estimera uniquement la pose du véhicule actuel, ce qui réduira efficacement la complexité du problème. Vous trouverez un aperçu de la tendance actuelle du SLAM dans (Bresson et al. 2017). Compte tenu de la précision des capteurs laser et du potentiel du SLAM, la combinaison de LiDAR-SLAM devient rapidement l'une des clés pour des véhicules totalement autonomes. Au fil des ans, les techniques d'estimation dans SLAM peuvent être classées en approches basées sur les filtres et en approches basées sur l'optimisation.

L'idée de base des approches basées sur les filtres provient du filtrage bayésien et comprend deux étapes: la prévision et l'observation. Lors de la première étape, une prédiction de la pose et de la carte du véhicule est effectuée à l'aide d'un modèle dynamique des véhicules. Le modèle pour faire correspondre une observation à la carte s'appelle un modèle d'observation. Les deux branches principales de cette approche sont les filtres étendus de Kalman et les filtres à particules SLAM.

Le SLAM basé sur l'optimisation (M. Liu et al. 2012) est également un algorithme en deux étapes itératives. La première étape identifie les contraintes du problème en fonction des données du capteur. Cela se fait en faisant correspondre les nouvelles observations à la carte. La deuxième étape calcule la pose du véhicule et la carte en fonction des contraintes identifiées. Les techniques basées sur la vision pour SLAM sont plus susceptibles d'utiliser cette approche, les techniques basées sur le laser sont également incluses dans la classe d'algorithme Graph-SLAM.

Une autre approche notable pour la localisation de véhicules est la technique basée sur des capteurs visuels. En utilisant un système de vision et des algorithmes de traitement d'image, un véhicule peut se localiser correctement dans un environnement pré-mappé. Cette approche est sensible aux conditions d'éclairage, ce qui en fait un candidat idéal pour la localisation à l'intérieur. La plupart des approches de localisation basées sur des caméras s'inscrivent dans des types de méthodes basées sur l'appariement de cartes. Dans ces approches, une carte détaillée de l'environnement est construite dans une phase hors ligne. Sur la base de l'entrée de caméra de phase en ligne et de la carte hors ligne, l'emplacement du véhicule est calculé. Semblable au laser SLAM, le SLAM visuel est une approche populaire pour la localisation de véhicules intelligents. Le concept SLAM reste le même que dans le SLAM laser, mais dans ce cas, un ensemble de caméras est monté sur le véhicule pour capturer non seulement des images mais également pour mesurer la profondeur de la scène.

Le calcul à mort est un processus d’estimation de la pose actuelle d’un véhicule à l’aide d’une pose préalablement déterminée et du modèle dynamique du véhicule. À l’origine, il s’agissait d’une approche développée pour les applications marines et qui est maintenant utilisée dans divers domaines tels que la navigation aérienne, le suivi des piétons ou la navigation autonome par robot. L'algorithme de calcul à rebours utilise différentes configurations de capteurs. Le calcul à mort avec unités de mesure inertielle (IMU) est largement utilisé dans la navigation de véhicules spatiaux, de navires de mer ou de véhicules terrestres. IMU a généralement des gyroscopes à trois axes et des accélérateurs pour mesurer la vitesse angulaire et la vitesse de déplacement de l'objet attaché.

L'un des inconvénients du GPS est sa disponibilité dans les scénarios urbains. Le plus souvent, les signaux GPS sont perdus ou mal reçus dans un tunnel, un parking ou lorsque le récepteur est entouré de bâtiments, obstruant ainsi la visibilité directe des satellites. Les signaux GPS standard souffrent également de l'effet de trajets multiples qui pourrait entraîner une erreur de localisation supplémentaire de 8 m (Kos, Markezic et Pokrajcic 2010). Néanmoins, le GPS (et

les autres GNSS) joue un rôle essentiel dans la localisation, en particulier à l'échelle mondiale, car il s'agit du seul système de positionnement qui affiche directement dans le repère global. Sans ces coordonnées de référence globales, chaque véhicule intelligent fonctionnera selon ses propres coordonnées locales. Aucune communication ni coopération n'est possible.

Au cours des dernières années, la communauté de recherche sur les véhicules intelligents a développé plusieurs systèmes dédiés à la localisation dans les zones interdites de GPS en général et les parkings en particulier. En raison du manque de signaux GPS, la plupart des solutions de localisation dans ce domaine se situent au niveau de la localisation locale. En fonction du choix du système de coordonnées de référence, ces travaux peuvent être classés en deux classes: méthodes de localisation absolue (ou basées sur une carte) et méthodes de localisation relative (autocentrées, sans carte). Les travaux récents des deux classes seront étudiés dans les sections suivantes.

Dans l'approche du positionnement absolu, il est nécessaire qu'une carte de l'environnement soit connue au préalable par le véhicule. Cette carte comprend deux composants principaux: les objets statiques qui contribuent à la structure de la carte (route, murs, portes, etc.) et les objets dynamiques qui constituent des obstacles dans l'environnement (autres véhicules, piétons, etc. .) Selon la solution, la carte peut contenir les deux ou uniquement des objets statiques.

Contrairement à la localisation absolue, la localisation relative ne nécessite pas une carte détaillée de l'environnement. L'approche vise à estimer la position du véhicule par rapport aux objets locaux environnants tels que les autres véhicules, le marquage des voies, etc.

Parmi ces deux approches, la méthode cartographique semble beaucoup plus précise. Un système bien défini peut localiser des véhicules avec une précision allant jusqu'à 0,1 m. Toutefois, pour ceux qui disposent d'une carte détaillée de l'environnement, la résolution et la précision des informations cartographiques ont une influence considérable sur l'erreur de localisation. Malheureusement, plus la résolution est élevée, plus la solution est complexe et moins évolutive. Ainsi, une nouvelle solution pour ce scénario est requise.

Chapter 3

Les réseaux de capteurs sans fil (WSN) font référence à un groupe de capteurs dispersés et dédiés dans l'espace pour surveiller et enregistrer les conditions physiques de l'environnement et organiser les données collectées à un emplacement central. Le GNSS, qui est une partie cruciale de ITS, est un exemple parfait de WSN pour des applications ITS. Le GNSS en général

ou le GPS en particulier ont établi une norme pour le système de navigation global des véhicules intelligents. Malgré ses faiblesses dans les zones obstruées, l'impact du GPS est toujours important. En outre, le concept de localisation dans le GPS suggère une application possible des réseaux à grande vitesse (WSN) pour couvrir également ces zones obstruées. Ce chapitre examinera la stratégie de localisation des véhicules intelligents en particulier des réseaux intelligents WSN.

Il existe différents types de capteurs sans fil ainsi que des formes de réseaux pour les tâches de localisation à l'aide de WSN. Les capteurs sont infrarouges, ultrasoniques, unités de mesure inertielle (IMU), antenne Wi-Fi, etc. Les exemples de réseaux peuvent être le réseau satellite de GPS, le réseau cellulaire GSM, les réseaux Wi-Fi ou des réseaux plus spécifiques tels que Zigbee ou Bluetooth. Malgré les différences de types de capteurs et de formes de réseaux, les stratégies de localisation à l'aide de WSN peuvent être classées en deux classes: approches basées sur les gammes et approches sans plages.

Les approches basées sur la distance pour la localisation des WSN sont un groupe de méthodes qui estiment l'emplacement de l'objet d'intérêt en fonction de mesures de distance déduites des sorties de capteurs sans fil. Ces approches comportent deux étapes: les mesures de distance et l’estimation de la position. Souvent, des capteurs dotés de fonctions de mesure de distance telles que les ultrasons, les UMI, les lasers, etc. peuvent directement être utilisés pour déduire la distance entre des objets d’intérêt et d’autres objets de l’environnement et permettre ainsi une estimation de la localisation possible. Cependant, il existe d’autres capteurs qui peuvent déduire indirectement la distance aux IO, tels que les signaux satellites, les signaux cellulaires, les signaux Wi-Fi, etc.), Algorithme Heure d'arrivée (TOA), décalage horaire (TDOA), ou angle d'arrivée (AOA), etc.

En revanche, les approches par fourchette de frais n’estiment pas la distance entre les OI et les OOI pour calculer la position. Ces méthodes utilisent des fonctionnalités de réseau et de capteurs telles que le graphe de connectivité réseau, la consommation d'énergie des capteurs et leur transmission ou la relation géométrique d'un réseau, etc. La plupart du temps, ces approches comportent deux étapes: l'extraction de caractéristiques et la reconnaissance de caractéristiques. Les algorithmes remarquables pour cette classe sont le saut de vecteur de distance (DV hop), le test de point approximatif de triangulation (APIT), l’empreinte digitale et l’algorithme de centroïde.

Le tableau 4 présente une comparaison rapide de ces approches.

Chapter 4

En comparant différentes approches de localisation des WSN, une méthode de prise d'empreinte est choisie car elle satisfait aux quatre critères énoncés dans la section 1.2, à savoir la disponibilité, l'évolutivité, l'universalité et la précision.

Le concept général de la localisation d'empreintes digitales Wi-Fi est présenté à la section 3.4.3. Il existe deux phases pour cette méthode: une phase hors ligne et une phase en ligne.

Dans la phase hors ligne, une base de données d'empreintes digitales (FP) est construite. Comme défini dans la section 3.4.3, une empreinte digitale peut être n'importe quel emplacement de l'environnement ciblé avec des coordonnées connues. Chaque enregistrement dans la base de données d'empreintes digitales est un mappage des coordonnées d'une empreinte digitale et de tous les RSSI numérisés à cette position. Dans la Figure 4.1, chaque point bleu est une empreinte digitale (FP) avec des coordonnées connues. À un certain FP, les RSSI des cinq points d'accès (AP0, AP1, .., AP4) sont enregistrés et mis en correspondance avec ses coordonnées. Répétez cette procédure pour tous les PF de l'environnement pour établir la base de données d'empreintes digitales. Un enregistrement dans cette base de données est écrit comme dans Eq.4.1.

Dans la phase en ligne où l’estimation de la localisation est effectuée, le véhicule se déplacera dans l’environnement tout en recherchant les RSSI des points d’accès environnants. Une fonction de vraisemblance basée sur les données de la phase hors ligne est définie par Eq.4.3. En général, l'empreinte digitale avec le score de vraisemblance le plus élevé sera choisie comme emplacement estimé.

Récemment, plusieurs tentatives d'utilisation du concept d'empreinte digitale Wi-Fi ont été utilisées pour déterminer la position d'un véhicule. Certaines approches utilisent les smartphones des utilisateurs pour aider et guider le conducteur vers un parking. D'autres approches visent directement des véhicules intelligents avec des capteurs montés sur des véhicules. Selon le choix des capteurs (smartphone ou capteurs montés), la précision du système de localisation risque d'être affectée. Le chapitre présente quatre études notables. Ces études permettent d’atteindre environ 3-4 m d’erreur de localisation moyenne.

Après avoir examiné ces études, nous avons identifié deux problèmes majeurs concernant la méthode de localisation d'empreintes digitales Wi-Fi pour les véhicules: une fréquence d'échantillonnage faible du balayage Wi-Fi et une forte variance des forces du signal reçu. Pour résoudre ces problèmes, des modifications sont proposées aux phases hors ligne et en ligne.

Dans la phase hors ligne, une base de données d'apprentissage hybride est mise en œuvre pour résoudre le problème de la vitesse de déplacement. De plus, un réseau de neurones d'ensemble (Dietterich 2000) pour la fonction de vraisemblance de phase en ligne est déployé pour résoudre le problème des signaux à forte variance.

La base de données hybride hors ligne est proposée avec une nouvelle définition d'empreinte digitale et un mélange d'analyses dynamiques et statiques. La distance entre deux lieux d'initiation et de fin de l'analyse est appelée une plage d'analyse. En fonction de la vitesse de déplacement de la cible, la plage de balayage peut également varier. Ainsi, une nouvelle définition d'empreinte digitale en tant que cercle est modélisée dans Eq.4.4. De plus, pour modéliser correctement les signaux reçus de la phase en ligne, en plus de la collecte classique de données statiques, des signaux sont également enregistrés pendant le déplacement des véhicules dans l'emplacement de l'empreinte digitale.

Dans la phase en ligne, une fonction de vraisemblance h est requise pour évaluer le vecteur RSSI d'entrée en temps réel. L'idée d'utiliser plusieurs modèles d'apprentissage pour améliorer les performances d'un seul est proposée dans (Krogh, Anders Jesper, 1995; Breiman, 1996; Hansen et Salamon, 1990). Dans certaines conditions, la combinaison d'estimateurs divers, non corrélés mais précis, devrait donner de meilleures performances qu'un seul. Cette section présente la stratégie d'ensemble visant à améliorer les résultats prévus (Eq.4.9 à Eq.4.13).

Les expériences relatives à la méthode proposée sont effectuées dans une place de parking ouverte du campus de l'INRIA Rocquencourt. En raison de la difficulté d'avoir un parking couvert pour les expériences, l'espace extérieur est utilisé. En même temps, ce parking extérieur bénéficie d'un RTK-GPS précis pour la vérité du terrain. Cela permet une meilleure évaluation du système. La zone d'essai est illustrée à la figure 4.16. Il existe deux véhicules dans les expériences: un Cybercar bleu conçu comme un prototype pour les véhicules intelligents et une Citroën C1 rouge modifiée à des fins expérimentales.

Tout d'abord, une étude de la zone de test est réalisée pour comprendre les caractéristiques de la méthode. Les résultats de cette enquête suggèrent qu'il existe une forte corrélation entre la force moyenne du signal Wi-Fi et la précision du résultat de la localisation. Ainsi, avec une attente réaliste d'une bonne force de signal moyenne dans le scénario réel, la zone d'essai est alors définie. Dans la figure 4.23, les empreintes digitales sont marquées d'un cercle rouge. La distance moyenne entre deux empreintes digitales adjacentes est de 6,1 m, ce qui correspond à la limite supérieure de l'inter-distance entre les empreintes digitales décrite à la section 4.1.

Avec cette distance, il ne faut que 25 empreintes digitales pour couvrir la zone de test. Pour chaque empreinte digitale, 60 analyses statiques et 20 analyses dynamiques sont enregistrées pour la base de données hors connexion. Un total de 156 points d'accès avec différentes adresses MAC est détecté sur 25 empreintes digitales. nous définissons ensuite un bon résultat de classification du réseau de neurones comme étant les empreintes digitales les plus proches de la vérité au sol en distance euclidienne. Comme mentionné dans l'équation 4.18, le résultat de Ensemble Neural Network est une liste des indices d'empreintes digitales et de leur confiance. Supposons que l'empreinte digitale de confiance la plus élevée est choisie comme résultat final de la classification. Un bon résultat de la classification doit satisfaire à l'Eq. 4.22. Pendant un an, avec plus de 60 expériences menées, la méthode proposée a surperformé toutes les solutions existantes et a une précision moyenne de 2,25 m.

Chapter 5

Ce chapitre présente un cadre de fusion pour le système de localisation de parkings utilisant plusieurs capteurs, notamment: l'empreinte Wi-Fi, l'IMU et le laser-SLAM. Pour compléter le faible taux d'échantillonnage, la localisation absolue à partir des empreintes Wi-Fi, un filtre à particules modèle de mélange gaussien est utilisé. Avec les entrées haute fréquence de l'IMU ou du laser-SLAM, les particules du filtre à particules évoluent en temps réel. Une fois que l'observation du système de localisation d'empreintes digitales Wi-Fi est disponible, une correction à l'aide de la fonction d'évaluation du mélange gaussien est effectuée pour éliminer l'erreur accumulée.

Une contribution majeure de ce chapitre est la fonction de notation du mélange gaussien, qui permet au filtre à particules de récupérer d'une mauvaise position initiale et de mauvaises observations pendant le mouvement. Tout d'abord, comme indiqué à la section 5.6.1.1, une bonne estimation de la position de départ augmenterait considérablement le taux de convergence du filtre à particules. L'utilisation du mélange de quelques empreintes digitales supérieures comme position initiale permet non seulement à la particule de converger plus rapidement, mais élimine également toute condition nécessaire au démarrage du système de localisation (c'est-à-dire à partir d'une position connue). De plus, même avec une mauvaise position de départ, la fonction d'évaluation du mélange gaussien aide la particule à converger rapidement. Ceci est montré dans les résultats d'expériences de cas de test où la position initiale est en dehors de la zone d'empreinte digitale. L'erreur de localisation est rapidement réduite lorsque le véhicule se rapproche d'une empreinte digitale. Deuxièmement, les observations du

système de localisation d'empreintes digitales Wi-Fi ne donnent pas toujours une bonne estimation de la position réelle. Au lieu de cela, il s'agit d'un cas de test réel présenté dans la section 5.3.2, dans lequel le résultat de classification de confiance le plus élevé de la localisation d'empreintes digitales Wi-Fi n'est pas un bon résultat de classification. Cependant, la fonction de notation du modèle de mélange gaussien donne au filtre à particules une chance de surmonter une telle situation en prenant en compte les autres résultats de classification supérieurs qui devraient théoriquement rapprocher l'estimation de la position réelle.

Une autre proposition intéressante de ce chapitre concerne la stratégie visant à fusionner le SLAM laser en un système de coordonnées global sans recourir à un processus d'initialisation ou à une carte laser prédéfinie. Contrairement aux autres solutions mentionnées au chapitre 2, ce framework de fusion ne nécessite pas de position initiale soigneusement calibrée pour le SLAM laser ni de carte prédéfinie pour la formulation d'une matrice de transformation entre la coordonnée SLAM et la coordonnée globale. Au lieu de cela, tirant parti de la haute précision du SLAM dans l’estimation par pas local, le cadre de fusion incorpore le laser-SLAM en tant qu’IMU, ce qui réduit le besoin d’une matrice de transformation.

Au cours d'une année d'expériences, la fusion de la localisation des empreintes digitales IMU et Wi-Fi est testée avec différents critères tels que: la stabilité du filtre à particules, le nombre de particules et le comportement du système avec différentes positions de départ.

Pour comprendre la stabilité du filtre à particules conçu, le système de fusion est testé sous deux perspectives: plusieurs exécutions sur le même jeu de données et différents jeux de données. Dans la première perspective, un seul jeu de données est introduit indépendamment dans l'algorithme pour 100 itérations. L'erreur de localisation moyenne et son écart type sont calculés au-dessus des 100 itérations. Une erreur moyenne faible (environ 0,8 m dans tous les cas et 0,5 m pour une bonne position de départ), ainsi qu'un faible écart type (~ 0,22) indiquent que le filtre à particules est stable. Pour la deuxième perspective, un total de 84 expériences indépendantes ont été menées. Les résultats finaux donnent un résultat similaire avec une erreur moyenne et un écart type de 0,859 m et 0,232 pour tous les cas et de 0,588 m et 0,127 pour une bonne position initiale. Ainsi, il a été prouvé que le filtre à particules conçu est stable.

Le nombre de particules dans un filtre à particules (ou sa dimension) est également un paramètre important. Cela détermine les ressources nécessaires pour que l'algorithme s'exécute en temps réel. Pour apprendre ce paramètre, différents nombres de particules sont testés dans le même

jeu de données. Enfin, avec seulement 2000 particules, la solution de fusion est capable d'obtenir un résultat optimal.

Différentes positions initiales pour les tests sont également étudiées pour comprendre la généralisation de l'algorithme. Il existe deux possibilités de lieu pour la position initiale: à l'intérieur ou à l'extérieur d'une zone d'empreinte digitale. Si la position initiale est dans une zone d'empreinte digitale, une bonne estimation initiale peut être attendue. Cela se traduit par une faible erreur de localisation moyenne de 0,588 m. Sinon, comme le filtre à particules a besoin de temps pour converger vers la position vraie, l'erreur de localisation moyenne dans ce cas est d'environ 0,859 m. Cette erreur moyenne élevée est principalement due à la grande erreur de positionnement initiale. En outre, il est raisonnable de s'attendre à ce que la position initiale d'un véhicule entrant dans un parc de stationnement soit relativement connue. Par conséquent, une bonne précision peut être attendue du système de fusion en général.

Bien que la vitesse de déplacement moyenne dans toutes les expériences soit d'environ 3,3 m / s, il est possible d'étendre le résultat de la thèse à une vitesse de déplacement supérieure. Pour ce faire, il faut trouver une solution permettant d'améliorer la fréquence d'échantillonnage de localisation des empreintes digitales Wi-Fi. Une solution potentielle consiste à utiliser plusieurs antennes Wi-Fi avec différents processeurs, chacun ayant un léger retard par rapport à l'autre. De cette manière, la fréquence d'échantillonnage du balayage Wi-Fi peut être augmentée proportionnellement au nombre d'antennes. Malheureusement, avec un temps limité, la thèse n'a pas pu être étendue pour couvrir l'idée.

Enfin, le cadre de fusion proposé permet non seulement de fusionner les empreintes Wi-Fi avec d'autres capteurs, mais il est également possible de combiner différentes stratégies telles que le GPS avec SLAM laser, le GPS avec système de localisation par caméra, etc. Cela étant dit, ce cadre peut être appliqué à plusieurs scénarios, mais pas uniquement à un sans GPS environnement ou à un parking privé.

Chapter 6

Le chapitre conclut la thèse avec deux contributions majeures et une perspective pour les travaux futurs. Après avoir défini le problème au début, une solution basée sur le réseau de capteurs sans fil est proposée. Le chapitre 4 explique pourquoi un système de localisation d'empreintes digitales Wi-Fi peut répondre aux quatre critères. À condition que, un réseau de neurones d'ensemble pour l'empreinte Wi-Fi est proposé. La base de données hybride d'empreintes digitales et un réseau de neurones d'ensemble destinés à aider la localisation

d'empreintes digitales Wi-Fi à s'adapter à la circulation d'un véhicule dans un parking sont deux contributions majeures. Des expériences sur des véhicules réels ont été menées pendant une année pour valider le système proposé. Avec deux véhicules différents, 64 expériences, le système fournit une erreur de localisation moyenne de 2,25 m. Cela prouve que le système de localisation d'empreintes digitales Wi-Fi proposé est capable de remplacer le GPS dans un environnement sans GPS.

Toutefois, comme indiqué dans le champ d'application, l'erreur de localisation souhaitée pour un véhicule intelligent est d'environ 0,2 m. De plus, le système devrait pouvoir localiser le véhicule à haute fréquence pour faire face aux mouvements à grande vitesse. Par conséquent, un cadre de fusion pour la localisation d'empreintes digitales Wi-Fi et un autre système tel que l'IMU ou le laser-SLAM est proposé. L'objectif de ces systèmes est d'améliorer progressivement la fréquence de localisation, la précision et la transition de l'environnement assisté par GPS à un environnement refusé par GPS. Afin d'accomplir cette tâche, le filtre de particules d'amorçage, une méthode de filtrage non linéaire est choisie. Comparé à un autre algorithme de filtrage, le filtre à particules semble offrir de meilleures performances en matière d'estimation non linéaire. En général, l'étape de correction du filtre à particules prendra en compte les observations disponibles pour peser sur l'ensemble candidat de positionnement (ou les particules). Compte tenu des observations absolues de méthodes telles que la localisation GPS, par caméra ou Wi-Fi, la meilleure estimation est souvent prise en compte pour évaluer l'ensemble de positionnement candidat. Dans cette thèse, la correction est prise à partir du système de localisation d'empreintes digitales Wi-Fi. Avec une étude statistique du chapitre 4, il est justifié que les 3 premiers résultats de la classification donnent une bien meilleure estimation de la position réelle que seulement le score le plus élevé. Par conséquent, au lieu de considérer uniquement le score de confiance le plus élevé du résultat de la localisation Wi-Fi, le filtre prend en compte plusieurs scores possibles (3 en haut dans cette thèse) sous forme d'observations. Une fonction de notation utilisant un modèle de mélange gaussien de ces observations est définie. Les avantages de cette approche sont décrits à la section 5.3.

Parmi les différents capteurs, deux des capteurs les plus courants pour véhicules autonomes sont choisis pour la fusion dans cette thèse, à savoir l'unité de mesure inertielle (IMU) et le LiDAR. Bien qu'il s'agisse d'un couplage standard du GPS et du LiDAR (ou Velodyme) dans l'environnement assisté par GPS pour la localisation précise de véhicules intelligents, ce n'est pas le cas pour l'environnement assisté par GPS. Ainsi, une combinaison de la localisation Wi-Fi et du SLAM laser est proposée. À ce jour, le travail de thèse est également la première

tentative de fusion de la localisation Wi-Fi et du laser-SLAM pour le positionnement de véhicules autonomes. Les détails de la stratégie de fusion sont expliqués au chapitre 5.

Enfin, avec de plus en plus d'études sur le même sujet chaque année, l'auteur estime que la solution de localisation de réseaux de capteurs sans fil deviendrait éventuellement une solution mature pour le positionnement de véhicules intelligents dans des environnements intérieurs.

9. APPENDIX 2: ABSTRACT

Chapter 1

The chapter presents the motivation, scope and goal of the thesis. This thesis begins with the collaboration of two research units RITS team, INRIA France and MICA Institute and funded by the Vietnamese government scholarship program 911. While benefits of intelligent vehicles are clear, much of the research attention is on GPS-aided, outdoor environment such as highway, urban streets etc. The GPS-denied environment, which is also an important scenario for intelligent vehicles applications, is not yet fully addressed. A notable environment for such scenario is an indoor carpark. This thesis aims to find a new solution for the localization problem for the GPS-denied environment. Existing solutions for this scenario are either costly to deploy or unable to fully resolve the problem. Hence, the solution must be a global localization method which allows seamless transition between GPS-aided and GPS-denied environment localization and satisfy four criteria: Availability, scalability, universality and accuracy. Two main contributions are proposed: a Wi-Fi Ensemble Fingerprinting Localization system which can replicate the GPS behaviour for the GPS-denied environment and a Gaussian Mixture Particle Filter fusion framework that enables fusion of multiple localization techniques together.

Chapter 2

In this chapter, some general techniques for intelligent vehicles localization are examined. Also, a survey of existing solutions for intelligent vehicles localization in GPS-denied environments are presented.

In general, IV localization techniques can be divided into two categories: global localization and local localization. Often, the global localization category is GNSS-based localization methods. These methods make use of satellite signals to determine 3D position information of the receiver in a global reference (such as WGS84). The term GPS refers to Global Positioning System which is governed by the United States of America. There are others Global Navigation Satellite Systems (GNSS) such as GLONASS (Russia), Galileo (Europe), and Beidou (China). To simplify the problem, the thesis will focus on GPS performance as a representative for other GNSSs. The principle of computing the receiver location is based on knowing the positions of

the satellites then deducing the respective “pseudo-ranges” from those satellites to the receiver as in Figure 2.2. Here, the term “pseudo-range” refers to the distance calculated from satellites to the mobile receiver. Since satellites are constantly moving, this distance is not a fixed value. To calculate the 3D position of a receiver, at least four satellites are required. An overview of the GPS system can be found in (Hofmann-Wellenhof, Lichtenegger, and Wasle 2018).

There are two level of GPS services namely Standard Positioning Service (SPS) and Precise Positioning Service (PPS). While SPS is accessible by public users, high precision PPS is only accessible by authorized users (military personnel, government agents). Summary of SPS and PPS performance are shown in Table 1 and Table 2. In general, SPS provides 7.8m of maximum localization error in 95% of the time and PPS offers a better accuracy with 5.9m of maximum localization error in 95% of the time. Also, vertical accuracy is expected to be lower than horizontal accuracy in all GPS measurements. In the best case scenario, a highly accurate DGPS solution known as Real Time Kinematic GPS (RTK GPS) can deliver up to few centimetres of accuracy. However, the method requires dedicated base stations, sensors, continuous GPS signals and an excessive price for deploying and maintaining. This makes the RTK not suitable for most urban application (“Real Time Kinematics - Navipedia” 2018).

Similar to the US, the European Union also develop a global positioning system called Galileo to provide an independent high precision global positioning system for the European nations. The system is supposed to help the EU countries not to rely on China’s BeiDou, Russian GLONASS or more significantly, the United States GPS. Under good conditions such as fully function satellites (up to 30 units), clear vision from receiver to satellites, etc. the free open access for navigation of the Galileo system within the EU border is expected to be around 4 meter of precision (“Galileo General Introduction - Navipedia” 2018). Another worth to mention global positioning system is the GLONASS developed by Russia in 1980s. By 2010, the GLONASS has covered the entire Russia territory then after October 2011, the global coverage is achieved. The evolution of the GLONASS positioning accuracy is shown in Figure 2.5. Up to now, under static sky, the GLONASS accuracy for public access is as good as 2.8 meters. A quick comparison of different global localization system can be found in Table 3.

One notable local localization method is laser-based localization. Using a rangefinder technique based on laser beams, the sensor accurately estimates the distance to other objects in the environment. An important form of laser sensor setup is LiDAR (James Eddy 2017) (Light Detection and Ranging) which fires continuously laser beams to the environment. This helps to estimate the distance to surrounding obstacles and allows to perform a mapping of the

environment at a high resolution. When it comes to laser sensor, the majority of its localization algorithms involve solving entirely or partially a Simultaneous Localization and Mapping (SLAM) problem (Smith and Cheeseman 2018), (Durrant-Whyte and Bailey 2006), (Dellaert et al. 2018).The SLAM objective is to estimate the vehicle's trajectory (or pose in online SLAM) and at the same time to map the neighbouring environment given inputs from the vehicle's sensors. A graphical representation of the full SLAM and online SLAM problem is shown in Figure 2.6a and Figure 2.6b respectively. In the full SLAM problem, the algorithm is supposed to estimate the whole trajectory of the vehicle formulated by a list of its poses over time step k: x_k given sensors reading z_k, control input u_k and at the same time building the map m of the environment. This demanding task becomes more and more complex over time and it is difficult to be handled in real time. The idea of online SLAM, which is supposed to be done in real time, is then introduced. Online SLAM will only estimate the current vehicle's pose thus effectively reduce the complexity of the problem. An overview of the current trend in SLAM can be found in (Bresson et al. 2017). Given the accuracy of laser sensors and the potential of SLAM, the combination of LiDAR-SLAM quickly becomes one of the keys towards fully autonomous vehicles. Over the years, the techniques of estimation in SLAM can be categorized into *filter-based* approaches and *optimization-based* approaches.

The core idea of filter-based approaches comes from Bayesian filtering and consists of two steps: prediction and observation. In the first step, a prediction of the vehicle's pose and map state is made using a dynamic model of the vehicles with control inputs u_k. Having this prediction, a correction is made based on the current observation from sensors inputs z_k. The model to match an observation with the map is called an observation model. Two major branches in this approach are *Extended Kalman Filter* and *Particle Filter* based SLAM.

Optimization-based SLAM (M. Liu et al. 2012) is also a two iterative steps algorithm. The first step identifies constraints of the problem based on sensor data. This is done by matching between new observations and the map. The second step computes the vehicle pose and the map given the identified constraints. Vision-based techniques for SLAM are more likely to use this approach, laser-based techniques are also included within Graph-SLAM algorithm class.

Another notable approach for vehicle localization is visual sensors based technique. Using a vision system and image processing algorithms, a vehicle can correctly localize itself within a pre-mapped environment. This approach is sensitive to lighting conditions making it a suitable candidate for indoor localization. Most of camera-based localization approaches fall into map-matching based method types. In these approaches, a detailed map of the environment is built

in an offline phase. Based on online phase camera input and the offline map, the location of the vehicle is calculated. Similar to Laser SLAM, visual SLAM is a popular approach for intelligent vehicles localization. The SLAM concept remains the same as in the laser SLAM but in this case a set of cameras is mounted on the vehicle to capture not only images but also to measure the depth of the scene.

Dead-reckoning is a process of estimating the current pose of a vehicle using a previously determined pose and the vehicle's dynamic model. Initially, it was an approach developed for marine applications and has now been used in a variety of fields such as air navigation, pedestrian tracking or autonomous robot navigation. The dead-reckoning algorithm makes use of different sensor configurations. Dead-reckoning with Inertial Measurement Units (IMU) is widely used in the navigation of spacecraft, marine ships or landline vehicles. IMU typically has three-axis gyroscopes and accelerators to measure angular and displacement velocity of the attached object.

One of the drawbacks of GPS is its availability in urban scenarios. More often, GPS signals are lost or poorly received in a tunnel, a carpark or when the receiver is surrounded by buildings thus obstructs line-of-sight to satellites. The standard GPS signals also suffer from the multi-path effect which could result in additional 8m of error in localization (Kos, Markezic, and Pokrajcic 2010). Still, GPS (and other GNSSs) plays a vital role in localization especially at the global scale as it is the only positioning system that directly outputs in the global coordinate frame. Without this global reference coordinates, each intelligent vehicle will work on its own local coordinates hence no communication or cooperation is possible.

In the last few years, the research community in Intelligent Vehicles has been developing several dedicated systems for localization in GPS-denied areas in general and carparks in particular. Due to the lack of GPS signals, most of the solutions for localization in this domain fall into the local localization level. Depending on the choice of the reference coordinate system, these works can be categorized into two classes: absolute localization (or map-based) methods and relative localization (self-centric, without a map) methods. The two classes' recent works will be studied in the following sections.

In the absolute positioning approach, it is required that a map of the environment is known beforehand by the vehicle. In this map, there are two main components: static objects which contribute to the structure of the map (e.g. road, walls, doors, etc.), and dynamic objects which

are moving obstacles in the environment (e.g. other vehicles, pedestrian, etc.). Depending on the solution, the map may contain both or just static objects.

In contrast to absolute localization, relative localization does not require an extensive map of the environment. The approach aims to estimate the vehicle position relative to its surrounding local objects such as other vehicles, lane marking, etc.

Among these two approaches, the map-based method appears to be much more accurate. A well-defined system can localize vehicles up to 0.1m of accuracy. However, for those with a detailed map of the environment, the resolution and precision of map information severely influence the localization error. Unfortunately, the higher the resolution the map is, the more complex and less scalable the solution is. Thus, a new solution for this scenario is required.

Chapter 3

Wireless Sensors Networks (WSNs) refer to a group of spatially dispersed and dedicated sensors for monitoring and recording the physical conditions of the environment and organizing the collected data at a central location. The GNSS, which is a crucial part of ITS, is a perfect example of WSNs for ITS applications. The GNSS in general or GPS in particular has set a standard for the global navigation system of intelligent vehicles. Despite its weaknesses in obstructed areas, the impact of GPS is still large. In addition, the concept of localization in GPS suggests a possible application of WSNs to cover those obstructed areas as well. This chapter will take a look at WSNs strategy for localization in general and intelligent vehicles localization in particular.

There are various types of wireless sensors as well as forms of networks for localization task using WSNs. The sensors are infrared, ultrasonic, Inertial Measurement Units (IMU), Wi-Fi antenna, etc. and Networks examples could be the Satellites network of GPS, the GSM cellular network, Wi-Fi networks or more specific networks such as Zigbee, or Bluetooth. Despite differences in sensors types and networks forms, the strategies of localization using WSNs can be categorized into two classes: *Range-based* and *Range-free* approaches.

Range-based approaches for WSNs localization are a group of methods that estimate the location of the object of interest based on distance measurements inferred from wireless sensors outputs. These approaches have two stages: distance measurements and position estimation. Often, sensors with distance measuring feature such as ultrasonic, IMU, lasers, etc. which can directly be used to infer the distance from/to objects of interest (OOIs) to other objects in the

environment and thus possible location estimation can be calculated. However, there are other sensors that can indirectly infer the distance to OOIs such as Satellites signals, cellular signals, Wi-Fi signals, etc. The distance computation from these sensors outputs is based on a signal propagation model using Received Signal Strength Indicator (RSSI), Time of Arrival (TOA), Time Difference of Arrival (TDOA), or Angle of Arrival (AOA) algorithm, etc.

Range-fee approaches, in contrary, do not estimate the distance to/from OOIs in order to calculate position. Those methods use network and sensors features such as network connectivity graph, sensors power consumption and transmission or geometric relationship of network etc. Most of the time, these approaches have two steps: feature extractions and feature recognition. Notable algorithms for this class are distance vector hop (DV hop), approximate point-in-triangulation test (APIT), fingerprinting and centroid algorithm.

A quick comparison of these approaches can be found in Table 4.

Chapter 4

By comparing different WSNs localization approaches, a fingerprinting method is chosen as it satisfies all of four criteria stated in Section 1.2 which are *availability*, *scalability*, *universality* and *accuracy*.

The general concept of Wi-Fi Fingerprinting localization is introduced in Section 3.4.3. There are two phases for this method: *an offline* and *an online* phase.

In the *offline* phase, a database of *fingerprints* (FPs) is built. As defined in Section 3.4.3, a *fingerprint* could be any location in the targeted environment with known coordinates. Each record in the database of *fingerprints* is a mapping of a *fingerprint* coordinates and all scanned RSSIs at that position. In Figure 4.1, each blue dot is a *fingerprint* (FP) with known coordinates. At a certain FP, RSSIs from all five access points (AP0, AP1, .., AP4) are recorded and mapped to its coordinates. Repeat this process for all FPs in the environment to establish the database of *fingerprints*. A record in this database is written as in Eq.4.1.

In the *online* phase where localization estimation is carried out, the vehicle will move inside the environment while scanning for RSSIs from surrounding APs. A likelihood function based on data from offline phase is defined as Eq.4.3. In general, the *fingerprint* with the highest likelihood score will be chosen as the estimated location.

Recently, there are several attempts to use the concept of Wi-Fi fingerprinting in determining position of a vehicle. Some approaches take advantages of users' smartphones to assist and

guide driver to a parking lot. Other approaches directly aim for intelligent vehicles with sensors are mounted on vehicles. Depending on the choice of sensors (smartphone or mounted sensors), the accuracy of the localization system is likely to be affected. The chapter presents four notable studies. These studies achieve around 3-4m of mean localization error.

Having these studies reviewed, two major issues of the Wi-Fi Fingerprinting localization method for vehicles are identified: Low sampling frequency of Wi-Fi scan and high variance in received signal strengths. To address these issues, changes in both *offline* and *online* phases are proposed. In the *offline* phase, a hybrid learning database is implemented to overcome the movement speed issue. Furthermore, an ensemble neural network(Dietterich 2000) for the *online* phase likelihood function is deployed to solve the high variance signals problem.

The hybrid offline database is proposed with a new definition for fingerprint and a mix of dynamic as well as static scan. The distance between two locations of scan initiation and termination is called a *scan range*. Depending on the movement speed of the target, the *scan range* can also vary. Thus, a new fingerprint definition as a circle is modelled in Eq.4.4. Also, to correctly model the received signals of the online phase, in addition to classical static data collection, signals are also recorded while vehicles moving through the fingerprint location.

In the *online* phase, a likelihood function *h* is required for evaluating the real-time input RSSIs vector. The idea of using multiple learning models to enhance performance of a single one is proposed in (Krogh, Anders Jesper 1995; Breiman 1996; Hansen and Salamon 1990). Under certain conditions, the combination of diverse, uncorrelated but accurate estimators should have better performance than one alone. This section presents the ensemble strategy to enhance the predicted results (Eq.4.9 to Eq.4.13).

Experiments for the proposed method are carried out in an open parking space of the INRIA Rocquencourt campus. Due to difficulties in having an indoor carpark for experiments, the outdoor space is utilized. At the same time, this outdoor carpark benefit from a precise RTK-GPS for localization ground truth. This allows a better evaluation of the system. The testing area is shown in Figure 4.16. There are two vehicles in the experiments: a blue Cybercar designed as a prototype for intelligent vehicles and a red Citroen C1 with modification for experimental purposes.

First, a survey of the testing area is conducted to understand the characteristic of the method. Results from this survey suggest that there is a strong correlation between the average Wi-Fi signal strength and the accuracy of localization result. Thus, with a realistic expectation of a

good average signal strength in the real life scenario, the testing area is then defined. In Figure 4.23, fingerprint locations are marked with red circles. The average distance between two adjacent fingerprints is 6.1m as this is the upper-bound of the inter-distance between fingerprints discussed in Section 0. With this inter-distance, it takes only 25 fingerprints to cover the testing area. For each fingerprint, 60 static scans and 20 dynamic scans are recorded for the offline database. A total 156 access points with different MAC addresses are detected across 25 fingerprints. we then define a *good classification result* of the neural network as the closest fingerprints to the ground truth in Euclidean distance. As mentioned in Eq. 4.18, result from the Ensemble Neural Network is a list of fingerprints' indices and their corresponding confidence. Assume that the highest confidence fingerprint is chosen as the final classification result, a good classification result must satisfy the Eq. 4.22. For one year period, with more than 60 conducted experiments, the proposed method outperformed all existing solutions and has 2.25m of mean accuracy.

Chapter 5

This chapter presents a fusion framework for the car park localization system using multiple sensors including: the Wi-Fi fingerprinting, the IMU and the laser-SLAM. To compliment the low sampling rate, absolute localization from Wi-Fi fingerprinting, a Gaussian mixture model particle filter is employed. With high frequency inputs from the IMU or laser-SLAM, particles in the particle filter are evolved in real time. Once observation from the Wi-Fi fingerprinting localization system available, correction using Gaussian mixture scoring function is made to eliminate the accumulated error.

A major contribution in this chapter is the Gaussian mixture scoring function that enables the particle filter to recover from both a bad initial position and bad observations during the movement. Firstly, as discussed in Section 5.6.1.1, a good initial guess of the starting position would significantly boost the convergence rate of the particle filter. Using the mixture of few top fingerprints as the initial position not only allows the particle to converge faster but also eliminate any condition required for the localization system to start (i.e. starting from a known position). Moreover, even with a bad starting position, the Gaussian mixture scoring function helps the particle to quickly converge. This is shown in experiment results of test cases where the initial position is out of the fingerprint area. The localization error is quickly reduced once the vehicle moves closer to a fingerprint. Secondly, observations from the Wi-Fi fingerprinting localization system is not always giving good estimation of the true position. Instead, a real test

case shown in Section 5.3.2 where the highest confidence classification result of the Wi-Fi fingerprinting localization is not a *good classification* result. However, the Gaussian mixture model scoring function gives the particle filter a chance to overcome such situation by taking into account other top classification results which should theoretically bring the estimation closer to the true position.

Another notable proposal in this chapter is the strategy to the fuse laser-SLAM into a global coordinate system without the need of an initialization process or a predefined laser map. Unlike other solutions mentioned in Chapter 2, this fusion framework does not require a carefully calibrated initial position for laser-SLAM nor a prebuilt map to formulize a transformation matrix between the SLAM coordinate and the global coordinate. Instead, taking advantage of the SLAM high precision in the local step estimation, the fusion framework incorporate the laser-SLAM as an IMU which reduces the need for a transformation matrix.

During a year of experiments, the fusion of IMU and Wi-Fi fingerprinting localization is tested with different criteria such as: stability of the particle filter, number particles and the behaviour of the system with different initial starting positions.

To understand the designed particle filter stability, the fusion system is tested in two perspectives: multiple runs on the same dataset and different datasets. In the first perspective, a single dataset is independently fed into the algorithm for a 100 iterations. The mean localization error and its standard deviation is calculated on top of all 100 iterations. A low mean error (around 0.8m for all cases, and 0.5m for a good starting position) as well as low standard deviation (~ 0.22) indicate that the particle filter is stable. For the second perspective, a total of 84 independent experiments were conducted. The final results yield a similar outcome with mean error and standard deviation is 0.859m and 0.232 for all cases and 0.588m and 0.127 for a good initial position. Thus, the designed particle filter is proven to be stable.

The number of particles in a particle filter (or its dimension) is also an important parameter. This decides the resources needed for the algorithm to run in real time. To learn this parameter, different number of particles are tested in the same dataset. Finally, with only 2000 particles, the fusion solution is able to achieve the optimal result.

Different initial positions for test runs are also studied to understand the generalization of the algorithm. There are two possibilities for place for the initial position: either within or outside a fingerprint area. If the initial position is within a fingerprint area, a good initial guess can be expected. This results in a low mean localization error of 0.588m. Otherwise, since the particle

filter needs time to converge to the true position, the mean localization error in this case is around 0.859m. This high mean error is mostly due to the initial large positioning error. In addition, it is reasonable to expect the initial position of a vehicle entering a car park is relatively known. Hence, a good accuracy can be expected from the fusion system in general.

Although, the average movement speed in all experiments is around 3.3m/s, there is a possibility of extending the thesis result to a higher movement speed. In order to accomplish this, a solution to enhance Wi-Fi fingerprinting localization sampling frequency must be found. One potential way is to use multiple Wi-Fi antenna with different processors, each has a small delay to the other. In this way, the sampling frequency of Wi-Fi scan can be increased proportional to the number of antennas. Unfortunately, with limited time, the thesis could not be extended to cover the idea.

Finally, the proposed fusion framework allows not only the fusion of Wi-Fi fingerprinting with other sensors but it has the potential to combine different strategies such as the GPS with laser-SLAM, GPS with camera-based localization system, etc.. With that being said, this framework can be applied to multiple scenarios but not just GPS-denied environment or car park.

Chapter 6

The chapter concludes the thesis with two major contributions and perspective for the future work. Having defined the problem at the beginning, a solution based on Wireless Sensors Network is proposed. Chapter 4 gives a discussion on why a Wi-Fi fingerprinting localization system could satisfy all four criteria. Provided that, an ensemble neural network for Wi-Fi fingerprinting is proposed. Two major contributions are the hybrid database of fingerprints as well as an ensemble neural network to help the Wi-Fi fingerprinting localization adapt to a vehicle movement inside a car park. Experiments on real vehicles were conducted for a duration of one year to validate the proposed system. With two different vehicles, 64 experiments, the system provides a 2.25m of average localization error. This proves that the proposed Wi-Fi fingerprinting localization system is capable of replacing the GPS in a GPS-denied environment.

Still, as stated in the scope, the desired localization error for an intelligent vehicle is around 0.2m. In addition, the system should be able to locate the vehicle in high frequency to cope with high-speed movement. Therefore, a fusion framework for the Wi-Fi fingerprinting localization and another system such as the IMU or laser-SLAM is proposed. The goal of such systems is to smoothly improve localization frequency, accuracy as well as the transition from the GPS-

aided environment to GPS-denied environment. In order to accomplish the task, the bootstrap particle filter, a non-linear filtering method is chosen. Compare to other filtering algorithm, the particle filter appears to have better performance when it comes to non-linear estimation. In general, the correction step of the particle filter will take into account available observations to put weight on the positioning candidate set (or the particles). Given absolute observations from methods such as GPS, camera or Wi-Fi localization, often, the best estimation is taken into account evaluate the positioning candidate set. In this thesis, the correction is taken from the Wi-Fi fingerprinting localization system. Having a statistic study from Chapter 4, it is justified that the top 3 classification results give a much better estimation of the true position than only the highest score one. Hence, instead of considering just the highest confidence score from the Wi-Fi localization result, the filter takes into account multiple possible ones (3-top in this thesis) as observations. A scoring function using Gaussian mixture model of those observations is defined. The benefit of this approach is described in Section 5.3.

Among different sensors, two of the most common ones for autonomous vehicles are chosen for fusion in this thesis namely the Inertial Measurement Unit (IMU) and LiDAR. While it is a standard coupling of the GPS and LiDAR (or Velodyme) in the GPS-aided environment for the precise localization of intelligent vehicles, it is not the case for the GPS-aided environment. Thus, a combination of the Wi-Fi localization and the laser-based SLAM is proposed. To this date, the thesis work is also the first attempt to fuse the Wi-Fi localization and the laser-SLAM for autonomous vehicles positioning. Details of the fusion strategy is explained in Chapter 5.

Finally, with more and more studies are being found in the same topic each year, the author believes that the wireless sensor networks localization solution would eventually be a mature solution for intelligent vehicles positioning in the indoor environments.